UNIVERSITÄT ZU LÜBECK

From the Department of Dermatology, Allergology, and Venerology

University of Lübeck

"Dectin-2: the C-type lectin receptor governs neutrophils by cooperating with Fcγ receptor IV to drive neutrophil-mediated skin inflammation"

Dissertation

for Fulfillment of

Requirements

for the Doctoral Degree

of the University of Lübeck

from the Department of Natural Science

Submitted by

Francesca Fagiani, MSc.

from Rome, Italy

Lübeck 2023

First referee: Prof. Dr. med. Christian Sadik

Second referee: Prof. Dr. Rudolf Manz

Date of oral examination: 28.06.2023

Approved for printing. Lübeck, 20.07.2023

ACKNOWLEDGEMENTS

I would like to dedicate this project in memory of the director of the clinic of Dermatology of the university of Lübeck, Prof. Dr. med. Detlef Zillikens and our beloved secretary Frau Stephanie Ollmann.

I would like to thank Prof. Dr. med. Christian Sadik for giving me the opportunity to work in his laboratory and towards my PhD degree. This work would not have been possible without his trust in me.

I appreciated the time I spent with my second family, the AG Sadik group, and thank you for being with me in the fun and hard times.

A special thanks to Dr. Paul Schilf, Dr. Sripriya Murthy and Dr. Tanya Sezin for teaching me how to perform the experiments and how to think outside the box. Thank you for being there not only as co-workers but also as friends.

Thank you to all the friends I met in Lübeck who spent with me beautiful moments by going out, eating, dancing and singing because this was what we loved the most.

It is 10 years I live abroad, far away from my family and friends and so it is hard to deal with problems and overcome them by yourself, however my mom, my father and my brother have been always there for me, they had to deal with my behaviour when I cried, when I was sad and when I was seeing everything blue. Thank you for the support you gave me every single time.

I would like to mention my husband Davide who, instead, lived my up and down mood 24/7 over all these years. I guess it must be hard let a PhD soul be calm when experiments failed after an entire day in the lab. Also, thank you so much for not letting me give up on writing the dissertation; the strength also came from a little one who felt my feelings for 9 months and especially during this writing period and is about to say “hello” to this world and so cheers to you baby girl, Gaia.

At last, I would like to thank myself for taking everything that happened in my life as a positive or negative example, to be better equipped in front of the same situations in the future. I think there is always a hidden reason why something happens in that moment and so I like to see it as a challenge and to think something better is coming.

Thank you all!

“In memory of

Prof. Dr. med. Detlef Zillikens

and Frau Stephanie Ollmann”

ABSTRACT

The recruitment of neutrophils into the skin is the hallmark of skin inflammation and their role in host defense against pathogen infection has been extensively studied in many disease contexts. The CLR dendritic cell-associated C-type lectin-2 (Dectin-2) is a single transmembrane protein that through the adaptive molecule Fcγ receptor IV (FcγRIV) contributes to host defense by activating myeloid cells upon binding to α-linked mannose-containing biomolecules expressed by certain fungi and bacteria. In the present study, I examine the role of Dectin-2 in the effector phase of the autoantibody-induced skin inflammation using a mouse model of epidermolysis bullosa acquisita (EBA). EBA is a prototypical example of blisters formation caused by autoantibodies (AAbs) against collagen 7 (COL7). The deposition of the AAbs at the base membrane zone, in the skin, leads to neutrophils recruitment inducing dermal-epidermal separation in the skin. Our findings describe the role of Dectin-2 and its cooperation with FcγRIV in driving neutrophils recruitment into the skin in antibody-transfer EBA mouse model. Accordingly, deficiency in Dectin-2 mice (*Clec4n*$^{-/-}$) confers a strong resistance to disease. Thus, C57BL/6J WT mice control manifest signs of EBA both at clinical and histopathological level, *Clec4n*$^{-/-}$ mice neither show signs of disease at the clinical level nor at histopathological level showing an intact dermal-epidermal junction. The leukotriene B4 (LTB_4) is a potent chemoattractant that leads to recruit more neutrophils to the inflamed tissue; *In vitro* studies in this work demonstrate a decrease in the response to LTB_4 release *Clec4n*$^{-/-}$ bone-marrow derived

neutrophils in response to the immune-complex activation. Contrary to the previous assumptions, ROS released by *Clec4n*$^{-/-}$ BM-derived neutrophils does not show a significant difference compared to C57BL/6J WT mice control. This suggests a divergence of signaling pathways leading to the production of LTB_4 and ROS requiring Dectin-2 mediated signaling for LTB_4 release but not ROS production in neutrophils. To narrow down the list of potential cell types required for Dectin-2 signaling mediated manifestation of EBA phenotype, I performed bone-marrow chimera (BMC) experiments, demonstrating that Dectin-2 expression on radiosensitive hematopoietic cells is required for AAb-induced skin inflammation. In support of this hypothesis, this study shows that indeed neutrophils activation mediated by Fc-receptor signaling is essential for the development of EBA as *in vivo* experiments using the passive EBA mouse model, and neutrophils specific FcαRIV deficient mice (*Fcgr4*$^{-/-}$) demonstrate complete protection from induction of antibody-transfer EBA, compared to normal manifestation of the disease observed matching MRP8-Cre-ires/GFP control mice. Overall, findings point towards a central role of Dectin-2 in neutrophils, and putative cooperative signaling with the FcγIV receptor to drive neutrophils-mediated skin inflammation.

ZUSAMMENSFASSUNG

Die Rekrutierung von Neutrophilen in die Haut ist das Kennzeichen der Hautentzündung, und ihre Rolle bei der Wirtsabwehr gegen Pathogeninfektionen wurde in vielen Krankheitszusammenhängen eingehend untersucht. Das CLR dendritische Zell-assoziierte C-Typ Lektin-2 (Dectin-2) ist ein einzelnes Transmembranprotein, das über das adaptive Molekül Fcγ-Rezeptor IV (FcγRIV) zur Wirtsabwehr beiträgt, indem es myeloische Zellen nach Bindung an α-verknüpfte mannosehaltige Biomoleküle aktiviert, die von bestimmten Pilzen und Bakterien exprimiert werden. In der vorliegenden Studie untersuche ich die Rolle von Dectin-2 in der Effektorphase der Autoantikörper-induzierten Hautentzündung anhand eines Mausmodells der Epidermolysis bullosa acquisita (EBA). EBA ist ein prototypisches Beispiel für eine Blasenbildung, die durch Autoantikörper (AAbs) gegen Kollagen 7 (COL7) verursacht wird. Die Ablagerung der AAbs in der Basismembranzone der Haut führt zur Rekrutierung von Neutrophilen, die eine dermale-epidermale Trennung in der Haut bewirken. Unsere Ergebnisse beschreiben die Rolle von Dectin-2 und seine Zusammenarbeit mit FcγRIV bei der Rekrutierung von Neutrophilen in die Haut im EBA-Mausmodell mit Antikörper-Transfer. Dementsprechend führt ein Mangel an Dectin-2-Mäusen (*Clec4n*$^{-/-}$) zu einer starken Resistenz gegen die Krankheit. Während Wildtyp-Mäuse C57BL/6J sowohl auf klinischer als auch auf histopathologischer Ebene Anzeichen von EBA aufweisen, zeigen *Clec4n*$^{-/-}$ Mäuse weder auf klinischer noch auf histopathologischer Ebene Krankheitsanzeichen und weisen eine intakte dermale-epidermale Grenzfläche auf. Leukotrien B4 (LTB_4) ist ein starkes

Chemoattraktionsmittel, das dazu führt, dass mehr Neutrophile in das entzündete Gewebe gelangen; In-vitro-Studien in dieser Arbeit zeigen eine Abnahme der LTB_4-Freisetzung von *Clec4n*$^{-/-}$ Neutrophilen aus dem Knochenmark als Reaktion auf die Aktivierung des Immunkomplexes. Im Gegensatz zu den früheren Annahmen zeigt die ROS-Freisetzung von *Clec4n*$^{-/-}$ Neutrophilen aus dem Knochenmark keinen signifikanten Unterschied im Vergleich zur C57BL/6J Kontrolle. Dies deutet auf eine Divergenz der Signalwege hin, die zur Produktion von LTB_4 und ROS führen, wobei Dectin-2 vermittelte Signale für die LTB_4-Freisetzung, nicht aber für die ROS-Produktion in Neutrophilen erforderlich sind. Um die Liste der potenziellen Zelltypen einzugrenzen, die für die durch Dectin-2-Signale vermittelte Manifestation des EBA-Phänotyps erforderlich sind, habe ich Knochenmarkschimären-Experimente durchgeführt und gezeigt, dass die Dectin-2-Expression auf strahlenempfindlichen hämatopoetischen Zellen für die AAb-induzierte Hautentzündung erforderlich ist. Zur Untermauerung dieser Hypothese zeigt diese Studie, dass die Aktivierung von Neutrophilen durch Fc-Rezeptor-Signale für die Entwicklung von EBA wesentlich ist, wie In-vivo-Experimente mit dem passiven EBA-Mausmodell zeigen. Neutrophilen-spezifische *Fcg4*-KO-Mäuse (*Fcgr4*$^{-/-}$) zeigen einen vollständigen Schutz vor der Induktion von EBA durch Antikörper-Transfer, verglichen mit der normalen Manifestation der Krankheit bei MRP8-Cre-ihres/GFP-Kontrollmäusen. Insgesamt deuten die Ergebnisse auf eine zentrale Rolle von Dectin-2 in Neutrophilen hin und auf eine mögliche Zusammenarbeit mit dem FcγIV-Rezeptor, um die von Neutrophilen vermittelte Hautentzündung zu steuern.

LIST OF ABBREVIATIONS

Abbreviation	Description
5LO	5-lipoxygenase
AAb	autoantibody
Ab; Abs	antibody; antibodies
AD(s)	autoimmune disease(s)
AIBD(s)	autoimmune blistering skin disease (s)
AP	alternative pathway
AUC	area under curve
BLT1	leukotriene receptor 1
BLT2	leukotriene receptor 2
BM	bone marrow
BMC	bone marrow chimera
BMDC(s)	bone-marrow derived dendritic cell(s)
BMDM(s)	bone-marrow derived macrophage(s)
BP	bullous pemphigoid
BPAG	bullous pemphigoid antigen
BSA	bovine serum albumin
C3	complement component 3
C5a	complement component 5 a
CL	classical pathway
Clec4n	C-type lectin domain family 4, member n
CLR(s)	c-type lectin receptor(s)
Col7	type VII collagen
CRD	carbohydrate recognition domain
CTLR(s)	C-type lectin-like receptors
CXCL	C-X-C chemokine ligand
CXCR	C-X-C chemokine receptor
DAMP	damage-associated molecular pattern(s)
DC(s)	dendritic cell(s)
DC-SIGN	dendritic cell-specific intercellular adhesion molecule-3-grabbing non-integrin
DDW	double distilled water
Dectin	dendritic cell-associated C-type lectin

DEJ	dermal-epidermal junction
DIF	direct immunofluorescence
DNA	deoxyriboNucleic Acid
Dsg	desmoglein
EBA	epidermolysis bullosa acquisita
ELISA	enzyme-linked immunosorbent assay
ER	endoplasmic reticulum
ESL	E-selectin ligand
FACS	fluorescence-activated cell sorting
Fc	fragment crystallizable region
FcγR(s)	Fc gamma receptor(s)
FLAP	5LO-activating-protein
FRET	fluorescence resonance energy transfer
G-CSF	granulocyte colony-stimulating factor
GM-CSF	macrophage colony-stimulating factor
GMP(s)	granulocyte–monocyte progenitor(s)
H_2O_2	hydrogen peroxide
H&E	hematoxylin and eosin
HAS	human serum albumin
HD(s)	hemidesmosome(s)
HEK	human embryonic kidney
HOCl	hypochlorous acid
HSC	hematopoietic stem cell
IC(s)	immuno-complex(es)
ICAM(s)	intercellular adhesion molecule(s)
IFAP300	intermediate filament associated protein
Ig	immunoglobulin
IHC	immunohistochemistry
IIF	indirect immunofluorescence
IL	interleukin
ITAM(s)	immunoreceptor tyrosine-based activation motif(s)
KO	Kockout
LAD	linear IgA disease
LD	lamina densa
LL	lamina lucida
LT(s)	leukotriene(s)
LTA_4	leukotriene A4

LTA_4H	leukotriene A4 hydrolase
LTB_4	leukotriene B4
LMPP(s)	lymphoid-primed multipotent progenitor(s)
LP	lectin pathway
Ly6G	lymphocyte antigen 6 complex locus G6D
ManLAM	lipoglycan mannose-capped lipoarabinomannan
MOI(s)	multiplicity of infection(s)
MMP	matrix metallopeptidase
MPP	multipotent progenitor
MΦ(s)	macrophage(s)
NADPH	nicotinamide adenine dinucleotide phosphate
NC	non-collagenous domain
NFκB	nuclear factor kappa-light-chain-enhancer of activated B cells
NOD(s)	cytoplasmic nod-like receptor(s)
$O_2^{\bullet -}$	superoxide anion
$OH^{\bullet}$	hydroxyl radical
OP	outer plaque
PAMP(s)	pathogen-associated molecular pattern(s)
PMN(s)	polymorphonuclear leukocytes
PRR	pathogen-recognition receptor(s)
qPCR	quantitative polymerase chain reaction
ROS	reactive oxygen species
RT	room temperature
SEM	standard error of mean
Syk	spleen tyrosine kinase
TLR(s)	toll-like receptor (s)
TNF-α	tumor necrosis factor - α
VCAM	vascular cell adhesion molecule
vWF	von Willebrand factor
WT	wild type

LIST OF FIGURES

Figure 1 Granulopoiesis of neutrophils. 2
Figure 2 Egression of neutrophils from the bone-marrow. 4
Figure 3 Mobilization of neutrophils to the inflamed tissue. 7
Figure 4 Host defense mechanisms for pathogen infection. 10
Figure 5 Schematic representation of the skin. 15
Figure 6 Clinical and histopathological features of EBA. 21
Figure 7 Animal passive transfer model. 24
Figure 8 Schematic illustration of passive EBA mouse induction. 35
Figure 9 Schematic representation of murine type VII collagen. 38
Figure10 Representative illustration of BM-derived neutrophils purity isolation. 49
Figure 11 Cell migration transwell setup. 56
Figure 12 Schematic illustration of bone marrow chimera generation. 58
Figure 13 *Clec4n*$^{-/-}$ mice are completely protected from EBA. 64
Figure 14 Expression of *Cxcl2* and *Il-1β*, was decreased at the mRNA level in *Clec4n* deficient mice. 66
Figure 15 Sera level of LTB_4, IL-6 and IL-17A in EBA. 67
Figure 16 Radiosensitive hematopoietic cells are responsible for EBA disease. 69
Figure 17 Bone-marrow cells are the drivers of disease progression in the EBA mouse model. 71
Figure 18 C57BL/6J WT BM-derived neutrophils express Dectin-2 upon 40 h GM-CSF stimulation. 72
Figure 19 C57BL/6J WT and *Clec4n*$^{-/-}$ BM-derived neutrophils migration towards C5a. 74
Figure 20 Dectin-2 is important for LTB_4 release by bone-marrow derived neutrophils upon IC stimulation. 76
Figure 21 *In vitro*: ROS release is Dectin-2 independent in both C57BL/6J WT and Clec4n$^{-/-}$ neutrophils. 78

Figure 22 The expression of the FcγRIV on neutrophils is important for their recruitment in the EBA pathogenesis. 80
Figure 23 Representative illustration of the expression of FcγIV receptor on neutrophils in mice blood after EBA induction 82
Figure 24 Representative illustration of the expression of FcγIV receptor on neutrophils in the bone marrow of mice after EBA induction 83
Figure 25 Representative illustration of the expression of FcγIV receptor on neutrophils in the lesional skin (ears) of MRP8-Cre-ires/GFP and FcγRIV neutrophils deficient mice after EBA induction 84
Figure 26 Dectin-2 interacts with FcγRIV to drive inflammation 86
Figure 27 FcγRIV is internalized after immune-complex stimulation 88

LIST OF TABLES

Table 1 C-type-lectin receptors: classification and ligands 11
Table 2 Abbreviations: Dsg-desmoglein; BPAG-bullous pemphigoid antigen. 19
Table 3 Scoring table used to calculate the disease severity in antibody-transfer EBA 36
Table 4 List of primers used in qPCR. 55

TABLE OF CONTENTS

ABSTRACT V

ZUSAMMENSFASSUNG VII

LIST OF ABBREVIATIONS IX

LIST OF FIGURES XII

LIST OF TABLES XIV

INTRODUCTION 1

1.1 GRANULOPOIESIS 1

1.2 NEUTROPHILS EGRESSION FROM THE BONE MARROW 3

1.3 NEUTROPHIL RECRUITMENT TO AN INJURED TISSUE 4

1.4 C-TYPE LECTINS IN IMMUNITY AND HOMEOSTASIS 8

1.4.1 THE ROLE OF DECTIN-2 IN HOST DEFENCE 11

1.4.2 DECTIN-2 ANTIGEN RECOGNITION THROUGH FCΓ RECEPTOR IV 13

1.5 THE SKIN STRUCTURE AND FUNCTION 14

1.6 AUTOIMMUNITY AND AUTOIMMUNE DISEASES 17

1.6.1 AUTOIMMUNE BULLOUS SKIN DISEASE 18

1.6.2 EPIDERMOLYSIS BULLOSA ACQUISITA (EBA) 20

1.7 EXPERIMENTAL MODEL FOR EBA 22

1.8 MECHANISMS MEDIATING AUTOANTIBODY-INDUCED SKIN INFLAMMATION AND TISSUE INJURY IN EBA 24

1.9 AIM OF THE PRESENT STUDY 26

MATERIALS AND METHODS 28

2.1 MATERIALS 28

2.1.1 CHEMICALS 28

2.1.2 COMMERCIAL BUFFERS & SOLUTIONS 29

2.1.3 ANTIBODIES 29

2.1.4 KITS AND OTHERS 31

2.1.5 LABORATORY EQUIPMENT 31

2.1.6 DISPOSABLE MATERIALS 32

2.1.7 MICE 33

2.2 METHODS 35
2.2.1 INDUCTION OF EXPERIMENTAL PASSIVE EBA MOUSE MODEL 35
2.2.1.1 SCORING DISEASE SEVERITY IN ANTIBODY TRANSFER EBA 35
2.2.1.2 GENERATION OF AFFINITY PURIFIED RABBIT ANTI-MURINE COL7C IGG 36
2.2.1.3 EXPRESSION OF RECOMBINANT NC-1 PEPTIDE AND IMMUNIZATION OF RABBITS 37
2.2.1.4 AFFINITY COLUMN CHROMATOGRAPHY FOR PURIFICATION OF TOTAL RABBIT IGG 37
2.2.1.5 EXPRESSION OF RECOMBINANT MCOL7C-HIS TAG PROTEIN 39
2.2.1.6 GENERATION OF MCOL7C AFFINITY CHROMATOGRAPHY COLUMN 39
2.2.1.7 PURIFICATION OF SPECIFIC RABBIT ANTI-MCOL7C IGG 40
2.2.2 *IN VITRO* ISOLATION OF BONE-MARROW DERIVED NEUTROPHILS (BM-NEUTROPHILS) 40
2.2.3 *IN VITRO* REACTIVE OXYGEN SPECIES (ROS) ASSAY 42
2.2.4 *IN VITRO* QUANTITATIVE DETERMINATION OF LEUKOTRIENE B4 (LTB_4) CONCENTRATION IN BM-DERIVED NEUTROPHILS SUPERNATANTS. 42
2.2.5 *IN VITRO* QUANTITATIVE DETERMINATION OF INTERLEUKIN 6 (IL-6) CONCENTRATION IN BM-DERIVED NEUTROPHILS SUPERNATANTS. 44
2.2.6 *IN VITRO* QUANTITATIVE DETERMINATION OF INTERLEUKIN 17A (IL-17A) CONCENTRATION IN BM-DERIVED NEUTROPHILS SUPERNATANTS. 45
2.2.5 FLOW CYTOMETRY 46
2.2.5.1 *IN VIVO* CHIMERA EXPERIMENT AND PASSIVE EBA SAMPLES 47
2.2.5.1.1 PERIPHERAL BLOOD SAMPLE PREPARATION FOR FLOW CYTOMETRY 47
2.2.5.1.2 LESIONAL SKIN TISSUE SAMPLE PREPARATION FOR FLOW CYTOMETRY 47
2.2.5.1.3 BM-DERIVED NEUTROPHILS SAMPLE PREPARATION FOR FLOW CYTOMETRY 48
2.2.5.1.4 BM-DERIVED NEUTROPHILS PURITY ANALYSIS 48
2.2.6 *IN VIVO* PASSIVE EBA IN NEUTROPHIL SPECIFIC FCΓRIV CONDITIONAL KNOCKOUT MICE 49
2.2.6.1 PERIPHERAL BLOOD SAMPLE PREPARATION FOR FLOW CYTOMETRY 49
2.2.6.2 LESIONAL SKIN TISSUE SAMPLE PREPARATION FOR FLOW CYTOMETRY 50
2.2.7 *IN VITRO* BM-DERIVED NEUTROPHILS STAINING 50
2.2.7.1 *IN VITRO* BM-DERIVED NEUTROPHILS EXTRACELLULAR STAINING 51
2.2.7.2 *IN VITRO* BM-DERIVED NEUTROPHILS INTRACELLULAR STAINING 51
2.2.8 TRIZOL RNA ISOLATION FROM TISSUES AND CELLS 52
2.2.8.1 FIRST STRAND COMPLEMENTARY DNA (CDNA) SYNTHESIS 53
2.2.8.2 REAL-TIME PCR (QPCR) AMPLIFICATION OF FIRST STRAND CDNA 54
2.9 *IN VITRO* CELL MIGRATION 55
2.10 BONE MARROW CHIMERA MOUSE MODEL 56
2.10.1 GENERATION OF BONE MARROW CHIMERA 57

2.11 Skin histopathology 59
2.11.1 Hematoxylin and eosin (H&E) staining 59
2.12 Immunofluorescence microscopy 59
2.12.1 Direct immunofluorescence (DIF) microscopy 60
2.12.2 Indirect immunofluorescence (IIF) microscopy 60
2.13 IMMUNOHISTOCHEMISTRY 60
2.13.1 Immunohistochemistry of complement 3 staining 61
2.13.2 Immunohistochemistry of mCOL7 IgG staining 62
2.14 Statistical analysis 62

RESULTS 63

3.1 Requirement of Dectin-2 for the induction and progression of antibody transfer EBA 63
3.1.1 *Clec4n*$^{-/-}$ mice are protected from induction of antibody-transfer EBA 63
3.1.1.1 Downregulation of Cxcl2 and Il-1ß are low expressed in *Clec4n*$^{-/-}$ mice in passive EBA model 65
3.1.1.2 Sera levels of LTB_4 are decreased in *Clec4n*$^{-/-}$ mice in EBA 67
3.1.2 Expression of Dectin-2 on radiosensitive hematopoietic cells is indispensable for manifestation of EBA in mice 68
3.1.2.1 Bone-marrow cells are the drivers of disease progression in the EBA mouse model 70
3.2 Studying the biological effects of Dectin2 on neutrophils functions 71
3.2.1 Neutrophils acquire Dectin-2 expression upon exposure to GM-CSF 71
3.2.2 Neutrophils migration towards the chemoattractant C5a is Dectin-2-independent 73
3.2.3 Dectin-2 is important for the release of LTB_4 by neutrophils to drive inflammation 74
3.2.4 Neutrophils ROS release is Dectin-2 independent 77
3.3 Cooperation of Dectin2 and FcγRIV on neutrophils 78
3.3.1 Neutrophils specific FcγRIV-KO mice are completely protected from induction of antibody-transfer EBA 78
3.3.1.1 Neutrophils require the cooperation between FcγIV receptor and Dectin-2 to elicit their function in EBA 81
3.3.2 Dectin-2 collaborates with FcγRIV to induce the release of ROS but not of LTB_4 from neutrophils 85
3.3.3 Dectin-2 enhances FcγRIV-triggered immune responses of neutrophils *IN VITRO* 86

DISCUSSION 89

4.1 Requirement of Dectin-2 for the progression of EBA 89

4.2 Biological effects of Dectin2 on neutrophils functions 92

4.3 Neutrophils require the cooperation between FcrIV receptor and Dectin-2 to elicit their function in EBA 94

4.4 Dectin-2 collaborates with FcrRIV to release ROS but not LTB_4 from neutrophils 96

4.5 Dectin-2 is expressed only when neutrophils are primed 97

4.6 Dectin-2 is expressed intracellularly upon recognition of autoantibodies 98

4.7 FcrRIV is expressed intracellularly when interacting with Dectin-2 98

CONCLUSION 99

LITERATURE 102

INTRODUCTION

Humans are exposed every day to a million of potential pathogens through contact, ingestion, and inhalation. Subsequently, these organisms enter our body and cause infections or diseases that arise when the immune system is compromised. The ability of the immune system to avoid the spread of infection is, mainly due to the adaptive response that has already encountered and therefore remember the specific pathogen to be destroyed again. However, the process by which the adaptive immune system recognizes a new pathogen is slow and can take weeks before a response is effective. Despite this, the first critical hours and days, during which our body has its first exposure to a new organism, are controlled by the innate response that protect us from infections (Janeway and Medzhitov R. 2002). The innate immune system comprises different components such as physical barriers (skin, epithelial membrane surfaces, mucus), phagocytes (neutrophils, monocytes, macrophages), serum proteins (e.g., lectins, complement system), cells that produce cytokines and inflammatory mediators (e.g., mast cells, macrophages, natural killer). Once the interaction host-pathogen occurs, an inflammatory cascade starts to generate different mechanisms to finally destroy the organism (Beutler, 2009). In this study, I focused my attention on neutrophils and their role in the innate immune response upon inflammation in autoimmune skin disease, specifically in the Epidermolysis bullosa acquisita (EBA). As neutrophils are the most abundant white blood cells and are often the first cells to migrate to the site of an injured tissue, it was hypothesized they may play an essential role in the manifestation of the disease in its earliest phase.

1.1 Granulopoiesis

Granulopoiesis is the process by which hemopoietic progenitor cells develop into neutrophils, basophils, and eosinophils under the influence of various growth factors and chemokines. Discovered for the first time in 1880 by Paul Ehrlich (Amulic et al., 2012), neutrophils are the most abundant white blood cells in humans and mice.

They are also known as polymorphonuclear (PMN) leukocytes produced in the bone marrow, from hematopoietic stem cells, around 10^{11} every day (Görgens et al., 2013). PMNs have a short lifespan dying after one day. Then, they are cleared by macrophages through their phagocytosis function. During the granulopoiesis process, the hematopoietic stem cells differentiate into multipotent progenitor (MPP) cells that form the lymphoid-primed multipotent progenitors (LMPPs), which differentiate into granulocyte–monocyte progenitors (GMPs). Under control of the granulocyte colony-stimulating factor (G-CSF), the GMPs is converted into the myeloblast that undergoes further differentiation steps from promyelocyte, myelocyte, metamyelocyte, band cell, and finally a mature neutrophil (von Vietinghoff and Ley 2008), (Figure 1). Also, the neutrophil nucleus changes its morphology from a round to a lobulated shape. When PMNs are mature they contain granules and vesicles important for destroying the pathogens. There are primary (azurophil) granules detectable at the myeloblast and promyelocyte stage; the secondary (specific) granules present at myelocyte and metamyelocyte stages and the tertiary (gelatinase) granules found at the band stage. The vesicles are presented only when neutrophils are mature. The granules, themselves contain many enzymes such as defensins, elastase, myeloperoxidase, matrix metalloproteinases and cathelicidins (Häger et al., 2010). In homeostasis conditions, the interaction between the ligand C-X-C motif chemokine 12 (CXCL12), that is expressed from the BM stromal cells and the chemokine receptor C-X-C Motif Chemokine Receptor 4 (CXCR4), expressed on the neutrophil membrane, allows the retention of the progenitor cells in the bone marrow.

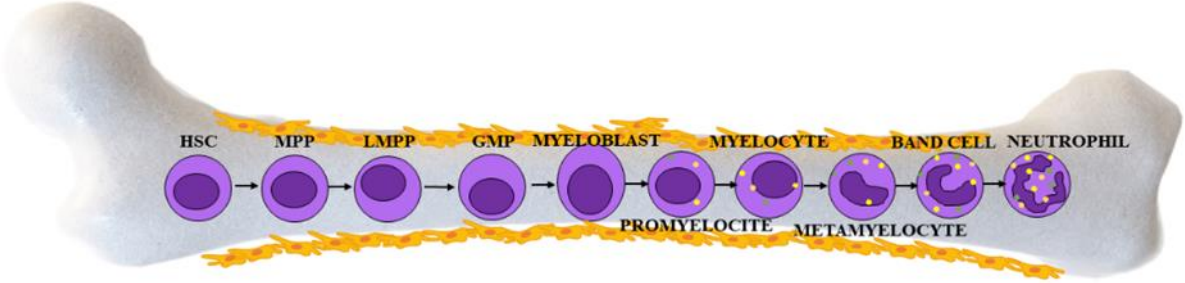

Figure 1 Granulopoiesis of neutrophils.

Schematic illustration of the generation of neutrophils in the bone-marrow. The continuous renew hematopoietic stem cell (HSC) forms the multipotent progenitor (MPP) cell. Subsequently, the

formation of the lymphoid-primed multipotent progenitor (LMPP) differentiates into granulocyte-monocyte progenitor (GMP). This latter turns into myeloblast, under the granulocyte colony-stimulating factor (GS-CSF), that follows the different develop stages that include promyelocyte, myelocyte, metamyelocyte, band cell and finally a neutrophil.

1.2 Neutrophils egression from the bone marrow

The egress of PMNs from the bone marrow (BM) to the blood circulation is promoted by the G-CSF. Mature neutrophils migrate across the sinusoidal endothelium through a process named “transcellular migration” during which they express CXCR4, a G-protein coupled receptor, at low level. In the meantime, the BM stromal cells produce the CXCL12 that is specific for CXCR4 and the interaction CXCR4-CXCL12 is important for the retention of PMNs in the marrow environment. G-SCF has an inhibitory effect on retaining neutrophils by interfering with the CXCL12-CXCR4 interaction and, therefore by reducing the expression of CXCL12 (Petit et al., 2002; Semerad et al., 2005) and CXCR4 (Kim et al., 2006). Mobilization from the bone marrow is promoted by the interaction of adhesion molecules expressed by neutrophils, the very late antigen-4, VLA-4, CD49d/CD29 (α4β1 integrin), the BM stromal cells and vascular cell adhesion molecule-1 (VCAM-1 or CD106). The interaction is, additionally, regulated by a cytokine arrange that includes the interleukin 23 (IL-23) produced by phagocytes and interleukin 17 (IL-17) created by T lymphocytes. In this process, both macrophages and dendritic cells phagocytose apoptotic PMNs (Gordy et al., 2011; Jiao et al., 2014) leading to a decrease of IL-23 (Stark et al., 2005) which in turn controls the expression of IL-17 by T lymphocytes (Gaffen et al., 2014). This latter is important to promote the granulopoiesis and neutrophils release, therefore low levels of IL-17 (von Vietinghoff and Ley, 2008) allows a steady-state of PMNs by reducing the expression of G-CSF (Figure 2). Also, neutrophils themselves release IL-17 attracting IL-17 producing T lymphocytes and, in turn, T helper (h) 17 cells recruit more PMNs. During their quiescent phase, neutrophils are limited to their antimicrobial function and appear to change their phenotype (aged neutrophils) in the absence of inflammation (Adrover et al., 2016). In the bloodstream, under physiological conditions, neutrophils are found to be less than 2% and they are cleared at the end of their resting phase in the spleen, liver, and the bone marrow (Rankin, 2010).

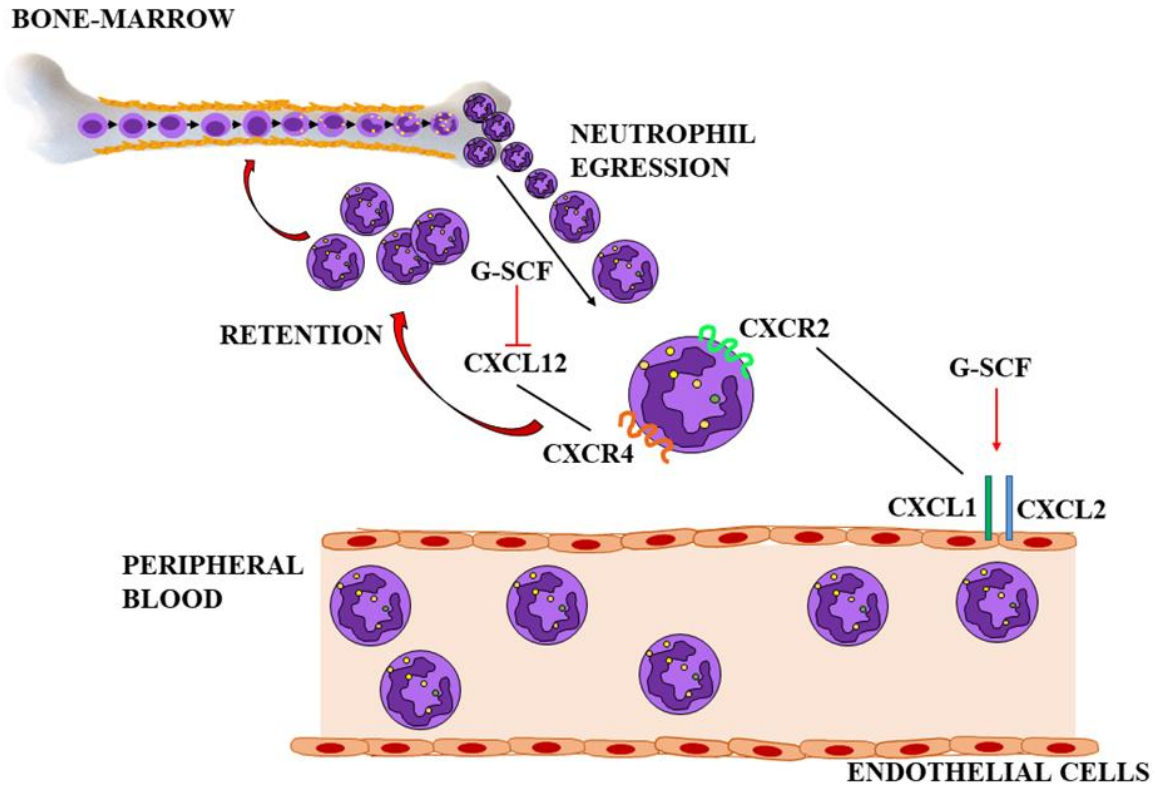

Figure 2 Egression of neutrophils from the bone-marrow.

Neutrophils mobilization from the bone-marrow is promoted by G-CSF which relies on CXCR2 and CXCR4. Neutrophil release is controlled by signals from CXCR4 and its ligand CXCL12 which retain neutrophils in the BM niche, while CXCR2 and its ligands CXCL1 and CXCL2 mediate the egression from the BM.

1.3 Neutrophil recruitment to an injured tissue

Mobilization of neutrophils to the inflamed tissue is mediated by the release of chemokines in the peripheral blood to guide the PMNs migration into peripheral tissue. The extravasation process consists of four steps: rolling, firm adhesion, trans endothelial migration (diapedesis) and chemotactic migration. In the inflamed site, the disruption of homeostasis is recognized by resident cells, like macrophages and mast cells, or stromal cells but it can be sensed, also from pathogen-associated molecular pattern (PAMPs) and damage-associated molecular pattern (DAMPs) molecules, which activates these sentinel cells to release pro-inflammatory mediators like, interleukin 1ß (IL-1β) and tumor necrosis factor (TNF), and neutrophil-active chemoattractants (e.g., chemokines and lipid mediators) (Arancibia et al., 2007). These mediators initiate the recruitment of neutrophils into

the tissue by diverse actions. To capture rolling PMNs, activated endothelial cells express adhesion molecules, such as P- and E- selectins, and members of integrins family like vascular cell adhesion molecules (VCAMs) and intercellular adhesion molecules (ICAMs) (Borregaard, 2010). These molecules interact with ligands expressed on neutrophils, the P-selectin ligand 1 (PSGL-1 or CD162), L-selectin (CD62L), E-selectin ligand 1 (ESL-1) and the cell adhesion receptor CD44. The process slows PMNs transit in shear flow and, depending on the interaction, the adhesion molecules ICAM-1 (CD54) and ICAM-2 (CD102) present on activated endothelial cells bind to their ligands, β2 integrins lymphocyte function associated antigen 1 (LFA-1, αLβ2, CD11a/CD18) and macrophage-1 antigen Mac-1 (αMβ2, CD11b/CD18) expressed on neutrophils (Harris et al., 2000). The next step comprises the transmigration of neutrophils via paracellular or transcellular route, therefore PMNs can migrate through the junctions between the endothelial cells or directly through an endothelial cell. In addition, chemokines released from both neutrophils and endothelial cells, the C-X-C Motif Chemokine Receptor 2 (CXCR2) particularly, contribute to the transmigration of neutrophils (Reutershan et al., 2006). The process by which neutrophils escape the blood vessel is known as diapedesis. After crossing the endothelial barrier, neutrophils must penetrate the perivascular basement membrane that is constituted by, mainly, laminin and collagen IV. To break through, PMNs release many proteases such as elastase, matrix metallopeptidase 8 (MMP-8), matrix metallopeptidase 9 (MMP-9), and matrix metallopeptidase 25 (MMP-25) that facilitate the penetration (Stefanidakis et al., 2004). However, the specific way of how neutrophils penetrate the basement membrane is still not clear. In the last step called “chemotactic migration”, neutrophils migrate into the inflammatory tissues following different gradients of many chemoattractants released by host or pathogen. Recruitment of PMNs into tissue, in response to an infection, requires them to exert their maximal functions, therefore they must be pre-instructed by internal or external agents. This process, also known as “priming”, is a remarkable key event whereby PMNs response to any stimulus is notably increased by a prior exposure to a priming agent (El-Benna et al., 2008). It has been described that a variety of agents can prime neutrophils: chemokines, cytokines, chemoattractants can all work together to build a strong pro-inflammatory network to enhance neutrophils antimicrobial activity. Specifically, one of the cytokines that primes PMNs is the Granulocyte-macrophage colony-

stimulating factor (GM-CSF), that induces the differentiation and proliferation of myeloid cells in the BM and, also the migration of these cells to the site of inflammation. Once in the inflamed tissue, exocytosis of neutrophil granules may result in high expression of surface receptors such as integrin alphaM (CD11b), lymphocyte antigen 6 complex locus G6D (Ly6G) and Fc-gamma receptors (FcγRs) (Borregaard et al., 1994). Conversely, L-selectin (CD62L) surface expression is diminished via enzymatic shedding (Walcheck et al., 1996). It was shown that chemoattractants act to initiate a cascade constituted from lipid-cytokine-chemokine that promote the recruitment of leucocytes in inflammation (Sadik et al., 2012). LTB_4 originates from the conversion of arachidonic acid to leukotriene A_4 (LTA_4) by 5-lipoxygenase (5LO) and 5LO-activating-protein (FLAP). LTA_4 is further converted into LTB_4 by LTA4 hydrolase (LTA_4H), or into cysteinyl leukotrienes (Peters-Golden et al., 2005). It is characterized by two receptors: leukotriene B4 receptor 1 (BLT1) with high affinity for LTB_4 and the bound LTB_4-BLT1 leads neutrophils adhesion to endothelial cells, degranulation of lysosomal enzymes, generation of superoxide, transmigration, and inhibition of apoptosis (Barcellos-de-Souza et al., 2012; Tager et al., 2000); In contrary, leukotriene B4 receptor 2 (BLT2) has low affinity for LTB_4 and was previously shown to mediate distinct biological roles from the BLT1 receptor (Yokomizo, 2014). The biological function of LTB_4 depends on the organ involved: patients with asthma, compared to the healthy one, were examined by Andrew Higham et al., who measured the level of the lipid mediator on the processed sputum neutrophil without finding any correlation in asthma patients (Higham, et al., 2016) These results suggested that LTB_4 was not the dominant mediator for neutrophilic inflammation in asthma; in contrary, in a mouse model of atopic dermatitis the importance of LTB_4 was demonstrated to drive the recruitment of neutrophils to the skin. In this model, accumulation of PMNs was found abundant in the dermis of tape-stripped mouse skin compared to unscratched skin. Thus, levels of LTB_4 and its receptor BLT1 were significantly increased at the mRNA levels compared to the control (Oyoshi et al., 2012). To increase the ability of killing pathogens, primed neutrophils stimulate the nicotinamide adenine dinucleotide phosphate-oxidase/Nox2 (NADPH) complex to generate the reactive oxygen species (ROS) during the respiratory burst. NADPH oxidase transfers its electron to the oxygen to form the superoxide anion ($O^{2\bullet-}$) and, subsequently to form the

hydroxyl radical (OH•). The superoxide anion is then converted to the hydrogen peroxide (H_2O_2) by the superoxide dismutase enzyme to convert it to the final product hypochlorous acid (HOCl) through the myeloperoxidase enzyme. Although these compounds together determine an efficient mechanism to kill pathogens, in turn, also this latter have developed skills to escape the toxicity: through an "intrinsic" resistant mechanism bacterium, for example, are able to detoxify the radical species into less damaging by-products or, moreover through an "extrinsic" mechanism, they can directly suppress ROS production by interfering with the NADPH oxidase activity (Fischer et al., 2016) (Figure 3).

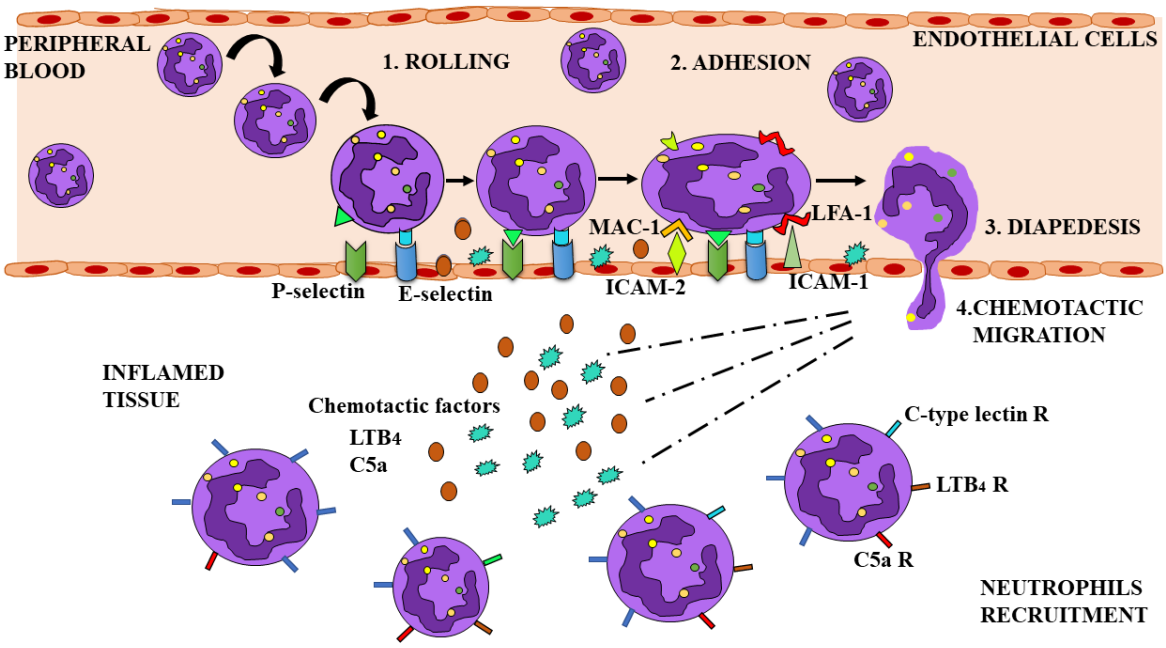

Figure 3 Mobilization of neutrophils to the inflamed tissue.

Chemotactic factors released from endothelial cells promote neutrophils migration to the injured tissue. In the blood neutrophils start to express to roll by binding the selectins, adhere onto the endothelium through ICAMs, MAC-1 and LFA-1 passing through the endothelial barrier following the gradient formed by the chemotactic factors, LTB_4 and C5a. Consequently, more neutrophils are recruited to defeat the insult.

As already mentioned above, production of chemoattractants by neutrophils to maximize host defence against pathogens is promoted by the recognition of receptors expressed on the PMNs surface membrane. The interaction receptor-pathogen initiates the transmission of a signal that spreads downstream to activate all the processes indispensable for the release of the pro- and inflammatory factors. Therefore, it is important to gain a detail attention to the variety of receptors known as pathogen-recognition receptors (PRRs) (Takeuchi and Akira, 2010) expressed on different immune cells for an early detection of the pathogen. PRRs includes the Toll-like receptors (TLRs), c-type lectin receptors (CLRs) and cytoplasmic nod-like receptors (NODs). They can recognize two classes of molecular patterns of infectious pathogens: pathogen-associated molecular patterns (PAMPs) and damage-associated molecular patterns (DAMPs). In this study, I will refer to the family members of c-type lectin receptors and their role in the innate immune response upon inflammation.

1.4 C-type lectins in immunity and homeostasis

Originally, the term was coined to discuss a group of animal proteins that could recognize carbohydrates. CLRs are a superfamily of more than 10,000 transmembrane proteins also known as PRRs that detect PAMPs, self-antigen or DAMPs (Hadebe et al., 2018). In mammals, CLRs are implicated in numerous physiological functions. They can be soluble proteins and can function as a growth factor, opsonins, antimicrobial proteins, or transmembrane proteins that, through a signalling pathway, modulate cellular, developmental, homeostatic, and immunological responses (Graham and Brown, 2009). However, there are several distinct patterns of evolution of CLRs like the absence of simple orthology in humans and mice. For example, in the collectin family mice express two different forms of mannose-binding protein while in humans there is only one functional gene. Moreover, human genome encodes two closely related proteins: the Dendritic Cell-Specific Intercellular adhesion molecule-3-Grabbing Non-integrin (DC-SIGN) and the Dendritic Cell-Specific Intercellular adhesion molecule-3-Grabbing Non-integrin receptor DC-SIGNR (L-SIGN) while there are eight genes for mouse SIGN proteins, none of which is organized in the same way as DC-SIGN and DC-SIGNR with

extended neck domains between the carbohydrate recognition domain (CRD) and the membrane. Despite this, CLRs properties in both humans and mice can be considered similar and so it is possible to use mice as a model that reflects the human one (Drickamer and Taylor, 2015). CLRs have a unique fold adaptable to many uses. It is a compact domain of 110-130 amino acid residues with a double-looped, two-stranded antiparallel β-sheet formed by the amino-and carboxy-terminal residues connected by two α-helices and a three-stranded antiparallel β-sheet. The domain has two conserved disulphide bonds up to four sites for Ca^{2+} depending on the lectin. It comprises at least one CRD that binds the sugar in a Ca^{2+}-dependent manner. Along the years, there were many studies on new molecules that have been identified in terms of the structures they have, what are their functions and so there was no doubt that CLRs changed their functions through evolution and no longer necessarily recognize only sugars. Despite this, the new term became C-Type Lectin-Like Receptors (CTLRs). CLRs are subdivided into 17 subgroups (Kerrigan et al., 2011) involved in many cellular functions like, for example, cell adhesion, complement activation, phagocytosis and innate immunity primarily expressed on myeloid cells such as monocytes, macrophages, dendritic cells (DCs) and neutrophils. Most of them, for example the dendritic cell-associated C-type lectin- (Dectin-1), a β-glucan receptor that belongs to group V, requires clustering that leads to the activation of the spleen tyrosine kinase (Syk) via immunoreceptor tyrosine-based activation motif (ITAM) in the cytoplasmic region of Dectin-1. The signal is made by the bound of Dectin-1 to the β-glucans on fungi, however, type II, IV and V which are present on immune cells, including Mincle and dendritic cell-associated C-type lectin-2 (Dectin-2) lack intrinsic signalling domains but activate Syk through the adaptive molecule such as FcγR (Kerscher et al., 2013). Therefore, the FcɣR chain allows the initiation of a cascade via ITAM that is present in their cytoplasmic tail and activates the SYK family kinases to catalyse the transfer of phosphate groups lead to the formation of the Card9/Bcl10/Malt complex. Subsequently, a downstream signal activates the nuclear factor kappa-light-chain-enhancer of activated B cells (NF-κB) pathway that is necessary to the final production of inflammatory and pro-inflammatory factors like chemokines, cytokines that are important for the recruitment of more proteins during an inflammation (Chiffoleau, 2018) (Figure 4). Based on CRD homology, even though they are present on different cells and have different function, CLRs overlap in ligand

recognition. The reason can be attributed to the number of their Ca^{2+} binding sites: langerin has only Ca-2 binding site, whereas DC-SIGN has Ca-1 and Ca-3 binding sites and this latter present more stability to the ligand recognition (van den Berg, 2012). As mentioned above, host defence by different immune cells starts with the innate response where mostly neutrophils are abundant in the early phase. The importance of neutrophils recruitment and, consequently the expression of, in this specific case PRRs in injured tissue may lead to a better understand of their role. It has been demonstrated that Dectin-2 is expressed on primed neutrophils and can exert different roles in experimental mouse models and *in vitro*.

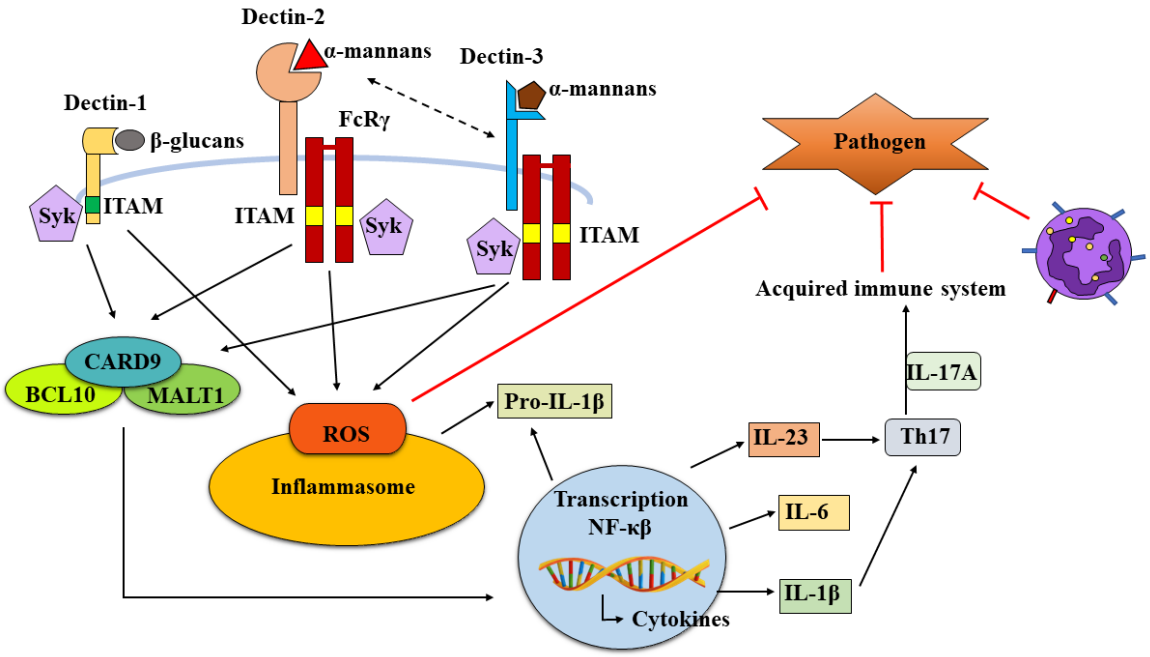

Figure 4 Host defense mechanisms for pathogen infection.

Upon b-glucan binding, Dectin-1 recruits Syk to the ITAM, following the activation of the CARD9-BCL10-MALT1 (CBM) complex. ROS production is also induced in a Syk-dependent manner, resulting in fungal killing in inflammasomes. Like Dectin-1, Syk is recruited to the ITAM of the FcRγ chain upon a-mannan binding to Dectin-2 and activates the CBM complex downstream. Then, the CBM complex activates NF-κB to activate cytokine genes including pro-IL-1b, IL-23 and IL-6. IL-23 and IL-1b promote the differentiation of Th17 cells, and IL-17A from Th17 cells recruits neutrophils to the inflammatory sites to contribute to the eradication of the pathogen. A small amount of IL-12 is also produced through activation of NF-κB and induces Th1 cell differentiation.

1.4.1 The role of Dectin-2 in host defence

Dectin-2 (gene symbol, *Clec4n*) is a transmembrane protein that belongs to the group II among the 17 groups of CLRs (table 1). It was discovered for the first time in Langerhan cells and subsequently shown to be expressed on a variety of myeloid cells like, monocytes, macrophages, DC and neutrophils. It comprises one extracellular carbohydrate domain that appears to have specificity for high mannose such as Man9GlcNAc2 and Man8GlcNAc2 (Eamon et al., 2006) and, therefore, can recognize many pathogens like *Candida albicans*, *Saccharomyces cerevisiae*, *Mycobacterium tuberculosis*, house dust mite allergens and many more (Kerscher et al., 2013). It is important to highlight the fact that a single C-type lectin role, in immunity, is not limited to one specific target but it can cover multiple responses to different pathogens.

Table 1 C-type-lectin receptors: classification and ligands

C-lectin-like receptors	Type	Group	Pathogen-associated molecular patterns
Mannose receptor	I	VI	Mannose, fucose, N-acetylglucosamine
DC-SIGN	II	II	Mannin
Langerin	II	II	Mannose, fucose, N-acetylglucosamine, mannin
MGL	II	II	GalNAc
ASGP-R	II	II	Galactose
Collectins	II	III	Mannose, fucose, N-acetylglucosamine
Dectin-1	II	V	β-Glucan
Dectin-2	II	VI	High-mannose oligosaccharide

Also, they can exert their function alone or with the interaction of other CLRs. For example, *C. albicans*, a regular commensal in the skin, has a fungal cell wall composed mainly of polysaccharides such as α- and β-mannans (components of mannoproteins), β-glucans, and chitin. When a lethal dose of candida was intravenously (i.v.) injected in C57BL/6J WT and Dectin-2 deficient (*Clec4n*$^{-/-}$) mice, after 28 days it was shown that *Clec4n*$^{-/-}$ mice were more susceptible to the infection (Daniela C Ifrim et al., 2016). The results suggested the importance of Dectin-2 in the recognition of the fungal for host defence. Another study conducted in C. albicans hyphae confirmed the constant formation of a heterodimers between

Dectin-2 and Dectin-3 (gene, *Clec4d*) to confer high sensitivity to the host cell for binding α-mannans more efficiently. In this model, Le-Le Zhu et. al., have stimulated RAW.264.7 cells stably expressing, singularly Dectin-2, Dectin-3 or together with *C. albican* hyphae at different multiplicity of infection (MOIs). By monitoring the hyphae-induced p65 (nuclear factor NF-kappa-B p65 subunit) nuclear translocation they have found that heterodimers of Dectin-2 and the dendritic cell-associated C-type lectin-3 (Dectin-3) have induced more p65 nuclear translocation than their homodimers (Le-Le Zhu et al., 2013). Dectin-2 has also been involved in the generation of an immune response when associated with Dectin-1 against the dermatophytosis, a common mycosis that compromised keratinized tissues. In this model, a soluble Fc chimera were constructed and, subsequently their binding to the fungi were investigated by fluorescence activated cell sorting (FACS) analysis. Both receptors have bound to the strain. Moreover, by analysing bone-marrow derived dendritic cells (BMDCs) incubated with dermatophytosis fungi has shown a rapid production of cytokines in a Dectin-1 and Dectin-2 dependent fashion. In addition to fungi, Dectin-2 plays a role in the recognition of the *Mycobacterium tuberculosis* that produces the lipoglycan mannose-capped lipoarabinomannan (ManLAM) which was identified as a ligand of Dectin-2 when used as a purified molecule (Decout et al., 2018; Yonekawa et al., 2014). Another *in vivo* study was conducted on C57BL/6J WT and Dectin- 2 deficient mice by investigating the role of Dectin-2 in skin wound healing process. Results have shown a significant acceleration of wound closure in Dectin-2 deficient mice compared to the C57BL/6J WT. In addition, immunohistochemical analysis have shown an increase of Dectin-2 in neutrophils infiltration at the early phase after wounding (Miura et al., 2019). Neutrophils are best known for their remarkable role in host defence. Dectin-2 expressed on primed PMNs seems to play different roles as shown above. The mechanism by which Dectin-2 recognizes microbes, viruses and autoantibodies present in the skin, lungs and other organs is still not well characterized. However, it is hypothesized that after recognition of its ligands, Dectin-2 signals through the molecule FcγR to subsequently produce pro- and inflammatory factors in damaged tissues.

1.4.2 Dectin-2 antigen recognition through Fcγ receptor IV

Neutrophils express a variety of receptors that enable to respond to inflammatory stimuli and danger signals. Among these, the FcγRs family stand out. In humans there are six different classes of FcγRs: FcγRI/CD64, FcγRIIA/CD32A, FcγRIIB/CD32B, FcγRIIC/CD32C, FcγRIIIA/CD16A, and FcγRIIIB/CD16B (Bruhns et al., 2009). In mice there are, four classes of FcγRs: FcγRI, FcγRIIB, FcγRIII and a novel, γ chain-dependent, activating IgG Fc receptor, FcγRIV (Nimmerjahn et al., 2005). They are all activating receptors, except for FcγRIIB with its inhibitory function both in human and mouse species (Ono et al., 1996). One of the factors that influence the affinity is the type of IgG subclasses (Scapini and Cassatella, 2014). For this reason, a single molecule of IgG cannot bind to most of the Fcγ receptors, however when IgG molecules form immune-complexes (antigen-antibody), they have a decrease in the affinity of the interaction with Fcγ receptors. Therefore, only immune complexes can facilitate the cross-linking of Fcγ receptors require for an activation of a cell in response to a stimulus. In mice, mouse IgG subclasses mediate selective FcγR engagement, for example IgG2a isotype antibodies preferentially interacts with FcγRIV; in contrary, IgG1 antibodies preferentially interact with the inhibitory antibody, FcγIIB (Bruhns and Jonsson, 2005). This dictates the *in vivo* outcome over the antibody responses whereas mouse IgG2a antibodies interact with activating FcRs to mediate the pro-inflammatory activities or the IgG1 antibodies that interact with inhibitor FcRs to mediate the anti-inflammatory activities. As described above, Dectin-2 couples to FcγR for an optimal expression and function. It has been demonstrated that bone-marrow derived macrophages (BMDMs) lacking FcRγ itself, Dectin-2 or mincle, were impaired in migration, engulfment, and phagosome maturation in fungal infection (Haider et al., 2019). Thus, many studies have been performed in fungal infection where Dectin-2 plays an antimicrobial activity by coupling FcγRs; however, the role of Dectin-2 in response to autoantibodies in autoimmune skin disease has not yet been characterized.

1.5 The skin structure and function

The skin covers the entire body surface and in correspondence of the natural orifices is in continuation with the mucous membranes that cover the internal cavities of the various organ systems (digestive, respiratory, urogenital) with everything regarding the structural organization of the skin and epidermis. Along with the skin appendages (hair, nails and sebaceous and sweat glands), it constitutes the integumentary apparatus. The main function of the skin is to constitute a barrier between the body interior and the exterior and to protect the body from dehydration and from possible infections by external pathogens. The skin also plays a key role in the process of thermoregulation and has sensory structures capable of receiving stimuli from the outside. The skin consists of three basic layers: epidermis, dermis, and hypodermis (Figure 5). The epidermis is the top layer, with variable thickness (0.07-0,12 mm). The epidermis is a pluri-stratified epithelium, the cellular elements differ as it proceeds from deeper layers to the more superficial. The most superficial layer of the epidermis, represented by the horny layer, is made from cellular elements fully keratinized, devoid of metabolic activity. The dermis, the underlying epidermis and separated from it by the basal membrane, is represented by dense connective tissue. The hypodermis, below the dermis, is represented by loose connective consists essentially of adipose tissue. The epidermis is made up of a multilayer epithelium of keratinocytes, which help to build the real scaffold epidermis; a structure overlying acellular, known as skin barrier, represented by a mixture of lipids derived from sebum and epidermal surface (Brogden et al., 2012; Elias 2015; Joo et al., 2015). The multi-layered epithelium of the epidermis consists of keratinocytes, which are continuously renewed, starting from the replication of stem elements present in the basal layer in contact with the underlying dermis, which play a trophic function. Generated cells then move to the outer surface and progressively differentiate. The process of keratinocyte differentiation is the gradual deposition of keratin filaments in the cytoplasm and morphological change of keratinocytes that arrive to turn up to constitute, in their entirety, foils flattened. Surface cells, now metabolically inactive, come off and die. This process, typical to terminal differentiation of keratinocytes, is known as keratinization or cornification. The turn-over of keratinocytes from the basal layer to the stratum corneum, is about 20-30 days. The skin appears, from histological observation, as a multi- layered

structure. Each layer shows different metabolic activity. These layers are commonly known as: basal or germinative layer; spinous layer or Malpighi; granular layer; shiny layer (present only in palms and soles of the feet); stratum corneum. The keratinization of the stratum corneum is strictly related to the construction of the "barrier function." The skin barrier is made up of lipids resulting from the sebaceous glands and the turn-over of the epidermis. This acellular structure exerts a key function in the protection against dehydration and as a barrier against infection by pathogens, preventing their penetration in the underlying layers (Joo et al., 2015; Elias 2015). The construction of the barrier is also associated to the release surface of peptides with antibiotic/bacteriostatic which thus constitute a further chemical filter protection against viruses and bacteria (Brogden et al., 2012).

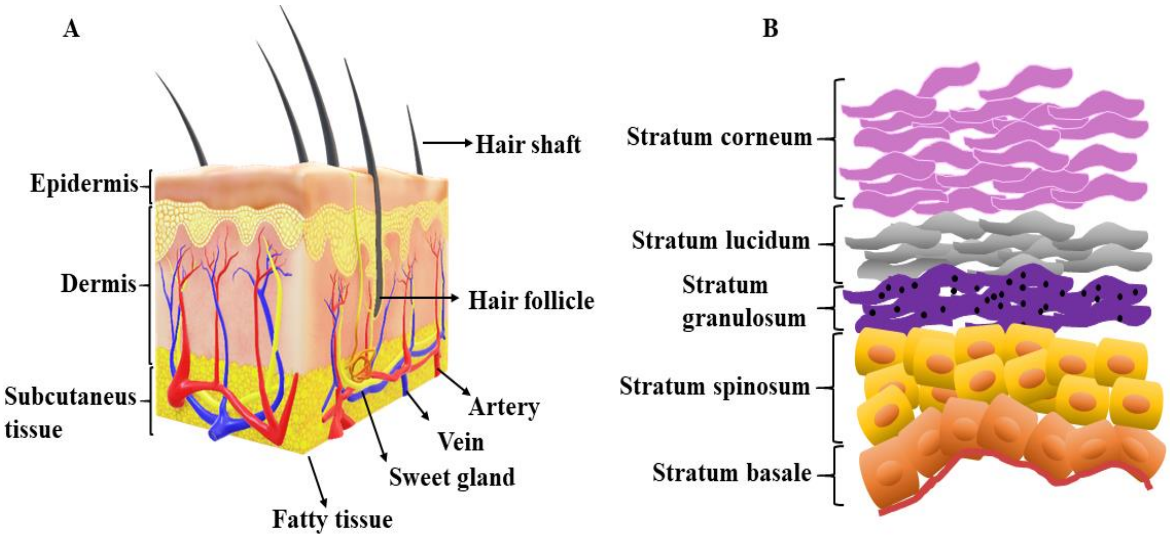

Figure 5 Schematic representation of the skin.

(A) image of the skin and skin appendages; (B) schematic representation of the epidermis and of the layers that comprise it.

The cellular cytoskeleton of the keratinocytes is attached to an intracellular junctions called desmosomes. They are organized in size and assembly by their adhesion molecules: the desmosomal cadherins, desmoglein and desmocollin, the plakin desmoplakin that links the adhesion molecules to the desmosome-intermediate filaments (DIFs), and the armadillo proteins plakoglobin and plakophilin that link the adhesion molecules to desmoplakin. When this adhesion fails, for example it can be

seen in autoimmune diseases, tissues that are subject to mechanical stress break down. In particular, the DIFs are divided in two intracellular and one intercellular component; the intracellular part is important to maintain the linkage between the intermediate filaments (IFs) and the adhesion molecules, while the intercellular one is constituted by an adhesion bond provided by the adhesion molecules. Failure of IFs can be found in epidermolysis bullosa simplex causes by a mutation in genes encoding for keratin 5 and 14 in the basal epidermis with a consequent manifestation of epidermal blisters (Garrod 2010; Garrod and Chidgey, 2008). While desmosomes are important to form the cell-to-cell adhesions, the hemidesmosomes (HDs) form adhesions between cells and the basement membrane. The zone between the epidermis and the dermis is called dermal-epidermal junction (DEJ) and has a wavy form. It is a highly specialized attachment between the epidermis and the papillary dermis where cells like keratinocytes, melanocytes and Merkel cells are abundant (Borradori and Sonnenberg, 1999). DEJ is important for: 1) maintaining the adherence of dermal-epidermal; 2) conferring a mechanical support for the epidermis and 3) being a barrier to the exchange of cells and molecules across the junction. It is constituted by 4 major subregions: (i) the basal cell plasma membranes of basal keratinocytes and the hemidesmosomal plaques: the inner plaque that is linked to keratins 5 and 14. They are formed by cytoplasmic proteins (e.g. HD1, plectin, intermediate filament associated protein (IFAP300), and bullous pemphigoid antigen 1 (BPAG1)), and the outer plaque that is formed by the transmembrane proteins α6β4 integrin and BPAG2 (type XVII collagen); a sub-basal plaque in (ii) the lamina lucida (LL) is attached to the anchoring filaments which is further attach to the HDs of the (iii) lamina densa (LD). This latter is constituted by the DEJ associated proteins, laminin 332 and laminin 331, and serve as a bridge between HDs and the dermal matrix (Walko et al., 2015). The dermis is a fibrous thick tissue that provides strength and flexibility to the skin. Moreover, it contains dense connective tissues like the blood vessels that carry the nutrients and help to regulate the temperature of the body, the nerve endings that provides different degrees of sensitivity to different areas, thus it comprises fibroblasts that are responsible for the production and secretion of procollagen and elastic fibers. The anchoring fibrils are abundant in collagen type VII (Col7). Depending on the type and organization, collagen can be classified into different groups: collagen I, III, and V are the most abundant in the human skin, while minor but still present in the

human skin of collagens VII, XVII and XXIX can be found. Col7 is an extracellular matrix protein and links the basal lamina and the underlying connective tissue. Its domain architecture is determined by an extend central triple-helical domain (145 kDa) edged by two non-collagenous domains, NC1 (145 kDa amino-terminal) and NC2 (34 kDa carboxyl-terminal) (Wegener H et al., 2013). NC1 comprises eleven submodules with homology of adhesion molecules like the fibronectin type III-like (NFIII) repeats and the A domain of von Willebrand (vWF) factor. It is important for the stabilization of DEJ by binding to laminin 332, laminin 331, and collagen IV while, on the other hand, NC2 comprises only a single module (Chen et al., 1997). Col7 synthesis takes place in epidermal keratinocytes and dermal fibroblasts. Protein synthesis, hydroxylation and glycosylation all take place inside the cell, while proteolytic processes in cross-linking takes place outside the cell. The most common amino acid in collagen is the glycine and, also proline and lysine. In the cytoplasm of the cell, specifically in the endoplasmic reticulum (ER), the preprocollagen, the pro α-chain backbone, is glycosylated to allow the sugar molecules to stick together and to form the procollagen, so the triple helix. Consequently, the triple helical molecules are secreted in the extracellular space. Procollagen is transported from the ER to the Golgi, and this step requires a conserved proteins called the coat protein complex II (Cop II). This latter is important for carrying the collagen out of the cell (Malhotra and Erlmann, 2011). A mutation that causes a disruption of glycosylation and so a loss of immunological tolerance led to the production of autoantibodies (AAbs) against Col7. Consequently, the integrity of the skin is compromised resulting in the development of autoimmune bullous skin diseases (AIBDs).

1.6 Autoimmunity and Autoimmune diseases

The term autoimmunity was coined for the first time by the physician Paul Ehrlich, over a hundred years ago, who proposed an existent mechanism to prevent the immune response against their own elements. Back to then, there were no experimental data at the molecular and cellular levels that could state what he tried to define as autoimmunity (Bell and Bird, 2005). The development of laboratory tools allowed scientists to investigate deeply into autoimmunity that led them to

distinguish the autoimmunity from autoinflammatory. The difference between the two terms was described as follow: autoimmunity is a self-direct inflammation caused by aberrant dendritic cells and T and B cells behaviour that disrupt tolerance resulting in an adaptive immune response; in contrast, autoinflammation leads to the activation of an innate immune response by which altered factors such as the production of cytokines by neutrophils, macrophages may result in tissue damage (Hayter and Cook, 2012). Thus, when the immune system is dysregulated and the response is a nature´s self-destruction, this can lead to an autoimmunity that can affect any system in the body; for example, it can affect lungs, kidneys, brain, skin and so many organs with severe consequences. To classify a disease as an autoimmune disease (AD), we can refer to at least two of the Witebsky´s postulates: 1) a direct immune response to an affected tissue or organ; 2) a high production of auto-reactive T cells or AAbs in the affected organ or tissue; 3) induction of the disease in animals by immunization with autoantigens; 4) an immune modulation, suppression of autoimmune response that enhances the clinical level (Rose and Bona, 1993). Statistically, 8% of the world population is affected by autoimmune disorders and 78% of those affected is represented by women. It is known that the immune response can differ between men and women. Sex differences highlight those women are more susceptible to infections with a consequent high production of antibodies that cause an inflammation as a result of protection against it, for what concern women, but can result as an increase of mortality in men (Fairweather et al., 2008). What causes autoimmunity is still unclear but if we can resume what science progresses until now, we can state that one component is our genetic and so if we have the wrong genes these can cause autoimmune disorders; another component can be the environment (Davidson and Diamond, 2001). ADs can be classified into two groups: the systemic ADs that refers to diverse affected organs, and an organ-specific ADs that refers to a single affected organ.

1.6.1 Autoimmune bullous skin disease

Autoimmune bullous diseases of the skin are rare disorders which are associated with the production of AAbs. The overall yearly incidence is between 0.3-1.0/100,000 Autoimmune bullous skin disease can be classified into two main

categories depending on the affected skin at the epidermal or at the dermal-epidermal junction level (Damoiseaux, 2013). In the pemphigus disease group, AAbs are directed against desmosomal proteins resulting in loss of adhesion between adjacent epidermal keratinocytes and formation of intraepithelial blisters (Foliaceus, 2008). In contrast, the group of pemphigoid diseases is characterized by the production of AAbs directed against hemidesmosomal proteins and type VII collagen, leading to de-adhesion of the lower layer of the skin, between the epidermis and the dermis with a consequent formation of subepidermal blisters.

Table 2 Abbreviations: Dsg-desmoglein; BPAG-bullous pemphigoid antigen.

Group of diseases	**Associated diseases**	**Target antigen(s)**
	Pemphigus vulgaris	Dsg1 & Dsg3
Pemphigus	Pemphigus foliaceus	Dsg1
	Paraneoplastic pemphigus	Dsg1, Dsg3,
	IgA pemphigus	Desmocollin
	Bullous pemphigoid	BPAG1 & BPAG2
	Pemphigoid gestationis	BPAG1 & BPAG2
Pemphigoid	Linear IgA bullous dermatosis	BPAG2
	Mucous membrane pemphigoid	BPAG1, BPAG2, laminin 332, α6β4
	Anti p200 pemphigoid	Unknown antigen
	Epidermolysis bullosa acquisita	type VII collagen

1.6.2 Epidermolysis bullosa acquisita (EBA)

Epidermolysis bullosa acquisita (EBA) is a rare subepidermal autoimmune blistering disorder (SEAIBD) caused by AAbs, mainly IgG class, against the 145-kDa non-collagenous amino-terminal (NC-1) domain of collagen VII, with an incident of 1/50,000 (Lehman, et al., 2009). Clinically, it is a heterogeneous disease that results of a defect in anchoring between the epidermis and dermis, resulting in friction and skin fragility. Indeed, EBA can be classified in two types: the inflammatory and non-inflammatory phenotype (Mihai and Sitaru, 2007). Patients with the non-inflammatory form of EBA (the classical EBA type) present skin fragility, blister and erosions heal with scarring and milia. In opposite, the inflammatory form of EBA is characterized by widespread tense vesicles surrounded by inflamed skin, with minimal scarring and milia (Mehren and Gniadecki, 2011). It resembles bullous pemphigoid (BP), linear IgA disease (LAD), mucous membrane pemphigoid (MMP) and Brunsting-Perry pemphigoid (Koga et al., 2019).

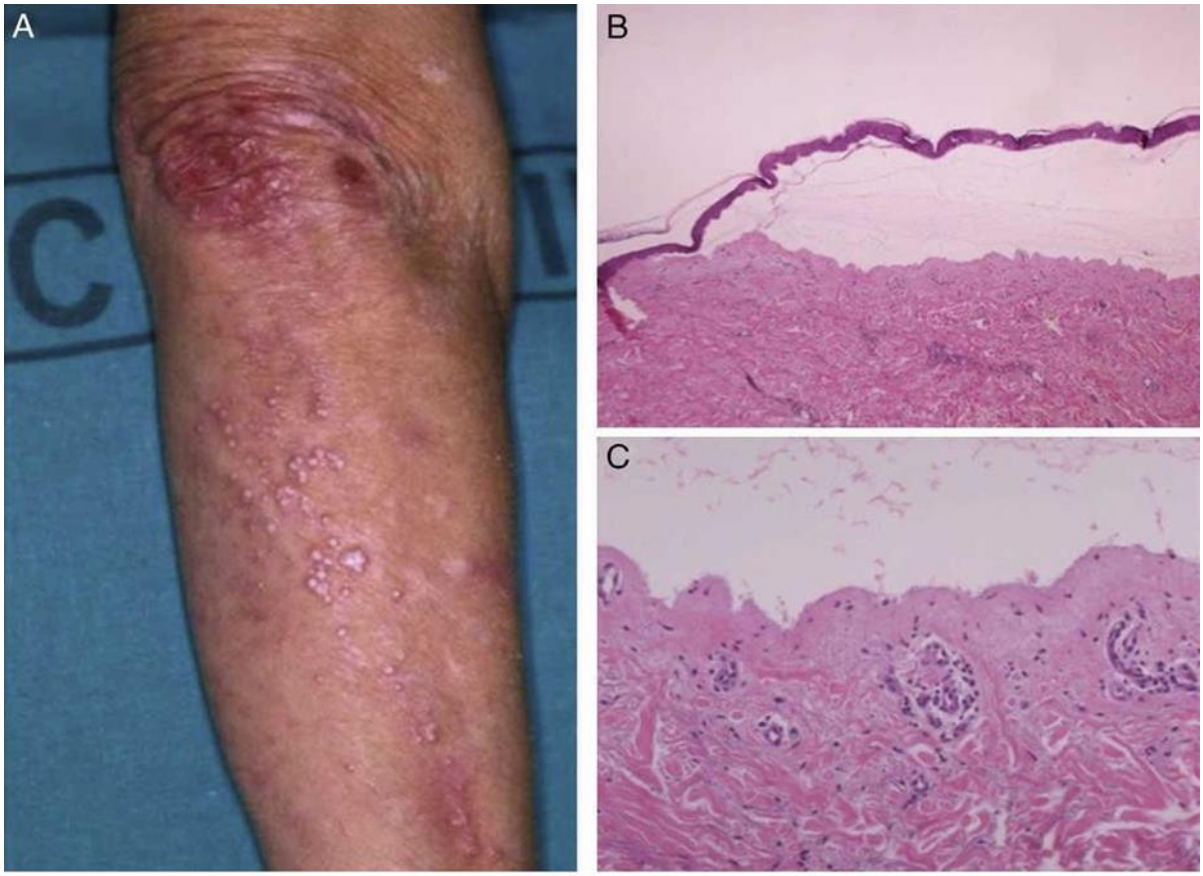

Figure 6 Clinical and histophatological features of EBA.

(A), Inflammatory epidermolysis bullosa acquisita. (B), Subepidermal blister. Hematoxylin-eosin, original magnification ×40. (C), Significant inflammatory infiltrate with predominance of neutrophils and scant eosinophils. Hematoxylin-eosin, original magnification ×100.

The routine screening test to diagnose EBA is the direct immunofluorescence (DIF) microscopy and enzyme-linked immunosorbent assay (ELISA). These techniques are important for the detection of the AAbs deposition on the dermal site of salt-split-skin ("floor pattern") and to evaluate the disease severity, respectively (Santi, C. G. et al., 2019). Besides deposition of IgGs as part of the adaptive immune response, DIF can also detect deposition of complement 3 (C3) at the DEJ, that is considered the hallmark of an injury inflammation (Edwards et al., 2019; Mihai et al., 2007). The complement system can be activated by three pathways: lectin, classical and alternative. The lectin pathway (LP) and the classical pathway (CL) are activated by exogenous materials where different enzymes cleave the C3 into the anaphylatoxin

C3a. On the other hand, the alternative pathway (AP) is continuously activated by spontaneous hydrolysis of thioester bond within C3 and, after changes in its conformational structure, leads to a strong and rapid response to an insult. The terminal phase of the three pathways ends with the formation of C5a generated from C3 cleavage, and can act as a potent chemoattractant for macrophages, neutrophils and activated B and T cells by binding its specific receptor expressed in the immune and non-immune cells (Noris and Remuzzi, 2013). There are no specific treatments for EBA due to the low prevalence of the disease, therefore the treatments applied to date rely on clinical experience. Patients are treated with corticosteroids with a doses range between 0.5 to 1.5 mg/kg per day. The treatment can be combined with other steroids like methotrexate, azathioprine, rituximab and, also an intravenous immunoglobulin (IVIG) to supply the antibody deficiencies. (Ludwig, 2013). Despite the initial improvements in EBA patients, after these treatments, there are several factors to be considered. The higher cost of some medications compared to other conventional one and, therefore the limitation to investigate new approaches on a large number of patients; the side effects that have been reported at the gastrointestinal, genitourinary, infectious levels. Close follow-up and monitoring for medication side effects is critical for successful treatment of these complex disorders. Hence, studies on EBA novel therapeutical approaches are still to be assessed. The mechanism by which the inflammatory response occurs is not yet fully understood. Therefore, many of *in vitro* and *in vivo* experiments are leading to the discover of new molecular mechanisms mediating AAb-induced inflammation and subsequent tissue damage in the skin in EBA (Bieber et al., 2010).

1.7 Experimental model for EBA

To understand the causes and the pathogenic mechanisms of EBA disease, many studies *in vivo*, *ex vivo* and *in vitro*) were evaluated for their fidelity in reproducing the human disease. In an *in vitro* assay model, neutrophils - treated with immune complexes – release reactive oxygen species (ROS) that are detected by the measurement of the luminol based chemiluminescence. In this assay, neutrophils from healthy blood donors are isolated and incubated with fixed immune complexes of anti-Col7 IgG. This in turn, results in neutrophil activation; the luminescence

signal is further quantitated by integrating the light emission over time, using a temperature-controlled luminescence plate reader (Ludwig, 2013). In an *ex vivo* model, human cryosections, obtained from human neonatal skin, were incubated with EBA patients' sera containing pathogenic AAbs. It is known that Ab alone itself does not induce any detachment of derma-epidermal junction however, by adding peripheral blood neutrophils from healthy donors leads to the localization of the PMN at the DEJ, induction of dermal-epidermal separation, production of reactive oxygen species (ROS) and secretion of matrix metalloproteinases (MMP9 and MMP12). Recently, an *in vivo* model was successfully developed (Sitaru et al., 2005, 2006) and gave scientists the chance to reproduce the clinical and the histological features of human EBA in a mouse model. To investigate the induction phase of EBA, an immunization-induced disease mouse model was established resulting in loss of tolerance and generation of anti-Col7 AAbs. In this model, mice were immunized with recombinant peptide fragment from immunogenic NC-1 domain of murine Col7. The result led to the production of fixing IgG2a/IgG2b murine anti-Col7 AAbs, their deposition at the DEJ and dermal-epidermal separation (Sitaru et al., 2006). To study the effector phase of EBA, specifically the AAb-mediated tissue injury mechanism, a passive antibody transfer model was developed (Figure 7). In this model, polyclonal antibodies against type collagen VII were generated in rabbits by immunization with the recombinant forms of the non-collagenous (NC1) domain of murine type VII collagen. Due to structural similarities between the murine and the rabbit Col7 proteins, cross reactivity of rabbit IgG with murine Col7 occurs. Hence, rabbit serum is subsequently used to affinity purify Col7 IgG that is injected into C57Bl6/J or BALB/c mice (Woodley D T et al., 2006). The mouse strains, C57BL/6 and BALB/c are susceptible to blister formation, reproducing human EBA at clinical, histological, electron microscopically, and immunopathological levels. This reactivity was induced by injecting IgG in a range of 20-500 µg/g body weight injection. The blister formation was visible in mice 2-4 days after the first injection and highlights their strength and closely resembling the human disease, at the clinical and histopathological level (Sitaru et al., 2005).

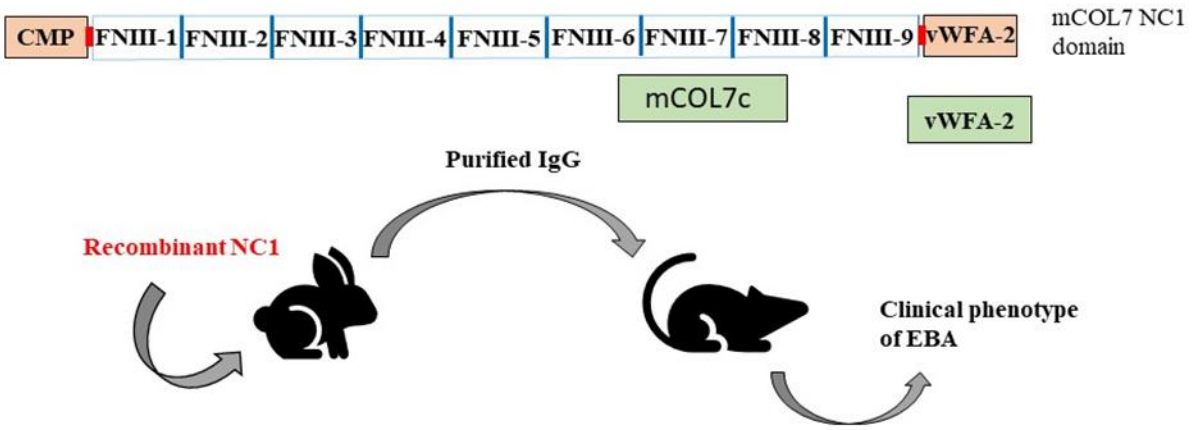

Figure 7 Animal passive transfer model.

In passive transfer model, rabbits were immunized with recombinant NC1 protein (mCOL7c or vWFA-1). Subsequently, rabbit IgG was purified and injected into the mouse to induce EBA.

1.8 Mechanisms mediating autoantibody-induced skin inflammation and tissue injury in EBA

The immune system plays an essential role in host defence by recognizing and eliminating foreign Ags. The breakdown of one of the mechanisms by which the immune system responds to avoid a potential harmful reaction may result in autoimmunity. Regarding the group of organ-specific autoimmune disease and in this case EBA, skin blister formation is related to the reaction of autoantibodies against structural epithelial proteins (Sitaru et al., 2005). The molecular mechanism by which skin blister formation is manifested is still unknown but there are many studies on the possible pathways involved in the onset of the disease. Depending on the different subpopulations where, for example, in patients with pemphigus and mucous membrane pemphigoid the only binding of the Abs to their targets causes blisters, lesion induction in patients with BP and EBA seemed to require more inflammatory pathways (Yancey, 2005). Data from the antibody passive transfer EBA mouse model suggest that the complement system is a key factor in mediating inflammation and blistering in EBA. It was shown that mice that were deficient in C5 response surprisingly failed to develop the EBA disease (Nandakumar and Holmdahl, 2006; Sitaru et al., 2005). Furthermore, products derived from the cleavage of C5, C5a, mediate CD18- dependent neutrophils extravasation into

inflamed skin (Chiriac et al., 2007). Other findings suggest that the granulocyte-macrophage colony stimulating factor (GM-CSF), a cytokine that stimulates neutrophils and other cells and promotes their recruitment to the site of inflammation, has been identified at high level in EBA, both in mouse serum and skin, promoting blister formation. Its contribution to innate immune mechanism, also promotes PMNs activation to initiate a cascade of pro- and inflammatory responses and, therefore the release of reactive oxygen species (ROS) that have been found (Samavedam et al., 2013). Based on these results, to investigate whether neutrophils may have an impact on the production of autoantibodies, EBA was induced in neutrophil-depleted mice. The results showed the disease phenotype was abolished in these mice, suggesting that PMNs could have been the main effectors of the AAb production and so skin inflammation in this model (Chiriac et al., 2007; Kasperkiewicz et al., 2012a). Focusing on the importance of neutrophils and their recruitment in the inflammatory skin, in EBA, Sezin et al., had investigated the presence of a potent chemoattractant, the lipid mediator B4 (LTB_4) indispensable for neutrophil´s recruitment. It is biosynthesized from arachidonic acid through sequential enzymatic conversion by 5-lipoxygenase (5-LO) and LTA_4-hydrolase and modulates PMNs functions such adhesion, degranulation, ROS release and apoptosis. These results are based on one of their *in vivo* experiments where they induced EBA disease in 5-LO–deficient mice (*Alox5*$^{-/-}$) and BLT1-deficient mice (*Ltb4r1*$^{-/-}$). They have found widespread skin lesions in the wild-type compared to the KO mice that showed no clinical signs of disease thus, at the histopathological levels, it has been seen that lesional wild-type skin was markedly infiltrated predominantly by neutrophils (Sezin et al., 2017). Expression of several cytokines, affecting neutrophils function, such as interleukin-1 (IL-17), interleukin-23 (IL-23), interleukin-8 (IL-8), (functional homologs in mice CXCL-2), interleukin-1β (IL-1β), tumor-necrosis factor-α (TNF-α) and GM-CSF (already mentioned above) were founded to be up-regulated in lesional skin and sera of diseased mice (Ludwig, 2013). Once in the skin, PMNs express, on their membrane surface, a variety of receptors with different functions and specificity for the recognition of AAbs that target the epitopes located in the NC1 domain of collagen type VII. Mainly, 50-60% of IgG were found in EBA patients and or in combination with IgA. Characterization of autoantibodies subclass distribution in the EBA sera contained IgG1, IgG2, IgG3 and IgG4 collagen type VII NC-1 specific autoantibodies (Bernard et al., 1991;

Oostingh et al., 2005). When neutrophils bind the Fc portions of the anti col7 Abs, they do so via the FcγRs that drive proinflammatory effector functions.

1.9 Aim of the present study

The pemphigoid disease Epidermolysis Bullosa Acquisita (EBA) is a severe autoimmune skin disease, and the current treatment relies on general immunosuppressive therapy, which does not lead to remission in all cases. Therefore, there is an urgent medical need for the development of novel therapeutic options. The progression of EBA depends on the recruitment of neutrophils into the skin by chemotactically active mediators. The mechanisms of regulation of neutrophils recruitment into the skin and their activity are only partially understood. Also, little is known about the biological effect of Dectin-2. Moreover, the expression of Dectin-2 has been described on different cells type which belong to the group of the radioresistant and radiosensitive cells. The present study was undertaken to elucidate the mechanism of the contribution of Dectin-2 in the development of skin inflammation in the model of passive EBA. Also, with the help of bone marrow chimera mouse model, the relative contribution of hematopoietic and non-hematopoietic cells to the development of the inflammation will help to validate Dectin-2 as a pharmacological target for the treatment of pemphigoid disorders.

MATERIALS AND METHODS

2.1 Materials

2.1.1 Chemicals

Chemicals	Cat. no.	Source
Aceton	5025.1	Carl Roth GmbH & Co. KG, Karlsruhe, Germany
β-mercaptoethanol	M6250	Sigma-Aldrich, Darmstadt, Germany
Bovine serum albumin fraction V-biotin free	163.2	Carl Roth GmbH & Co. KG, Karlsruhe, Germany
Recombinant Mouse Complement Component C5a Protein	2150-C5-025/CF	Bio-Techne/ R&D System
EDTA solution 0.5M pH 8	A3145.0500	AppliChem GmbH, Darmstadt, Germany
Ethanol 70%	T913.3	Carl Roth GmbH & Co. KG, Karlsruhe, Germany
Ethanolamine	E9508	Sigma-Aldrich, Darmstadt, Germany
FBS superior	S0615	Merck KGaA, Darmstadt, Germany
Glycin	3908.2	Carl Roth GmbH & Co. KG, Karlsruhe, Germany
Haematoxylin	104302	Merck KGaA, Darmstadt, Germany
Human serum albumin	A1653	Sigma-Aldrich, Darmstadt, Germany
Ketamin hydrochloride	K2753	Sigma-Aldrich, Darmstadt, Germany
Leukotriene B4	20110	Biomol GmbH, Hamburg, Germany
Luminol sodium salt	A4685	Sigma-Aldrich, Darmstadt, Germany
Methanol	T169.1	Carl Roth GmbH & Co. KG, Karlsruhe, Germany

Mouse GM-CSF	130-095-746	Miltenyi Biotec
Protein G sepharose beads	L00209	Hölzel Diagnostika Handels GmbH, Köln, Germany
Roti-Histofix (4% solution)	P087.2	Carl Roth GmbH & Co. KG, Karlsruhe, Germany
RPMI 1640 with L-glutamine	BE12-702F	Lonza Cologne GmbH, Köln, Germany
RPMI 1640 with L-glutamine w/o glucose w/o phenol red	C4116.0500	Genaxxon bioscience GmbH, Ulm, Germany
Xylazine hydrochloride	X1251	Sigma-Aldrich, Darmstadt, Germany

2.1.2 Commercial buffers & solutions

Name	**Cat. No.**	**Source**
PBS pH 7.2 0.1 M	70013-016	Invitrogen GmbH, Darmstadt, Germany
DPBS pH 7.2 0.01 M	14190-094	Invitrogen GmbH, Darmstadt, Germany
1 M HEPES	L1613	Biochrom GmbH, Berlin, Germany
Normal goat serum	X0907	Dako Deutschland GmbH, Hamburg, Germany
MACS® BSA Stock Solution	130-001-376	Miltenyi Biotec
autoMACS® Rinsing Solution	130-091-222	Miltenyi Biotec
FcR Blocking Reagent, mouse	130-092-575	Miltenyi Biotec

2.1.3 Antibodies

A. Primary Antibodies			
Name	**Cat. no.**	**Application**	**Source**
Rat anti-mouse Complement 3	CL7503AP	IHC	CEDARLANE
APC mouse anti-mouse CD45.1	533772	FC	BD Bioscience
FITC mouse anti-mouse CD45.2	109806	FC	BD Bioscience

PerCP-Cy5.5 rat anti-mouse Ly6G	130-103-232	FC	Miltenyi Biotec
APC mouse anti-mouse CD11b	130-113-232	FC	Miltenyi Biotec
PE anti-mouse F4/80	123109	FC	BioLegend
Mouse Dectin-2/CLEC6A alpha Isoform APC-conjugated	FAB1525A	FC	R&D System
Polyclonal rabbit anti-human serum albumin	A0433	*in vitro* assay	Sigma-Aldrich, Darmstadt, Germany
Ly-6G Antibody, anti-mouse, PerCP-Vio® 700, REAfinity™	130-117-500	FC	Miltenyi Biotec
Ly-6G Antibody, anti-mouse, APC-Vio® 770, REAfinity™	130-119-126	FC	Miltenyi Biotec
FITC anti-mouse Ly-6C	128005	FC	BioLegend
PE anti-mouse CD16.2 (FcγRIV)	149503	FC	BioLegend
Viobility™ 488/520 Fixable Dye	130-109-812	FC	Miltenyi Biotec

Isotype Antibodies			
Name	**Cat. no.**	**Application**	**Source**
Purified Armenian Hamster IgG Isotype Ctrl	400901	*in vitro* assay	BioLegend
Dectin-2 Antibody, anti-mouse, pure	130-094-481	FC	Miltenyi Biotec

B. Secondary Antibodies			
Name	**Cat. no.**	**Application**	**Source**
Fluorescence dyes			
Alexa Fluor® 594 AffiniPure Goat Anti-Rat IgG (H+L)	112-585-167	IHC	Jackson ImmunoResearch
Alexa Fluor® 488 AffiniPure Goat Anti-Rabbit IgG (H+L)	111-545-144	IHC	Jackson ImmunoResearch
DAPI fluoromount G	0100-20	IHC	BIOZOL, Munich, Germany

2.1.4 Kits and others

Name	**Cat. no.**	**Source**
Thermo Scientific RevertAid First strand cDNA Synthetic kit	K1622	Thermo Fisher Scientific, Germany
LTB_4 parameter assay	KGE006B	R&D Systems GmbH, Wiesbaden-Nordenstadt, Germany
ELISA MAX™ Standard Set Mouse IL-6	431301	BioLegend
ELISA MAX™ Standard Set Mouse IL-17A	432501	BioLegend
True-Nuclear™ Transcription Factor Buffer Set	424401	BioLegend

2.1.5 Laboratory equipment

Equipment	**Source**
Accu-jet pro pipette	BRAND GmbH, Wertheim, Germany
Analytical scale ABS/ABJ-BA-def- 1019	Kern & Sohn GmbH, Balingen, Germany
Bio-photometer plus 8.5 mm	Eppendorf AG, Hamburg, Germany
Centrifuge 5810R	Eppendorf AG, Hamburg, Germany
CFI Plan Apo λ 10x lense	Keyence Deutschland GmbH, Neu-Isenburg, Germany
CFI Plan Apo λ 20x lense	Keyence Deutschland GmbH, Neu-Isenburg, Germany

Cryostat CM3050 S	Leica Mikrosysteme Vertrieb GmbH, Wetzlar, Germany
FACSCalibur	Becton Dickinson GmbH, Heidelberg, Germany
Freezer -20˚	Liebherr Hausgeräte GmbH, Ochsenhausen, Germany
Freezer -80˚	Thermo Fisher Scientific GmbH, Dreieich, Germany
HandyStep S dispenser	BRAND GmbH, Wertheim, Germany
Hemavet 950	Drew Scientific Inc. Miami Lakes, Florida, USA
HERAcell incubator	Heraeus Instruments GmbH, Hanau, Germany
Infinite M200 PRO ELISA reader	Thermo Fisher Scientific GmbH, Dreieich, Germany
Keyence microscope BZ-9000E	Keyence Deutschland GmbH, Neu-Isenburg, Germany
Laminar hood	NuAire, Plymouth, Minnesota, USA
Magnetic hotplate stirrer VMS-C4	VWR International GmbH, Darmstadt, Germany
Mastercycler ep realplex	Eppendorf AG, Hamburg, Germany
Micro centrifuge Micro Star 17R	VWR International GmbH, Darmstadt, Germany
Microtome	Leica Mikrosysteme Vertrieb GmbH, Wetzlar, Germany
Mini protean tetra system	Bio-Rad Laboratories GmbH, Munich, Germany
NanoDrop 2000c spectrophotometer	Thermo Fisher Scientific GmbH, Dreieich, Germany
Neubauer cell counting chamber	Laboroptik GmbH, Friedrichsdorf, Germany
pH meter HI208	HANNA instruments, Vöhringen, Germany
Power Pac basic	Bio-Rad Laboratories GmbH, Munich, Germany
Refrigerator	Siemens, Munich, Germany
Transferpette S (10 µl, 100 µl, 1000 µl)	BRAND GmbH, Wertheim, Germany
Vortex	Vortex-Genie® 2-Scientific Industries Inc., Bohemia, New-York,USA

2.1.6 Disposable materials

Type of article	**Source**
Amicon Ultra-15 (10 kDa)	Merck Millipore, Darmstadt, Germany
Amicon Ultra-15 (30 kDa)	Merck Millipore, Darmstadt, Germany
Cell strainer 70 µm	Becton Dickinson GmbH, Heidelberg, Germany
Cover glass slides (24x60)	Paul Marienfeld GmbH, Lauda-Königshofen, Germany
Crystalcruz Chromatography columns 1.5 cm x 10 cm	Santa Cruz Biotechnology, Heidelberg, Germany
Dako-pen	Dako Deutschland GmbH, Hamburg, Germany

Dialysis tubing visking cellulose type 36/32 inch 0.020 mm thick	Carl Roth GmbH & Co. KG, Karlsruhe, Germany
ELISA high binding 96-well plate	Fisher Scientific GmbH, Schwerte, Germany
Falcon tubes (15 ml; 50 ml)	Sarstedt AG&Co., Nuembrecht, Germany
Ministart 0.2 µm	Sartorius Stedim Biotech GmbH, Göttingen, Germany
Parafilm	Th. Geyer GmbH & Co. KG, Renningen, Germany
Pipette tips (10 µl; 100 µl; 1000 µl)	Sarstedt AG&Co., Nuembrecht, Germany
Reaction tubes (1.5 ml; 2 ml)	Sarstedt AG&Co., Nuembrecht, Germany
Serological pipettes (5 ml; 10 ml; 25 ml)	Sarstedt AG&Co., Nuembrecht, Germany
SuperFrost/Plus-slide glasses	Gerhard Menzel, Glasbearbeitungswerk, GmbH&Co. KG, Germany
Syringe (5 ml; 20 ml)	Becton Dickinson GmbH, Heidelberg, Germany
Syringe 1 ml	Becton Dickinson GmbH, Heidelberg, Germany

2.1.7 Mice

C57BL/6J WT mice were purchased from The Jackson Laboratory. In the present study, C57BL/6J WT serves as control group when I compared disease progression when comparing EBA development and progression in Dectin-2 deficient mice (*Clec4n*$^{-/-}$).

Clec4n$^{-/-}$ mice were generated by homologous recombination by means of the embryonic stem cell line E14.1 (Saijo et al., 2010); they were backcrossed for eight generations to C57BL/6J (Nihon SLC, Shizuoka, Japan).

B6.SJL-Ptprc^{a}Pep^{b}/BoyJ is a C57BL/6 congenic strain used widely in transplant studies because it carries the differential *Ptprca* pan leukocyte marker commonly known as CD45.1 or Ly5.1. Wild-type C57BL/6 inbred mice express the *Ptprcb* (CD45.2 or Ly5.2) allele. The strain was purchased from The Jackson Laboratory. In the present study, B6.SJL-Ptprc^{a} Pep^{b}/BoyJ serves as controls in the BM chimera experiments.

B6.Cg-Tg(S100A8-cre,-EGFP)1Ilw/J transgenic mice, also known with the common name MRP8-Cre-ires/GFP, have the human S100 calcium binding protein A8 (calgranulin A) (MRP8 or S100A8) promoter directing bicistronic Cre and EGFP protein expression to granulocytes and granulocyte/macrophage progenitors (GMPs). EGFP fluorescence and cre expression is evident in hemizygotes in 20% of granulocyte/macrophage progenitors (GMPs) and 100% of granulocytes during myeloid differentiation. When bred with mice containing a loxP-flanked sequence of interest, the resulting offspring can have Cre-mediated recombination of the flanked sequence in these cells. Mice were purchased from The Jackson Laboratory. In the present study, I used MRP8-Cre-ires/GFP mice as control group when I compared disease progression when comparing EBA development and progression in neutrophils specific FcgRIV-KO ($MRP8^{Cre}$ x $FcγRIV^{flx/flx}$).

FcγRIV-deficient mice were purchased from The Jackson Laboratory. A targeting vector was constructed with loxP sites flanking the first three exons of the *Fcgr4* gene. Upon homologous recombination in embryonic stem cells derived from C57BL/6 mice and generation of an FcγRIV-floxed mouse, ubiquitous deletion of the floxed *Fcgr4* gene was achieved by crossing this mouse to the CAG-cre mouse strain, which results in a ubiquitous deletion of the floxed first three exons of the *Fcgr4* gene. In the present study, neutrophil specific FcγRIV-KO mice are designated as $MRP8^{Cre}$ x $FcγRIV^{flx/flx}$.

Animals were maintained on a 12-hour light–dark cycle at the animal facility of the University of Lübeck. Mice were held under SPF conditions and fed acidified drinking water and standard chow *ad libitum*.

All protocols were approved by local authorities of the Animal Care and Use Committee (Kiel, Germany) and performed by certified personnel.

In all experiments 6-12-weeks old age- and sex- matched mice were used.

2.2 Methods

2.2.1 Induction of experimental passive EBA mouse model

For induction of passive EBA in the mice, a previous established protocol was performed in this study. Briefly, mice were injected, subcutaneously, with 50 µg of rabbit anti-COL7 IgG on day 0, 2 and 4, into the neck, foreleg, and hind leg, respectively. Mice were weighted from day 0 and scored from day 4 and, every second day for their general condition and evidence of skin lesions until day 14. Disease severity was measured as a percentage of body surface area affected by skin lesions. On the day of termination, lesional biopsies were collected for histopathological analysis (stored in 4% buffered formalin and -80°C nitrogen for cryosection) and hind legs were collected for neutrophils isolation studies from the bone marrow (Figure 8).

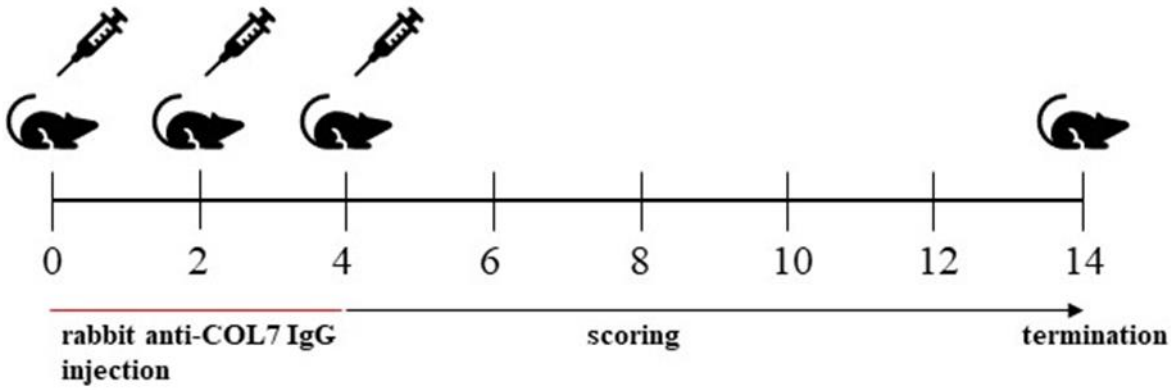

Figure 8 Schematic illustration of passive EBA mouse induction.

Mice were injected on day 0 (neck), 2 (foreleg) and 4 (hind leg) with 50µg of rabbit anti-COL7 IgG and scored from day 4 until day 14.

2.2.1.1 Scoring disease severity in antibody transfer EBA

The disease severity of passive EBA was scored by the % of affected surface body area. This latter was calculated by assigning individual percentile fraction to each part of the body. Integration of the affected area in distinct body parts of the mouse (Table 3) gave the overall score of EBA on that particular day. Subsequently, the area under the curve (AUC) was calculated with Graph-Pad Prism 6. The software computes the AUC using the trapezoid rule: a curve (created by nonlinear

regression) is a series of connected XY points, with equally spaced X values. Therefore, disease scores (Y values) obtained on different days are plotted against time series (X values). Subsequently, Prism uses the following formula $AUC = \Delta x*(y1+y2)$ to calculate an area that is formed under each adjacent pair of Y values that are represented on the XY plot.

Table 3 Scoring table used to calculate the disease severity in antibody-transfer EBA

The columns “Type of lesion” and “Affected surface body area (%)” are filled with example data.

Body parts	Percentile fraction from the total body area	Type of lesion	Affected surface body area (%)
left ear	2.5	Erosion	10
right ear	2.5		
right eye	0.5		
left eye	0.5		
Snout	2.5		
oral mucosa	2.5		
head& neck	9.0	Crust, alopecia	10
left foreleg	5.0		
right foreleg	5.0		
left hindleg	10.0		
right hindleg	10.0		
Tail	10.0		
Trunk	40.0	Erythema	10
Total score	100		5.15

2.2.1.2 Generation of affinity purified rabbit anti-murine Col7c IgG

To generate rabbit anti-murine Col7c IgG that can further react with the murine type VII collagen in the skin and induce EBA in mice, a 3-step procedure was performed. At the first step rabbits were immunized with recombinant NC-1 domain of murine

type VII collagen. Subsequently, total rabbit IgG were purified from rabbit sera using protein G resin affinity column chromatography. Finally, affinity column chromatography was used to specifically purify the pathogenic rabbit anti-murine Col7c IgG (also referred in this work as rabbit anti-mCol7c IgG). Each step of this procedure is described in detail in the following paragraphs. The procedures were made by our laboratory technicians, and I personally performed the last step regarding the purification of the specific rabbit anti-mCOL7c IgG.

2.2.1.3 Expression of recombinant NC-1 peptide and immunization of rabbits

To produce immune rabbit sera New Zealand white rabbits were immunized with the recombinant NC-1 domain of murine type VII collagen (Figure 9). The generation of recombinant NC-1 domain of murine type VII collagen, comprised from A, B, and C peptides was performed by a technician in our laboratory, Mrs. C. Kauderer according to a previously established protocol at the Department of Dermatology, Lübeck (Sitaru et al., 2005). The obtained proteins were sent to Eurogentec GmBH, Germany for immunization of New Zealand white rabbits. Rabbits were immunized subcutaneously with 250 µg of an equimolar mixture of the 3 purified recombinant proteins suspended in complete Freund's adjuvant. The animals were boosted thrice (at 15-day interval) with the same preparation in incomplete Freund's adjuvant. Immune sera were obtained at regular intervals and used to affinity purify specific IgG reactive against the pathogenic C domain of murine type VII collagen which will refer to in the present study as rabbit anti-mCol7c IgG.

2.2.1.4 Affinity column chromatography for purification of total rabbit IgG

Affinity column chromatography is an important technique in biochemistry that offers high selectivity and recovery for separation of proteins (or other macromolecules) from crude extracts. The separation of the protein occurs based on a reversible interaction between a protein and its specific ligand that is coupled to a chromatography matrix. Following its binding, the target protein is recovered by changing conditions to favor elution of the bound molecule. This is performed by either using a competitive ligand, or by changing the pH, ionic strength, or polarity.

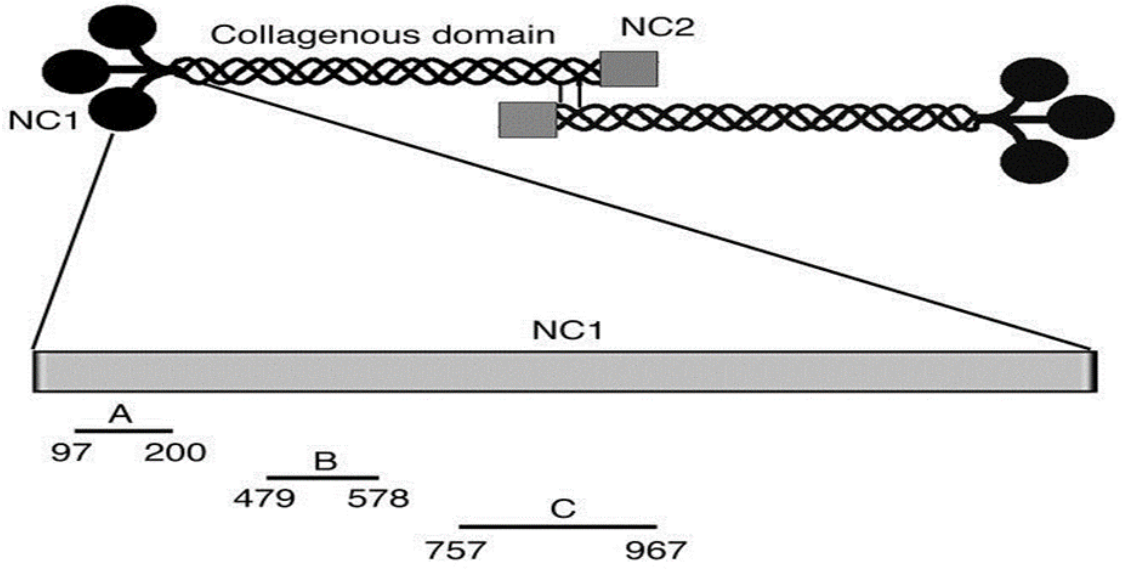

Figure 9 Schematic representation of murine type VII collagen.

Col7 is composed of 3 identical α chains, each one composed of a central triple helical C domain, flanked by a large amino-terminal NC-1 domain and a smaller carboxy-terminal NC-2 domain. Two Col7 molecules form antiparallel tail-to-tail dimers, stabilized by disulfide bonding through a carboxy-terminal overlap between the NC-2 domains. Three peptides (A, B, and C) of murine type VII collagen cDNA were cloned in linearized pGEX-6P-1 vector and expressed in E. Coli BL21. Amino acid residue numbers are shown below the fragments (source: Sitaru et al., 2005).

In this study, to isolate total IgG fraction from immunized rabbit sera, recombinant protein G resin affinity column chromatography was performed. Protein G is a bacterial cell wall protein isolated from group of G Streptococci bacteria that binds to the Fc portion of mammalian IgG with a reported binding capacity of > 20 mg sheep IgG/ml settled resin. The isolation of rabbit IgG was performed as follows. Briefly, 100 ml of rabbit serum was incubated with 5 ml of protein G resin. Consequently, IgG were eluted with 0.1M glycine buffer (pH 2.9) and neutralized with 1M Tris-HCl buffer (pH 9.0). The obtained IgG fraction was concentrated using dialysis membrane in polyethylene glycol 20,000 and dialyzed overnight against 0.01 M PBS pH 7.2 (Howe et al., 1964). Subsequently, anti-mCol7c IgG fraction was isolated from the total IgG fraction using affinity chromatography column coupled to mCol7c-His tag protein.

2.2.1.5 Expression of recombinant mCol7c-His tag protein

To affinity purify rabbit anti-mCol7c IgG; a specific mCol7c affinity chromatography column was generated. To do so, murine Col7c-his tag protein with an estimated size of ~ 23 kDa was generated as previously described (Sesarman et al., 2008). In brief, recombinant mCol7c-His tag protein was expressed in E. Coli BL21 and purified using TALON-immobilized cobalt affinity chromatography following manufacturer's instructions. TALON is an immobilized metal affinity chromatography resin charged with cobalt, which binds to His-tagged proteins from bacterial, mammalian, yeast, and baculovirus-infected cells. Thus, allowing their high purification under native or denaturing conditions. The purity of the eluted protein fractions was assessed by 15 % SDS PAGE gel and visualized with coomassie brilliant blue R-250. The Coomassie R- 250 dye binds to proteins through ionic interactions between the dye sulfonic acid groups and positive protein amine groups as well as through van der Waals attractions. The formation of the protein-dye stabilizes the negatively charged anionic form of the dye, producing a bright blue color that allows visualization of the protein. This technique is often used to stain proteins due to its high sensitivity and availability.

2.2.1.6 Generation of mCol7c affinity chromatography column

To generate mCol7c affinity chromatography column the expressed mCol7c-His tag protein was coupled to affinity media according to the following procedure. Briefly, the eluted mCol7c-His protein was concentrated with 0.01M PBS (pH 7.2) using Amicon Ultra-15 (10 kDa). Buffer exchange using Amicon Ultra-15 device is preferrable over overnight dialysis due to the high precipitation rate of the protein Thereafter, the PBS buffer was exchanged to 0.1 M MOPS pH 7.5 buffer for efficient coupling to the affinity media, Affigel 10. 10 mg of mCol7c-His tag protein (5 mg/ml) was coupled to 4 ml of gel bed Affigel 10 for 4 hours at 4˚C. Ninety percent of the maximal coupling is reported to be achieved within an hour, while within 4 hours the reaction is complete. Affigel 10 affinity media contains a neutral 10-atom spacer arm with N-hydroxysuccinimide ester that is highly reactive with free amino groups. Upon addition of a ligand, in our case the mCol7c protein, the N-hydroxysuccinimide is displaced, and a stable amide bond is formed. After completion of the coupling, the

gel bed is spun down at 500 g for 4 min at RT. A sample of 10 µl from the supernatant is collected, to check the efficacy of the coupling by 15 % SDS gel. Consequently, 0.2 ml of 1 M ethanolamine pH 8 is added to 2 ml 0.1 M MOPS pH 7.5 buffer and incubated for 1 hour at RT with the gel bed. This step blocks the remaining active ester groups that were not coupled to the protein. Following blocking, the gel bed is spun down again (500 g, 4 min, RT) and transferred to a CrystalCruz chromatography column 1.5 cm x 10 cm. The column is washed thrice with 50 ml 0.01 M PBS pH 7.2 and stored at 4˚C in 20 % ethanol for further use.

2.2.1.7 Purification of specific rabbit anti-mCol7c IgG

Total rabbit IgG fraction was subjected to mCol7c affinity chromatography and rabbit anti-mCol7c IgG were isolated. Briefly, 100mg of total rabbit IgG was incubated for 20 min at 40C. Subsequently, the column was washed once with 0.01 M PBS pH 7.2 and once with 850 mM NaCl solution containing 0.1% Triton X100. The column was further washed with 0.01 M PBS pH until OD was below 0.01 as determined by spectrophotometer. Consequently, the IgG fraction was eluted from the column with 0.1M glycin buffer (pH 2.9) and neutralized with 1M Tris-HCl buffer (pH 9.0). The column was regenerated with 20 mM Tris HCl pH 7.2 and another cycle of 20 mM solution containing 0.5 M NaCl pH 7.2. The column was washed with 0.01 M PBS pH 7.2, and the flow fraction was added for two additional isolation cycles. The obtained anti-mCol7c IgG fraction from all 3 cycles was concentrated using dialysis membrane in polyethylene glycol 20,000 and dialyzed overnight against 0.01 M PBS pH 7.2 (Howe et al., 1964). Purified anti-mCol7c IgG was concentrated using Amicon Ultra-15 (50 kDa) and filter-sterilized (pore size 0.2 µm). While its concentration was determined using Nano-Drop 2000c, its reactivity was assessed by indirect immunofluorescence microscopy using normal murine tail.

2.2.2 *In vitro* Isolation of Bone-Marrow derived neutrophils (BM-neutrophils)

Mice were anesthetized by intraperitoneal injection of ketamine (100 µg/g)/xylazine (15 µg/g) mixture and sacrificed by cervical dislocation. A sterile incision was made in the extremity feet and the skin from the distal part of the mouse was removed.

Using scissors and forceps, the acetabulum was gently twisted and removed from the hip joint. Subsequently, tibia and femur were transferred into sterile falcon tube containing the Magnetic-Activated cell sorting (MACS) buffer on ice. All subsequent procedures were performed sterile, under the hood to avoid any possible contamination and so activation of the cells. Using a scalpel, the remaining muscles were removed from the bones and scissors were used to separate the femur from the tibia at the knee joint. Both edges of the bone were cut to allow the BM to be flushed from the bone cavities using a 25-gauge needle and a 20-cc syringe with MACS buffer. The obtained BM was filtered into a new falcon tube and centrifuged at 1200 rpm 4 min at 8 °C. The pellet was resuspended in 1 mL MACS buffer and counted using the Neubauer chamber. After cell number was determined, cells were centrifuged at 400xg for 5 minutes. The supernatant was aspirated completely, and the cell pellet was resuspended in 200 µL of MACS buffer per 5x10^7 total cells with the addition of 50 µL of Neutrophil Biotin-Antibody Cocktail per 5x10^7 total cells. Cells were incubated for 10 minutes on ice. After incubation, cells were washed by adding 5-10 mL of MACS buffer per $5x10^7$ and were centrifuged at 400xg for 5 minutes. The supernatant was aspirated completely, and cell pellet was resuspended in 400 µL of MACS buffer per $5x10^7$cells and 100 µL of Anti-Biotin Microbeads per $5x10^7$. Cells were incubated for 15 minutes on ice. After incubation, cells were washed by adding 5-10 mL of MACS buffer per $5x10^7$ and were centrifuged at 400xg for 5 minutes. The supernatant was aspirated completely, and cell pellet was resuspended up to 10^8 cells in 500 µL of MACS buffer. Subsequently, cells were separated through a magnetic separation with MS column per negative selection. Columns were first prepared by rinsing with 500 µL of MACS buffer. Cell suspension was applied onto the column. Collected flow-through containing unlabeled cells was represented by enriched neutrophils. Column was washed three more times with 500 µL every step. Once BM-neutrophils were collected, cell suspension was centrifuged at 400xg for 5 minutes and the supernatant was aspirated completely. Cell pellet was resuspended with 1 mL of neutrophils buffer and cells were counted using the Neubauer chamber.

2.2.3 *In vitro* Reactive Oxygen Species (ROS) assay

ROS production in murine neutrophils were used as a read-out technique to investigate a response by neutrophils following activation with immune complex and C5a. In this assay, 5-luminol is oxidized by ROS (HOCl, OH-and OH.) generated during the respiratory burst of neutrophils. This results in production of 3-aminophthalate anion that relaxes to the ground state and emits light at 425 nm. This emission of light can be further detected by ELISA reader One day prior stimulation, a high binding 96 well ELISA plates (cat No.136102, poly styrene) was coated with 50 mM carbonate/bicarbonate buffer (adjusted pH= 9.6) and 20 µg/mL of human serum albumin (HAS) (Sigma-Aldrich), diluted 1:50. The plate was incubated overnight at 4°C. The day after, the plate was washed with 0.01 M sterile PBS 1X pH=7.2 and blocked for 1h with 200µl of 5% FBS in 0.01 M PBS pH=7.2. Subsequently, wells were washed again with sterile 0.01 M PBS 1X pH=7.2 and incubated with 100µl of rabbit polyclonal anti-human serum albumin Serum IgG (anti-HAS) (Sigma Aldrich) diluted 1:400 in PBS for 3 hours at RT. Antigen coated wells incubated with PBS only were used as a negative control. In parallel BM-derived neutrophils were isolated from C57BL/6J WT and *Clec4n*$^{-/-}$. Afterwards, the plate was washed once more with sterile PBS 1X and cells were adjusted to a concentration of 10^6/mL in RPMI without phenol red supplemented with 1 g/L of glucose and 25 mM HEPES. Cells were added in each well and luminol X20 (3-aminophthalhydrazide) diluted 1:20 in RPMI was added too. To measure the values, the plate was inserted in the TECAN Infinite M200PRO plate reader that was previously preheated at 37 °C. The chemiluminescence reaction was monitored for 2 hours.

2.2.4 *In vitro* quantitative determination of Leukotriene B4 (LTB_4) concentration in BM-derived neutrophils supernatants.

The Parameter™ LTB_4 assay is based on the forward sequential competitive binding technique in which LTB_4, present in a sample, competes with a fixed amount of horseradish peroxidase (HRP)-labeled LTB_4 for sites on a chicken polyclonal antibody. During the incubations, the chicken polyclonal antibody becomes bound to the rabbit anti-chicken antibody coated onto the microplate. Following a wash to

remove excess conjugate and unbound sample, a substrate solution is added to the wells to determine the bound enzyme activity. In this study, to investigate whether the presence of Dectin-2 is indispensable for the LTB_4 released by BM-derived neutrophil isolation, cells (10^6/mL) were stimulated with IC or C5a for 1 hour at 37 °C. After incubation, cells were collected in a falcon tube and centrifuged at 400 x g for 5 minutes. The resulting supernatant was collected and ready to be plated into a 96 well polystyrene microplate (12 strips of 8 wells) coated with a rabbit anti-chicken polyclonal antibody. All the reagents were brought to room temperature before use and so LTB_4 Standard was reconstituted with distilled water for a final production of stock solution (50,000 pg/mL). The standard was then sat for a minimum of 15 minutes prior to making the dilutions. Subsequently, a serial dilution was made to coat the standard deviation onto the plate to obtain a decreased concentration of A1: non-specific binding well (NSB) well was added with 100 µL of Calibrator Diluent RD5-52; B1: zero standard (B0) was added with 50 µL of Calibrator Diluent RD5-52; C1: 2500 pg/mL (It serves as the high standard), D1: 833 pg/mL, E1: 278 pg/mL, F1: 92.6 pg/mL, EG1: 30.9 pg/mL and H1 10.3 pg/mL. The supernatant, 50 µL, was added to the remained wells. A Primary Antibody Solution, 50 µL was added to each well (excluding the NSB well). All wells, except NSB, will now be blue in color. The plate was covered with adhesive strip provided and incubated for 1 hour at room temperature on a horizontal orbital microplate shaker (0.12” orbit) set at 500 ± 50 rpm. After incubation, the plate was not washed but was added with 50 µL of LTB_4 Conjugated to each well. All wells will now be violet in color except the NSB well, which will be pink. The plate was covered with a new adhesive strip and incubated for 3 hours at room temperature on the shaker. After the incubation time ended, the plate was washed 3 times by filling each well with 300 µL of Wash Buffer. In the last wash, the plate was inverted and blotted against clean paper towels. Each well was filled with 200 µL of Substrate Solution and incubated for 30 minutes at room temperature on the benchtop protected from light. After incubation, 100 µL of Stop Solution was added to each well. The color should change from blue to yellow. The plate was, therefore read by Magellan software and the optical density was determined (the microplate used was set up in the software with absorbance at 450 nm), with the correction wavelength set at 450 or 570 nm.

2.2.5 *In vitro* quantitative determination of Interleukin 6 (IL-6) concentration in BM-derived neutrophils supernatants.

One day prior to running the ELISA, Capture Antibody was diluted in Coating Buffer. The amount of 100 µL of this Capture Antibody solution was added into all wells of a 96-well plate provided in the set. Plate was sealed and incubated overnight between 2°C and 8°C. All reagents were brought to room temperature (RT) prior to use. Plate was washed 4 times with at least 300 µL Wash Buffer per well and blot residual buffer by firmly tapping plate upside down on absorbent paper. All subsequent washes were performed similarly. To block non-specific binding and reduce background, 200 µL Assay Diluent was added into each well. Plate was sealed and incubated at room temperature for 1 hour with shaking on a plate shaker (e.g. 500 rpm with a 0.3 cm circular orbit). All subsequent incubation with shaking were performed similarly. While the plate was blocked, standard dilutions were prepared. Plate was washed 4 times with Wash Buffer. The amount of 100 µL/well of standard dilutions and samples were added into the appropriate wells. The plate was sealed and incubated at room temperature for 2 hours with shaking. Plate was washed 4 times with Wash Buffer. The amount of 100 µL of diluted Detection Antibody solution was added into each well, plate was sealed and incubated at room temperature for 1 hour with shaking. The plate was washed 4 times with Wash Buffer. The amount of 100 µL of diluted Avidin-HRP solution was added into each well, plate was sealed and incubated at room temperature for 30 minutes with shaking. The plate was washed 5 times with Wash Buffer. For this final wash, wells were soaked in Wash Buffer for 30 seconds to 1 minute for each wash to minimize background. The amount of 100 µL of TMB Substrate Solution was added into each well and plate was incubated in the dark for 15- 30 minutes or until the desired color develops. Positive wells should turn blue in color. To stop the reaction, 100 µL of Stop Solution was added into each well. Positive wells should turn from blue to yellow. Read absorbance at 450 nm within 15 minutes.

2.2.6 *In vitro* quantitative determination of Interleukin 17A (IL-17A) concentration in BM-derived neutrophils supernatants.

All reagents were brought to room temperature prior to use. The amount of 500 µL of the 500 pg/mL top standard was prepared by diluting 12.5 µL of the standard stock solution in 487.5 µL of Assay Buffer A. A six two-fold serial dilutions of the 500 pg/mL top standard was performed in separate tubes using Assay Buffer A as the diluent. Thus, the Mouse IL-17A/F standard concentrations in the tubes were 500 pg/mL, 250 pg/mL, 125 pg/mL, 62.5 pg/mL, 31.3pg/mL, 15.6 pg/mL, and 7.8 pg/mL, respectively. Assay Buffer A served as the zero standard (0 pg/mL). The plate was washed 4 times with at least 300 µL of 1X Wash Buffer per well and blotted any residual buffer by firmly tapping the plate upside down on absorbent paper. All subsequent washes were performed similarly. A 50 µL of Assay Buffer A was added into each well that contained either standard dilutions or samples. The amount of 50 µL of standard dilutions or samples was added into the appropriate wells. The plate was sealed with a Plate Sealer included in the kit and incubated at room temperature for 2 hours while shaking at 200 rpm. The contents of the plate were discarded into a sink, then the plate was washed 4 times with 1X Wash Buffer as in step 4. The amount of 100 µL of Mouse IL-17A/F Detection Antibody solution was added into each well, the plate was sealed and incubated at room temperature for 1 hour while shaking. The contents of the plate were discarded into a sink, then the plate was washed 4 times with 1X Wash Buffer as in step 4. The amount of 100 µL of Avidin-HRP D solution was added into each well, the plate was sealed and incubated at room temperature for 30 minutes while shaking. The contents of the plate were discarded into a sink, then the plate was washed 5 times with 1X Wash Buffer as in step 4. For this final wash, wells were soaked in 1X Wash Buffer for 30 seconds to 1 minute for each wash to minimize the background. The amount of 100 µL of Substrate Solution F was added into each well and incubated for 15 minutes in the dark. Wells contained mouse IL-17A/F should turn blue in color with an intensity proportional to its concentration. To stop the reaction 100 µL of Stop Solution to was added into each well. The solution color should change from blue to yellow. Read absorbance at 450 nm within 30 minutes.

2.2.5 Flow cytometry

Flow cytometry is a powerful tool to analyze a variety of parameters on an individual cell basis. Specifically, the technology is helpful to count and analyze the size, shape, and properties of individual cells within a heterogeneous fluid mixture, by using a combination of antigens both on the surface and intracellularly. Essentially, flow cytometers illuminate a single cell at a time, detect fluorescence and light scattered from the cell and record this information to be further analyzed by a specific software program. Data obtained is extremely quantitative. Once a suspension of individual cells has been prepared from blood or tissues, the sample is inserted in the machine, and it is ready to be measured. Flow cytometry contains a variety of lasers, optics to gather the light, detectors to sense the light and a computer system to output the data. The passage from the whole cell population to a single cell is due to the presence of a funnel that lets each cell to form a single file line and, subsequently move across the laser beam that will scatter in multiple directions. The flow cytometer detects light scatter in a forward manner called forward scatter and, in a side, manner called side scatter. The detector converts the scatter light into a voltage pulse and finally the computer will convert this data into a histogram plot. In immunology, flow cytometry has been widely used for analyzing, simultaneously, many different populations in a sample and this capability is the immense strength of this experimental technique (Villas, 1998). In this study, the flow cytometry technique was used to analyze the expression markers both extra – and intracellularly on neutrophils under different conditions; when PMNs where stimulated with the immune complex or primed for 40 hours with GM-CSF, we were curious to analyze whether these stimuli would have changed the expression of different receptors by the granulocytes in the *Clec4n*$^{-/-}$ BM-derived neutrophils compared to the C57BL/6J WT; also, the extent of BM reconstitution in recipient mice in chimera experiment was studied by analyzing the peripheral blood on day 0 and lesional tissue after EBA, on day 14. This study allowed us to determine the congenic origin of the circulating neutrophils and to determine which cells are radiosensitive. Hence, flow cytometry was helpful to track the congenic origin of neutrophils infiltrating the skin of the bone marrow chimera mice.

2.2.5.1 *In vivo* chimera experiment and passive EBA samples

For this experiment, compensation was made to avoid many fluorochromes would have overlapped. To compensate, single beads were prepared. Also, the fluorescence minus one control (FMO) was prepared for each fluorochrome and used as a control. FMO is used to identify and gate cells in the context of data spread due to the multicolor panel.

2.2.5.1.1 Peripheral blood sample preparation for flow cytometry

Peripheral blood for FACS analysis was prepared as follows. Briefly, 100 µl from submandibular vein was collected into a tube supplemented with 50 µl of 50 mM EDTA. Subsequently, blood was lysed by adding 500 µl of erythrocyte lysis buffer. The reaction was stopped by adding 500 µl of FACS buffer (3 % BSA in 0.01 M DPBS pH 7.2). After supernatant was discarded, cells were washed thrice with FACS buffer and labelled with the respective antibodies (all diluted in FACS buffer) for 45 min at 4°C: APC-conjugated anti-mouse CD45.1 (0.2 mg/ml), FITC-conjugated anti-mouse CD45.2 (0.5 mg/ml), PerCP-Vio700-conjugated anti-mouse Ly6G (30µg/ml), APC-Vio770-conjugated CD11b (30µg/ml), PE-conjugated anti-mouse F4/80 (0.2 mg/ml), PE/Cyanine-conjugated anti-mouse CD45 (0.2 mg/ml), APC-conjugated anti-mouse Dectin-2 (0.2 mg/ml) and viobility 405/452 fixable dye. 104 cells were acquired on the MACSQuant Analyzer 10 cytometer and analyzed with MACSQuantifyTM software.

2.2.5.1.2 Lesional skin tissue sample preparation for flow cytometry

To prepare lesional tissue sample, both ears, (left and right), of the mouse were collected on day 14 of the EBA experiment. The procedure is the follow: ears were collected and cut in small pieces into a tube containing 1 ml RPMI medium (5% Pen-strep, 10% FBS) with L-glutamine supplemented with 400 µg of liberase TL research grade at 37˚C for 90 min. To stop the enzymatic digestion 1 ml of cold RPMI was

added into the tube. Subsequently, ears were minced with a 70 µm nylon cell strainer to obtain single cell suspension. The strainer was washed with the same cell solution to collect the remaining cells. The cell suspension was centrifuged at 1300 rpm for 5 min. at 4°C. Supernatant was discarded and the pellet was re-suspended in 1ml PBS. The antibodies' staining procedure was the same as the one for the blood with the same antibodies. 10^4 cells were acquired on the MACSQuant Analyzer 10 cytometer and analyzed with MACSQuantifyTM software.

2.2.5.1.3 BM-derived neutrophils sample preparation for flow cytometry

To prepare the BM-derived neutrophils for flow cytometry analysis, neutrophils were isolated from the bone marrow by following the procedure already mentioned above in chapter 2.3.2. Briefly, on day 14 of the experimental passive EBA model of chimera mice both legs were carefully detached. The procedure went into different steps by following the neutrophil isolation protocol to finally obtain BM-derived neutrophils. The samples were centrifuged, and the supernatant was discarded. The pellet was resuspended in FACS buffer (3 % BSA in 0.01 M DPBS pH 7.2) and the antibody staining procedure was the same as the one for the blood and skin with the same antibodies. 100.000 cells/100 µL cells were acquired on the MACSQuant Analyzer 10 cytometer and analyzed with MACSQuantifyTM software.

2.2.5.1.4 BM-derived neutrophils purity analysis

To ensure the isolation of neutrophils from the BM was effective after MACS, each experiment consisted of analyzing the PMNs by labelling them with Ly6G antibody, known to be a neutrophils marker, following the staining protocol assessed in our laboratory. Briefly, samples were centrifuged, and the supernatant was discarded. The pellet obtained was resuspended in FACS buffer to have 10^4 cells/100µl. Cells were blocked with Fc blocking reagent (1:10) for 10 minutes at RT. Viobility dye (1:100) was added without washing the cells and samples were incubated for 5 minutes at RT in the dark. Cells were stained with Ly6G antibody (1:10) for 1h in the dark at 4°C. The samples were centrifuged, and the supernatant was discarded. The pellet was resuspended in FACS buffer (3 % BSA in 0.01 M DPBS pH 7.2) and

10^4 cells were acquired on the MACSQuant Analyzer 10 cytometer and analyzed with MACSQuantifyTM software. In our laboratory, isolation of neutrophils from murine BM was obtained at the percentage of 87 -95 purity (Figure 10).

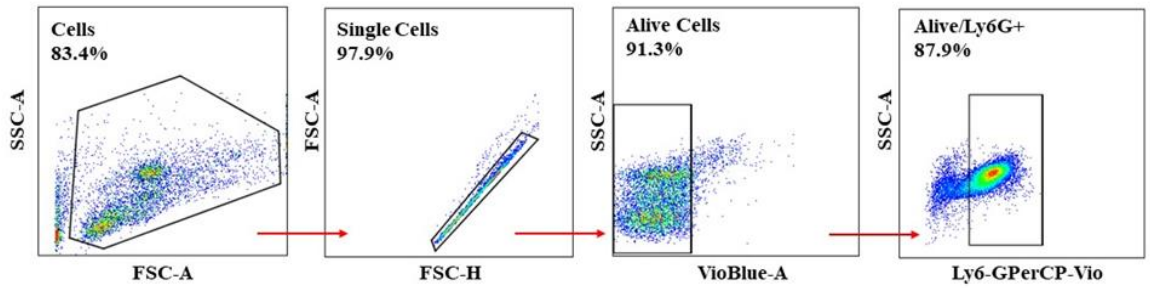

Figure 10 Representative illustration of BM-derived neutrophils purity isolation.
BM-derived neutrophils were isolated from C57BL/6J WT and Clec4n$^{-/-}$ mice, through a magnetic separation with MS column per negative selection. Each sample (10^4 cells/100µl) was labeled with anti – Ly-6GPerCP-Vio 700 antibody (1:10) and analyzed by flow cytometry. The purity of neutrophils was typically 87-95%.

2.2.6 *In vivo* passive EBA in neutrophil specific FcγRIV conditional knockout mice

For this experiment, compensation was made to avoid many fluorochromes would have overlapped. To compensate, single beads were prepared. Also, the fluorescence minus one control (FMO) was prepared for each fluorochrome and used as a control. FMO is used to identify and gate cells in the context of data spread due to the use of a multicolor panel.

2.2.6.1 Peripheral blood sample preparation for flow cytometry

Peripheral blood for FACS analysis was prepared as follows. Briefly, 100 µl from submandibular vein was collected into a tube supplemented with 50 µl of 50 mM EDTA. Subsequently, blood was lysed by adding 500 µl of erythrocyte lysis buffer. The reaction was stopped by adding 500 µl of FACS buffer (3 % BSA in 0.01 M DPBS pH 7.2). After supernatant was discarded, cells were washed thrice with

FACS buffer and labelled with the respective antibodies (all diluted in FACS buffer) for 45 min at 4°C: FITC-conjugated anti-mouse Ly6C (30µg/200 µl), PerCP-Vio700-conjugated anti-mouse Ly6G (30µg/ml), APC-conjugated anti-mouse F4/80 (0.2 mg/ml), PE-conjugated anti-mouse CD16.2 (FcγRIV) (0.2 mg/ml), APC-conjugated anti-mouse Dectin-2 (0.2 mg/ml), APC-Vio770-conjugated anti-mouse CD11b and viobility 405/452 fixable dye. 10^4 cells were acquired on the MACSQuant Analyzer 10 cytometer and analyzed with MACSQuantifyTM software.

2.2.6.2 Lesional skin tissue sample preparation for flow cytometry

To prepare lesional tissue sample, both ears, (left and right), of the mouse were collected on day 14 of the EBA experiment. The procedure was the follow: ears were collected and cut in small pieces into a tube containing 1 ml RPMI medium (5% Pen-strep, 10% FBS) with L-glutamine supplemented with 400 µg of liberase TL research grade at 37˚C for 90 min. To stop the enzymatic digestion 1 ml of cold RPMI was added into the tube. Subsequently, ears were passed through a 70 µm nylon cell strainer to obtain single cell suspension. The strainer was washed with the same cell solution to collect the remaining cells. The cell suspension was centrifuged at 1300 rpm (400xg) for 5 min. at 4°C. Supernatant was discarded and the pellet was re-suspended in 1ml PBS. The antibodies´ staining procedure was the same as the one for the blood with the same antibodies. 10^4 cells were acquired on the MACSQuant Analyzer 10 cytometer and analyzed with MACSQuantifyTM software.

2.2.7 *In vitro* BM-derived neutrophils staining

To assess whether the main receptors involved in the inflammation process were expressed externally or internally on neutrophil membrane, samples were prepared by isolating neutrophils from BM using the method in paragraph 2.2.2. Once isolated, neutrophils were stained as follow:

2.2.7.1 *In vitro* BM-derived neutrophils extracellular staining

Isolated neutrophils were stimulated with the immune complex on a pre-coated plate for 1 h at 37°C. Subsequently, samples were centrifuged, and the supernatant was discarded. The pellet obtained was resuspended in FACS buffer to have 10^4 cells/100µl. Cells were blocked with Fc blocking reagent for 10 minutes at RT. Viobility dye was added without washing the cells and samples were incubated for 5 minutes at RT in the dark. Cells were stained with the follow fluorochromes: APC-conjugated anti-mouse Dectin-2 (0.2 mg/ml), APC-Vio770-conjugated anti-mouse CD11b, APC-conjugated anti-mouse F4/80 (0.2 mg/ml), PE-conjugated anti-mouse CD16.2 (FcγRIV) (0.2 mg/ml), PerCP-Vio700-conjugated anti-mouse Ly6G (30µg/ml) and viobility 405/452 fixable dye. 10^4 cells were acquired on the MACSQuant Analyzer 10 cytometer and analyzed with MACSQuantifyTM software.

2.2.7.2 *In vitro* BM-derived neutrophils intracellular staining

To stain intracellularly, BM-derived neutrophils (100.000/100 µL) were centrifuged at 400 x g x 5 minutes. Supernatant was discarded and pellet was resuspended with 90 µL of MACS buffer with 10 µL of FcR block solution and incubated for 10 minutes at RT. Without washing the suspension, 1 µL of viobility dye was added and incubated for 5 minutes at RT in the dark. After incubation, 1 mL of MACS buffer was added, and cell suspension was centrifuge at 400 g x 5 minutes. Following the protocol, 0.5 mL of the Transcription Factor 1X solution was diluted (1:4) with Fix diluent and added in the suspension and incubated for 60 minutes in the dark at RT. Subsequently, without washing step 1 mL of the Transcription Factor 1X Permanent buffer diluted with DDW (1:10) was added and cells were centrifuged at 400 x g for 5 minutes. Supernatant was discarded and pellet was resuspended in 0.5 mL of Transcription Factor 1X Permanent buffer diluted with DDW (1:10). Cells were centrifuged at 400 x g for 5 minutes and the supernatant was discarded. The pellet was resuspended in 100 µL of MACS buffer and Dectin2-APC conjugated was applied (1:10) into the cells. After the sample was incubated 1 hour at RT in the dark, 0.5 µL of Transcription Factor 1X Permanent buffer diluted with DDW (1:10)

was added, without washing step, into the cells and centrifuged at 400xg for 5 minutes. Cells were washed twice with 1 mL of MACS buffer band centrifuged at 400xg for 5 minutes. Pellet was resuspended in 200 µL of MACS buffer and were acquired on the MACSQuant Analyzer 10 cytometer and analyzed with FlowJo 6.00.

2.2.8 TRIZOL RNA isolation from tissues and cells

To define a cellular gene expression from tissues or cells under conditions, a good readout is RNA isolation. RNA is short-lived and is prone to degradation by enzymes called RNAses. For this reason, the protocol has been used from W.M. Keck Foundation Biotechnology Microarryay Resource Laboratory at Yale University (Chomczynski and Mackey, 1995), comprises the use of TRIZOL reagent, a potent protein denaturant that inactivates all the enzymes responsible for RNA denaturation. In this study, lesional skin tissues from passive EBA mice were harvested, snap frozen samples were first homogenized by using a mortar and pestle that has been cooled with liquid nitrogen. Samples were transferred into a sterile Eppendorf and were lysed with 1 mL of TRIZOL.

To isolate RNA from fresh isolated BM-derived neutrophils in suspension were spined for 5 minutes at 300 x g. Media was removed and cells were resuspended in ice cold PBS. After a second centrifugation, supernatant was discarded, and the pellet resuspended with 1 mL TRIZOL reagent.

In both procedures, samples were incubated for 5 minutes at RT to permit the complete disassociation of nucleoprotein complexes. Subsequently, samples were centrifuged, and the supernatant was transferred into a new sterile tube. The procedure is the follow: PHASE SEPARATION: samples were treated with 200 µl of chloroform. Vortex for 15 seconds and incubated for 3 minutes at RT. After incubation, they were centrifuged for 15 minutes at 2-8°C to a final separated mixture: lower red, phenol-chloroform phase, an interphase and a colorless upper aqueous phase where RNA resides. Subsequently, the upper aqueous phase was carefully transferred into a new sterile tube; RNA PRECIPITATION: the aqueous phase was mixed with 500 µl isopropyl alcohol, incubated for 10 minutes at RT and centrifuged at 12,000 x g; RNA WASHING STEP: supernatant was discarded, and

the RNA pellet was washed with 1 mL of 75% ethanol. Subsequently, the sample was vortex and centrifuged at 7,500 x g for 5 minutes at 2-8°C. This step was repeated one more time; REDISSOLVING RNA: RNA pellet was air-dried and dissolved in 25 µl of DEPEC-treated water; SPECTROPHOTOMETRIC ANALYSIS: finally, sample concentration was determined by measuring the optical density (OD) unit at 260 nm and 280 nm by using 10 µl microcuvette. The samples were then adjusted to 100 ng/µl to proceed with the cDNA synthesis.

2.2.8.1 First strand Complementary DNA (cDNA) synthesis

The total RNA obtained from the tissues or cells was used as a template for an efficient synthesis of first strand cDNA. Briefly, PCR reaction was performed by using the RevertAid First Strand cDNA Synthesis Kit (Thermo Scientific, #K1621). To prepare the reaction the following reagents were added into a sterile, nuclease-free tube on ice in the indicated order:

Table 4: First strand Complementary DNA (cDNA) synthesis

The PCR was carried out using the following thermal cycling conditions:

Template RNA	total RNA	1 µL
Primer	Oligo $(dT)_{18}$ primer	1 µL
Water, nuclease-free		12 µL
5 x reaction buffer		4 µL
RiboLock RNase Inhibitor (20 U/µL)		1 µL
10 mM dNTP Mix		2 µL
RevertAid M-MuLV RT (200 U/µL)		1 µL

2.2.8.2 Real-Time PCR (qPCR) amplification of first strand cDNA

The product of the first strand cDNA synthetis was used directly in qPCR by preparing the regents as follow:

Forward (10 µM stock)	0.5 µL
Reverse (10 µM stock)	0.5 µL
Syber green	5 µL
cDNA	4 µL
Total volume	10 µL

The cDNA was loaded (4 µL) into the pre-sterilized PCR plate half skirt flat, 0.2ml 96 well following the addition of 6 µL of the master mix. The PCR was carried out using the following thermal cycling conditions:

Hold	2 min.	50 °C	
Denaturation	2 min.	95 °C	1 cycle
Annealing	15 sec.	95 °C	
Extension	1 min.	60 °C	40 cycles
Cooling	∞	4 °C	

Table 4 List of primers used in qPCR.

All the primers were constructed in our laboratory to be specific for the genes used in the experiments.

OLIGONAME	SEQUENCE 5´ → 3´	Tm (°C)
m Clec4n_forward	GCGAGCTGTGTGGTGACTTAC (21)	52
m Clec4n_reverse	CAGTGATTTGGGCAGCATCC (20)	55
m IL-17_forward	TCAGCGTGTCCAAACACTGAG (21)	59,8
m IL-17_reverse	CGCCAAGGGAGTTAAAGACTT (21)	57,9
m IL-23_forward	TGTCACGGAGGAATCACAAGT (21)	52
m IL-23_reverse	GGCATGAGGTTCCGAAAAGC (20)	56
m CXCL2_forward	CCAAGGGTTGACTTCAAGAACATC (24)	56
m CXCL2_reverse	TTTGACCGCCCTTGAGAGTG (20)	55
m IL-1beta_forward	GAAATGCCACCTTTTGACAGTG (22)	58,4
m IL-1beta_reverse	TGGATGCTCTCATCAGGACAG (21)	59,8
m TNFα_forward	GGTGATCGGTCCCCAAAGG (19)	56
m TNFα_reverse	GTTTGCTACGACGTGGGCTA (19)	53
m GM-CSF_forward	GGCCTTGGAAGCATGTAGAGG (21)	61,8
m GM-CSF_reverse	GGAGAACTCGTTAGAGACGACT (22)	60,3
m HPRT_forward	TCAGTCAACGGGGGACATAAA (21)	57,9
m HPRT_reverse	GGGGCTGTACTGCTTAACCAG (21)	61,8

2.9 *In vitro* cell migration

Cell migration is widely used in immunology to investigate the response of a cell towards chemoattractants. In this study, C5a (10 nM) was chosen as chemical signals to study the response of C57BL/6J WT and *Clec4n*$^{-/-}$ neutrophils. To prepare the reagents, an established protocol, in the laboratory, was followed. Briefly, freshly isolated BM-derived neutrophils were isolated as previously described. Cells were

counted by using the propidium iodide solution (1:10) in MacsQuant devised and adjusted to a work concentration of 1.6 x 10^6 /mL. Meanwhile, a 24 transwell polycarbonate membrane cell culture insert was primed with 100 µL neutrophil media and incubated for 1h at 37 °C. Subsequently, the upper part buffer was removed, and cells were added following the setup:

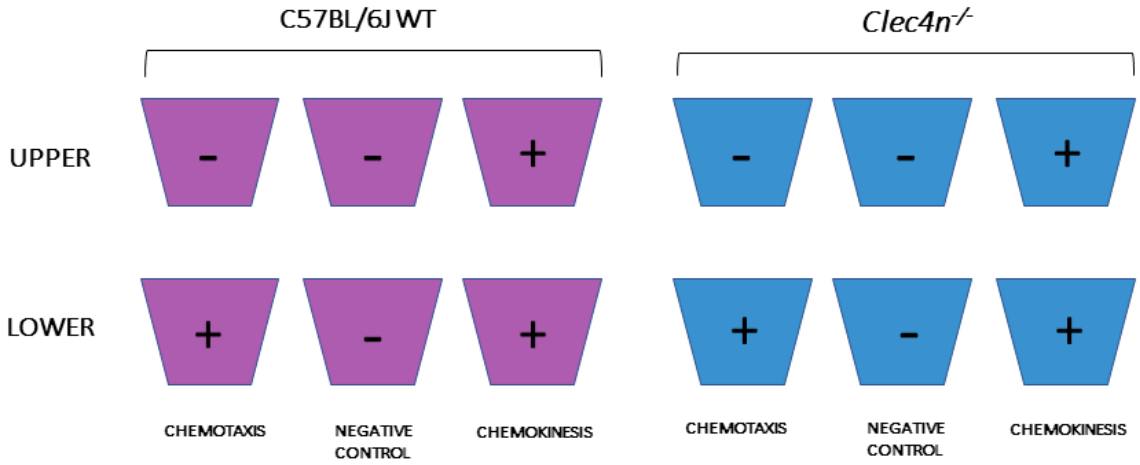

Figure 11 Cell migration transwell setup.

The transwell insert is constituted by two compartments: the upper and the lower part. The insert is constituted by the membrane that contains pores to let the cells migrate through it. The chemoattractants (+) and the respective vehicle controls (-) were loaded in the lower part and the cells treated with the chemoattractants (+) and, only cells (-) were loaded in the upper part.

Cells were incubated for 2 hours at 37 °C and, subsequently only the lower part was collected, carefully, to be analyzed in MacsQuant device. The measurement was taken as illustrated in Figure 11 by analyzing the chemotaxis, the negative control and the chemokinesis.

2.10 Bone marrow chimera mouse model

Transplantation of congenically labeled bone marrow (BM) into lethally irradiated mice is a valuable tool to study cellular processes in immunology. This approach is utilized in immunological research to study the contribution of various cell types of hematopoietic versus non-hematopoietic during the *in vivo* passive EBA experiment. It is based on the concept that radiosensitivity of cells is proportional to

the rate of cell division and inversely correlating to the degree of their differentiation; thus, positioning hematopoietic cells in the bone marrow as highly radiosensitive cells. To generate bone marrow chimera, recipient mice are subjected to predetermined lethal or sublethal doses of X-ray or γ radiation and reconstituted with donor bone marrow. To prepare the bone marrow cells, femurs, tibias and fibulas were retrieved from two adult donor mice for each group (4 months old). The mice are then monitored by flow cytometry for the presence of donor cells four to six weeks post BM transplantation. This protocol utilizes congenic mouse strains that differ at the common leukocyte antigen (CD45) locus. The CD45 antigen is expressed by all nucleated cells and allows donor cells to be easily distinguished from host cells by differential expression of CD45.1 and CD45.2 alleles between the donor and the host cells (Shen et al., 1985). The expression of Dectin-2 has been described on different cell types, some of which belong to the radioresistant and others to the radiosensitive cell group. In this study, the bone marrow chimera was conducted to identify the relative contribution of radiosensitive and radioresistant cells to the development of inflammation. Bone marrow chimaera was produced between congenic B6 wild type (carrying the CD45.1 allele, B6.SJL-Ptprc^{a} Pepc^{b}/BoyJ) and *Clec4n*$^{-/-}$ mice (carrying the CD45.2 allele) and the course of passive EBA in these animals was investigated. In the experiment, it was planned to produce bone marrow chimera mice and to induce an experimental EBA in these mice 3-4 weeks after the irradiation necessary to produce the chimera. After 3-4 weeks, the bone marrow has usually already recovered and has been almost completely replaced by the donor bone marrow. After 3-4 weeks from irradiation, however, skin-derived macrophages have not yet been replaced by donor cells via the blood. By bringing forward the induction of the experimental EBA to 3-4 weeks after irradiation, it was possible to determine whether the molecule Dectin-2 on skin-derived macrophages is important for the EBA or not.

2.10.1 Generation of bone marrow chimera

All reciprocal combinations of bone marrow chimera were generated by lethal (10Gy) γ irradiation of 11-weeks-old recipient mice (Figure 12). Subsequent BM

reconstitution was performed by intravenous injection of 10^7 isolated BM cells from two of the donor strains (as indicated in the text).

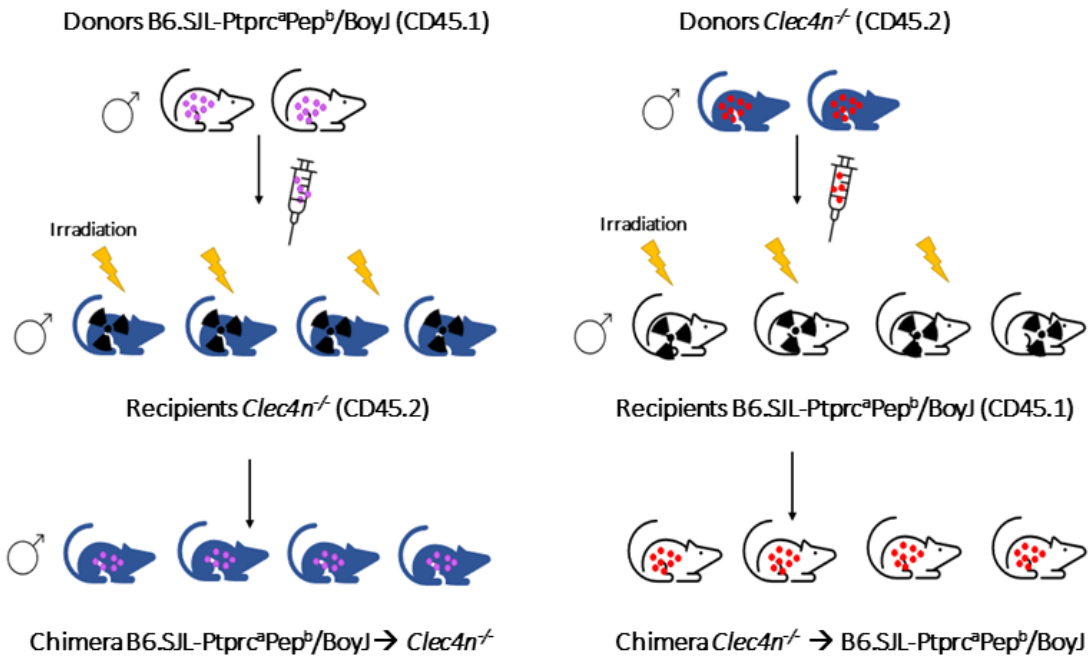

Figure 12 Schematic illustration of bone marrow chimera generation.

Recipients from each group (B6.SJL-Ptprc^{a}Pep^b/BoyJ and *Clec4n*$^{-/-}$) were first irradiated with (10Gy) γ irradiation and injected with BM donor cells. The B6.SJL-Ptprc^{a}Pep^b/BoyJ CD45.1 mice had received the *Clec4n*$^{-/-}$ BM cells and the *Clec4n*$^{-/-}$ mice had received the B6.SJL-Ptprc^{a}Pep^b/BoyJ CD45.1 BM cells.

To study the possible cellular sources of Dectin-2 in EBA, BMC mice, using B6.SJL-Ptprc^{a}Pep^b/BoyJ (CD45.1+) and *Clec4n*$^{-/-}$ (CD45.2+) mice, were generated as demonstrated in Fig. 11. All reciprocal combinations of Ptprc^{a}Pep^b/BoyJ and Clec4n-/-mice (i.e., *Clec4n*$^{-/-}$ → Ptprc^{a}Pep^b/BoyJ; Ptprc^{a}Pep^b/BoyJ → *Clec4n*$^{-/-}$) were generated (abbreviated as genotype of donor bone marrow → genotype of recipient mouse). To verify successful transplantation of donor bone marrow into the recipient mice, four weeks after reconstitution, 100 µL of peripheral blood was collected from submandibular vein and analyzed for CD45.1 and CD45.2 expression on Ly6G+ cells by flow cytometry.

2.11 Skin histopathology

Histopathology of the skin is an important test for dermatological diagnosis. It is a technique that involves examining tissues or cells under the microscope. Regarding EBA disease, subepidermal blisters that appear in the late stage of inflammation can be observed. It can be seen the presence of neutrophils infiltration or mixed with eosinophils and mononuclear cells at the dermal level.

2.11.1 Hematoxylin and eosin (H&E) staining

In this study, the clinical phenotype of EBA was assessed by histopathology and direct immunofluorescence technique. Briefly, for histopathology analysis, lesional skin biopsies from sacrificed mice on day 14 were fixed with 4% histofix solution and embedded in paraffin block. Skin paraffin sections were cut on microtome (6 µm) and stained for hematoxylin and eosin (H&E) according to a standard protocol used in the routine histopathological laboratory at the Department of Dermatology Lübeck. All sections were visualized using the BZ-9000E series Keyence microscope.

2.12 Immunofluorescence microscopy

Immunofluorescence microscopy is a technique that researchers use to assess the localization and the expression levels of the protein of interest. In clinical immunodermatology, there are two methods used to determine a specific bound of an antibody to its antigen: direct and indirect immunofluorescence (DIF and IDIF, respectively). Once the bound through a fluorescein linked Abs to a protein, immunoglobulin occurs, the excitation of the coupled fluorophore molecules allows the visualization of the protein using the fluorescence microscope.

2.12.1 Direct immunofluorescence (DIF) microscopy

To detect tissue bound rabbit anti-mCol7c IgG in murine perilesional skin, direct immunofluorescence microscopy was performed. In brief, 6µm of perilesional skin cryosections were prepared from tissue biopsies. Consequently, sections were air dried for 10 min at RT, fixed in cold aceton (10 min, -20˚C) and washed in 0.01 M PBS (5 min x 3) before staining. Pre-fixed skin sections were incubated with AlexaFluor 594-conjugated AffiniPure Donkey anti-rabbit IgG (0.003 mg/ml) antibody for 1 hour at RT. All antibodies were diluted in 0.01 M PBS pH 7.2.

Following extensive wash in 0.01 M PBS (5 min x 3) slides were mounted with diamidino-2-phenylindole dihydrochloride (DAPI) fluoromount G (Southern Biotech, USA) that intercalates with DNA and stains the nuclei of cells. Slides were stored at -20˚C until further visualization using the BZ-9000E series Keyence microscope (Keyence Deutschland GmbH, Neu-Isenburg, Germany).

2.12.2 Indirect immunofluorescence (IIF) microscopy

Before conducting the experimental EBA *in vivo*, the purified rabbit anti-mCOL7c IgG to type VII collagen in murine skin was tested to assess its reactivity. Briefly, 6 µm frozen skin sections obtained from normal mouse tail skin were incubated with serial dilutions of rabbit anti-mCol7c IgG (1:100-1:256,000; diluted in 0.01 M PBS pH 7.2). Following an extensive washing step (5 min x 3; 0.01 M PBS pH 7.2) IgG binding along the DEJ was visualized using a secondary AlexaFluor 594-conjugated AffiniPure Donkey anti-rabbit IgG (3 µg/ml) antibody. After 1 hour of incubation with the secondary antibody, slides were washed (5 min x 3; 0.01 M PBS pH 7.2) and mounted with DAPI fluoromount G.

2.13 IMMUNOHISTOCHEMISTRY

To determine the nature of the cells that are infiltrated in the perilesional skin of mice suffering from EBA, an immunohistochemistry (IHC) staining was performed. The

IHC method comprises different fixatives: fixation of tissue to a glass result in a strong defragmentation of membrane systems, thus leading to optimal access of Abs to different cellular epitopes. Following fixation, the tissues are incubated with primary antibodies directed against specific antigenic targets. The binding of the primary Ab can be further visualized by direct fluorescein or enzymatic labelling, or by addition of secondary Abs that are covalently linked to fluorophores and recognize the Fc portion of the primary antibody. Upon their excitation, fluorophores emit light at a certain wavelength that can be detected by immunofluorescence microscopy. In this study, frozen perilesional skin sections were stained for infiltration of neutrophils, and macrophages, using Ly6G, and CD68 monoclonal Abs. Following embedding in Tissue-Tek cryomold, sections were cut on cryostat and stored at -20˚C until further use. In all protocols frozen skin sections were air dried for 10 min at RT and fixed in cold aceton (10 min, -20˚C) before staining. All dilutions and washing steps were performed using 0.01 M PBS pH 7.2 (5 min x 3), unless indicated otherwise.

2.13.1 Immunohistochemistry of complement 3 staining

Cryosection slides of lesional skin, from *Clec4n*$^{-/-}$ and wild-type mice, were incubated for 10 minutes at RT. To later prevent liquids from drifting and mix, the interested sections were circled with the hydrophobic pen. Subsequently, slides were incubated for 10 minutes with cold acetone, at 4°C, to be fixed. Slides were washed 3 times for 5 minutes with PBS, pH 7.2, and blocked with 5% goat serum, diluted in PBS, pH 7.2, for 20 minutes at RT in humid chamber. No washing step was required and a primary antibody, rat anti-mouse complement 3 diluted 1:200 in PBS, pH 7.2, was applied on the lesional skin sections and incubated for 1 hour at RT. After incubation, slides were washed 3 times for 5 minutes with PBS, pH 7.2, and incubated with a secondary antibody, goat anti-rat IgG, diluted 1:500 in PBS, pH 7.2, for 1 hour at RT. After incubation, slides were washed 3 times for 10 minutes with PBS, pH 7.2 and incubated with Alexa fluor conjugated 594 goat anti-rat diluted 1:500 in PBS, pH 7.2, for 30 minutes at RT in the dark. Slides were washed 3 times for 5 minutes with PBS, pH 7.2, and DAPI was mounted on the slides. The slides were kept overnight in the dark. The detection of complement 3 deposition was

determined by capturing the images of chosen sections using BZ-II-Analyzer, Keyence.

2.13.2 Immunohistochemistry of mCOL7 IgG staining

Cryosection slides of lesional skin, from *Clec4n*$^{-/-}$ and wild-type mice, were incubated for 10 minutes at RT. To later prevent liquids from drifting and mixing, the interested sections were circled with the hydrophobic pen. Subsequently, slides were incubated for 10 minutes with cold acetone, at 4°C, to be fixed. Slides were washed 3 times for 5 minutes with PBS, pH 7.2, the mCOL7c IgG antibody was applied 1:100 on the skin sections and incubated for 1 hour in the dark at RT in a humid chamber. After incubation, slides were washed 3 times with PBS, pH 7.2, 50 µl of secondary antibody, streptavidin 488, was applied following 1 hour incubation fat RT. Slides were washed 3 times for 5 minutes with PBS, pH 7.2, and DAPI was mounted on the slides. The slides were kept overnight in the dark. The detection of mCOL7 IgG deposition was determined by capturing the images of chosen sections using BZ-II-Analyzer, Keyence.

2.14 Statistical analysis

Data was organized using Microsoft Excel. Statistical analysis was performed using the software GraphPad Prism 6 (GraphPad, San Diego, California, USA). Unless otherwise state data was presented as mean ± SEM. Statistical tests used are stated where applicable.

RESULTS

3.1 Requirement of Dectin-2 for the induction and progression of antibody transfer EBA

To address if Dectin-2 plays a broader role in the regulation of neutrophil activity beyond the recognition of pathogen-associated molecular patterns, the antibody transfer EBA mouse model was used. The EBA transfer model reflects the effector phase of the autoimmune blistering skin disease epidermolysis bullosa acquisita (EBA).

3.1.1 *Clec4n*$^{-/-}$ mice are protected from induction of antibody-transfer EBA

To study the role of Dectin-2 in the pathogenesis of AAb-induced skin inflammation, antibody-transfer EBA mouse model was induced in C57BL/6J WT and *Clec4n*$^{-/-}$ mice. Injection of 50 µg of affinity purified rabbit anti-mCol7c IgG into the neck, right foreleg, and hindleg of *Clec4n*$^{-/-}$ mice (n=18) demonstrated that these mice were largely protected from EBA in compared to age- & sex-matched C57BL/6J WT mice (n=18). C57BL/6J WT mice developed severe signs of erythema and crusts on the ears and alopecia around the eyes, starting from day 6 of the experiment, while *Clec4n*$^{-/-}$ remained completely protected from disease and did not show EBA lesions on their skin through the entire observation period. Figure 13A showed a clinical score of experimental EBA in C57BL/6J WT and *Clec4n*$^{-/-}$ mice. Since the beginning of the score, on day 4, it can be seen a slight difference but still not significant raise of the disease trend between the two groups. On day 8 there was a significant increase of the clinical manifestation in the C57BL/6J WT mice while, in contrary, while the *Clec4n*$^{-/-}$ mice demonstrated a complete protection with no presence of lesions in the skin. WT mice exhibited EBA-lesions spreading to their entire body; figure 13B representatively illustrated the development of crusts and erosions on the head and neck regions, right foreleg, and trunk. The clinical score of the disease in C57BL/6J WT mice peaked on day 12 of the experiment whereas, a complete protection can be observed a complete protection in the *Clec4n*$^{-/-}$ mice during the

entire observation period of the experiment. Observations of residual inflammation activity in *Clec4n*$^{-/-}$ mice could be attributed to either negligible AAb-induced inflammation or unrelated scratching/biting induced-induced inflammation. Histopathological analysis of the lesional skin, showed separation of derma-epidermal junction and mononuclear cellular infiltration. Despite lack of dermal-epidermal separation in *Clec4n*$^{-/-}$ mice both groups of mice showed the immunofluorescence staining of C3 and linear deposition of IgG, figure 13 E and F.

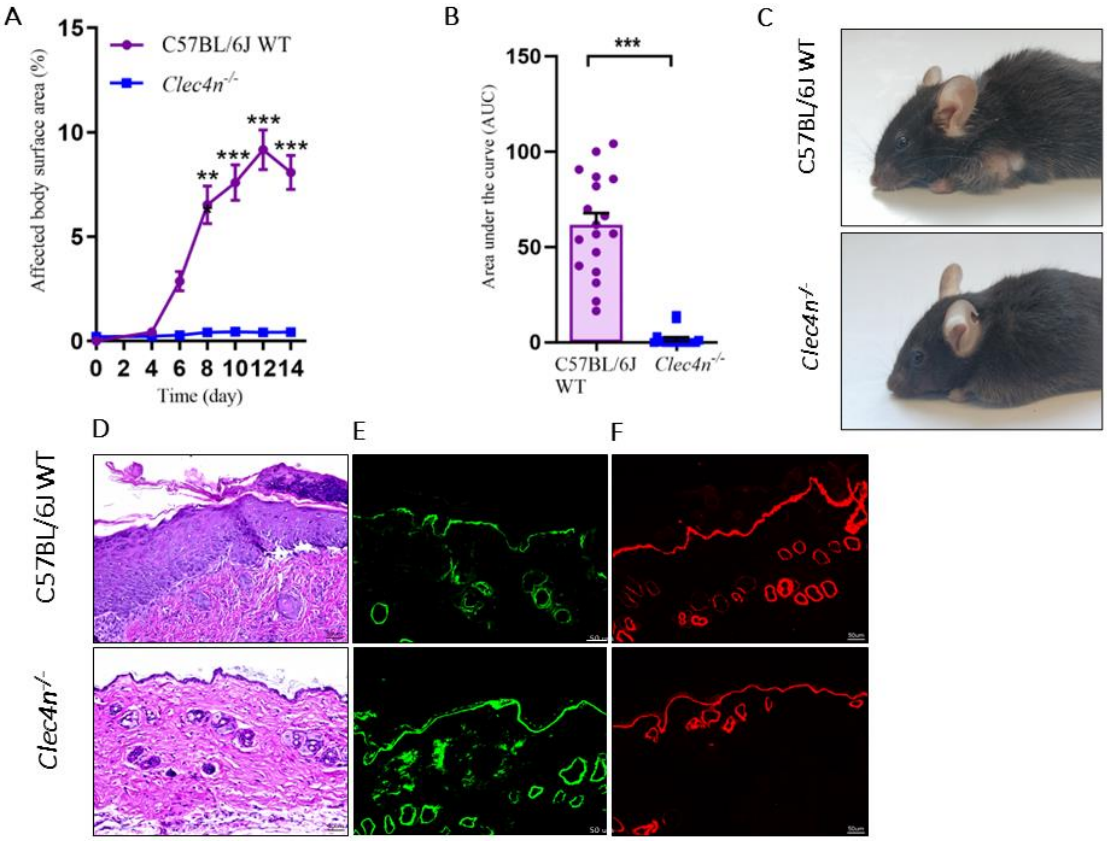

Figure 13 *Clec4n*$^{-/-}$ mice are completely protected from EBA.

Experimental EBA was induced as described in paragraph 2.2.1. (A) Clinical score of experimental EBA in WT (●) vs. *Clec4n*$^{-/-}$ (■). *Clec4n*$^{-/-}$ mice show a complete protection from the disease as compared to C57BL/6J WT animals (n=18); (B) Area under the curve (AUC) of affected ear surface area representing clinical score is shown. (C) Representative clinical pictures of C57BL/6J WT and *Clec4n*$^{-/-}$ mice on day 14 of the experiment; erosion and alopecia are manifested only in the C57BL/6JWT mice; (D) Histological sections of lesional skin highlight derma-epidermal junction separation in the C57BL/6J WT mice and an abundant cellular infiltrate. In contrast, there is no evidence of skin inflammation in the *Clec4n*$^{-/-}$ animals; Immunohistochemistry analysis reveal linear deposition of rabbit anti-mCol7c IgG and (E) C3 deposition (F) in the skin of both C57BL/6J WT and

Clec4n$^{-/-}$ mice. (All data are presented as mean ± SEM; One-Way ANOVA test; * p ≤ 0.05; Scale bar, 50µm).

3.1.1.1 Downregulation of *Cxcl2* and *Il-1ß* are low expressed in *Clec4n*$^{-/-}$ mice in passive EBA model

Pro-inflammatory cytokines contribute to the initiation and propagation of autoimmune inflammation (Moudgil K.D., Choubey D. 2011). The cytokines IL-17 and IL-23 are involved in neutrophils recruitment and migration through the induction of granulopoiesis and production of IL-1β, TNF- α and neutrophils chemoattractant chemokines like CXCL-2. To investigate whether deficiency in Dectin-2 compromised the expression of genes involved in the inflammatory response, mRNA levels of (interleukin 17) *Il-17*, (interleukin 23) *Il-23*, (chemokine (C-X-C motif) ligand 2) *Cxcl2*, (interleukin-1beta) *Il-1β*, (tumor necrosis factor-alpha) *Tnf-α* and (colony stimulating factor 2) *Csf2* (encoding for GM-CSF) genes in lesional skin of C57BL/6J WT and *Clec4n*$^{-/-}$ mice on day 14 after induction of EBA was analyzed. RNA was extracted from inflamed skin as described in paragraph 2.2.8. As expected, the *Clec4n*$^{-/-}$ mice showed no expression of *Clec4n*$^{-/-}$ gene compared to the C57BL/6J WT, figure 14 A. No significant difference was observed in the expression of IL-17 and IL-23 between C57BL/6J WT and *Clec4n*$^{-/-}$ that both *Il-17* and *Il-23* genes were not statistically different expressed in both C57BL/6J WT and *Clec4n*$^{-/-}$ mice in EBA figure 15 B-C. Additionally, no significant difference was found in the expression of the pro-inflammatory cytokines, TNF-α and GM-CSF between the two groups, figure 15 F-G. In contrary, *Cxcl2* and *Il-1β* genes were not expressed at higher level in *Clec4n*$^{-/-}$ mice compared to the C57BL/6J WT, figure 15 D-E These results suggested that IL-17, IL-23, TNF-α and GM-CSF receptors are continuously expressed during inflammation to promote the migration of neutrophils, however the expression of *Cxcl2* gene is low expressed. Thus, this latter is regulated by the potent pro-inflammatory IL-1β that is, also, decreased in the *Clec4n*$^{-/-}$ mice. Although, the expression of the genes *Il-17*, *Il-23*, *Tnf-α* and *Csf2* remained constantly highly expressed during EBA inflammation, it may be that the absence of Dectin-2 leads to a disruption of the signal downstream where an efficient expression of certain cytokines and chemokines, in this case Cxcl2 and Il-1β, is not

well orchestrated. Subsequently, the recruitment of the leukocytes might be lower because the transcription of these genes to a final protein product is compromised. Furthermore, Il-1β promotes the release of free radicals, ROS, by helping the digestion of the autoantibodies by neutrophils through phagocytosis. Consequently, the existent signal cascade loop could be disrupted and might not facilitate PMNs exocytosis/degranulation of immune components to induce blister formation and visible signs of inflammation at the skin surface.

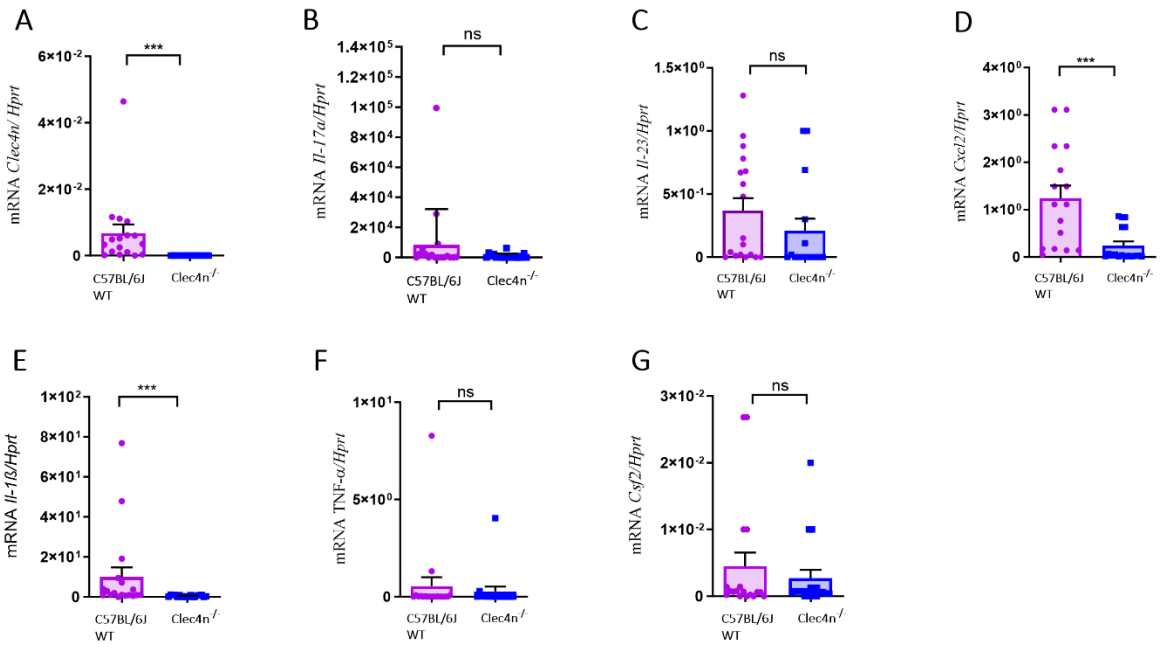

Figure 14 Expression of *Cxcl2* and *Il-1β*, was decreased at the mRNA level in *Clec4n* deficient mice in inflamed EBA skin.

Profiled genes expression at mRNA levels in EBA. RNA was extracted from inflamed tissues on day 14 in both C57BL/6J WT and *Clec4n*$^{-/-}$ mice. Measurement was normalized to the housekeeping gene Hprt. *Clec4n* gene was used as a control (A). No difference in the expression of the genes *Il-17*, *Il-23, Tnf-α* and *Csf2* (B, C, F and G). The chemokine gene *Cxcl2* and its regulator pro-inflammatory cytokine gene *Il-1ß* showed a significant decrease in the *Clec4n*$^{-/-}$ mice compared to the C57BL/6J WT. All data are presented as mean ± SD; n=3 * $p \leq 0.05$. Statistical analysis was made with Man-Whitney test.

3.1.1.2 Sera levels of LTB_4 are decreased in *Clec4n*$^{-/-}$ mice in EBA

Results observed in the clinical score of EBA mouse model suggested, at first approach, that *Clec4n*$^{-/-}$ mice were not affected by any inflammatory process during the experimental model. To understand whether there is a correlation between the absence of Dectin-2 and the release of inflammatory mediators, the levels of IL-6, LTB_4 and IL-17A in the sera of EBA mice was evaluated. Peripheral blood from both C57BL/6J WT and *Clec4n*$^{-/-}$ mice was taken on day 14 and after centrifugation, serum was collected and analyzed. Samples were measured by using the company protocol described in chapter 2.2.4, 2.2.5 and 2.2.6, and were diluted 1:10 to be in the range of the standard curve. No significant difference was observed in serum concentration level of IL-6 and IL-17A, in contrast, expression of LTB_4 was decreased in *Clec4n*$^{-/-}$ mice compared to the C57BL/6J WT mice. These results suggested that Dectin-2 activation, during EBA, may be important to produce LTB_4 as a chemoattractant to recruit more leukocytes during inflammation as figure 15C showed.

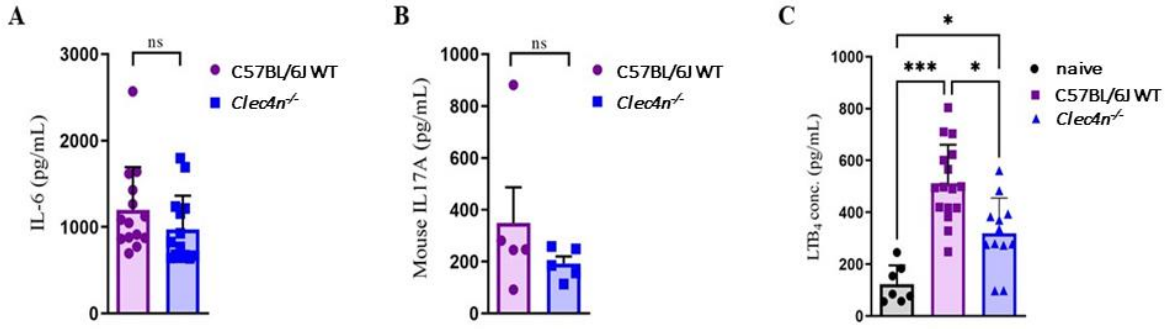

Figure 15 Sera level of LTB_4, IL-6 and IL-17 in EBA.

Sera level of LTB_4, IL-6 and IL-17A were analyzed on day 14 of EBA in C57BL/6J WT and *Clec4n*$^{-/-}$ m (A) Levels of IL-6 (n= 14 C57BL/6J WT and 14 *Clec4n*$^{-/-}$) and (B) IL-17A (n= 5 C57BL/6J WT and 5 *Clec4n*$^{-/-}$) showed high concentrations in both groups. No significant difference in the concentration of these two interleukins in both groups was seen. In contrast, (C) the concentration of LTB_4 (n= 14 C57BL/6J WT and 14 *Clec4n*$^{-/-}$) was decreased in sera of *Clec4n*$^{-/-}$ mice compared to C57BL/6J WT mice. Hereby, a control group (n=7) was used. All data are presented as mean ± SD; * $p \leq 0.05$. Statistical analysis was made with Man-Whitney test for A and B and two-way ANOVA multiple comparison for C.

3.1.2 Expression of Dectin-2 on radiosensitive hematopoietic cells is indispensable for manifestation of EBA in mice

To study the contribution of various cell types of hematopoietic versus non-hematopoietic origin during the *in vivo* passive EBA experiment, bone marrow chimera experiments were conducted in the *Clec4n*$^{-/-}$ mice and were compared to B6.SJL-Ptprc^{a} Pep^{b}/BoyJ mice. The protocol was followed according to the strategy previously described in the method section. In this experiment, two groups were generated: the *Clec4n*$^{-/-}$ → B6.SJL-Ptprc^{a} Pep^{b}/BoyJ and B6.SJL-Ptprc^{a} Pep^{b}/BoyJ → *Clec4n*$^{-/-}$ (abbreviated as genotype of donor bone marrow → genotype of recipient mouse). Four weeks after successful bone marrow engraftment, peripheral blood from mice was analyzed for chimerism exploiting the allelic variant of CD45 marker present in the *Clec4n*$^{-/-}$ (CD45.1 isoform) mouse strains, in accordance with the strategy described previously; thus, neutrophils originated from B6.SJL-Ptprc^{a} Pep^{b}/BoyJ mice were Ly6G+CD45.1+, while neutrophils originated from the *Clec4n*$^{-/-}$ mice were Ly6G+CD45.2+. Briefly, after induction of EBA by injection of affinity purified rabbit anti-mCol7c IgG, conventional *Clec4n*$^{-/-}$ mice (n=4) demonstrated the previously observed resistance to EBA as opposed to age- & sex-matched C57BL6/J WT mice (n=4). Remarkably, while B6.SJL-Ptprc^{a} Pep^{b}/BoyJ → *Clec4n*$^{-/-}$ mice, Dectin-2 deficient mice carrying bone marrow of B6.SJL-Ptprc^{a} Pep^{b}/BoyJ mice, developed severe signs of erythema and crusts on the ears and alopecia around the eyes, starting from day 4 of the experiment, and *Clec4n*$^{-/-}$ → B6.SJL-Ptprc^{a} Pep^{b}/BoyJ, B6.SJL-Ptprc^{a} Pep^{b}/BoyJ mice carrying bone marrow of Dectin-2 deficient mice, showed much less signs of the disease and did not show or at most showed a light EBA lesions on their skin on day 10 of the experiment (Figure 16 A). Since the beginning of the clinical observation, on day 4, 6 and 8 a slight difference but no significant increase raise of the disease trend could be seen between the two groups. At later stages of the disease progression, from day 10 onwards, there was a significant increase of the clinical manifestation in the B6.SJL-Ptprc^{a} Pep^{b}/BoyJ → *Clec4n*$^{-/-}$ mice while, in contrast, *Clec4n*$^{-/-}$ → B6.SJL-Ptprc^{a} Pep^{b}/BoyJ mice demonstrated protection with no presence or at most slight presence of lesions in the skin. B6.SJL-Ptprc^{a} Pep^{b}/BoyJ mice exhibited EBA-lesions spreading to their

entire body; figure 16 B representatively illustrated the development of crusts and erosions on the head and neck regions, right foreleg, and trunk. Histopathological analysis of the lesional skin, figure 16 C, showed separation of derma-epidermal junction and mononuclear cellular infiltration. Despite lack of dermal-epidermal separation in *Clec4n*$^{-/-}$ mice both groups of mice showed the immunofluorescence staining of C3 and linear deposition of IgG, figure 16 D and E. In addition, these results strongly confirmed the importance of Dectin-2 on radiosensitive hematopoietic cells.

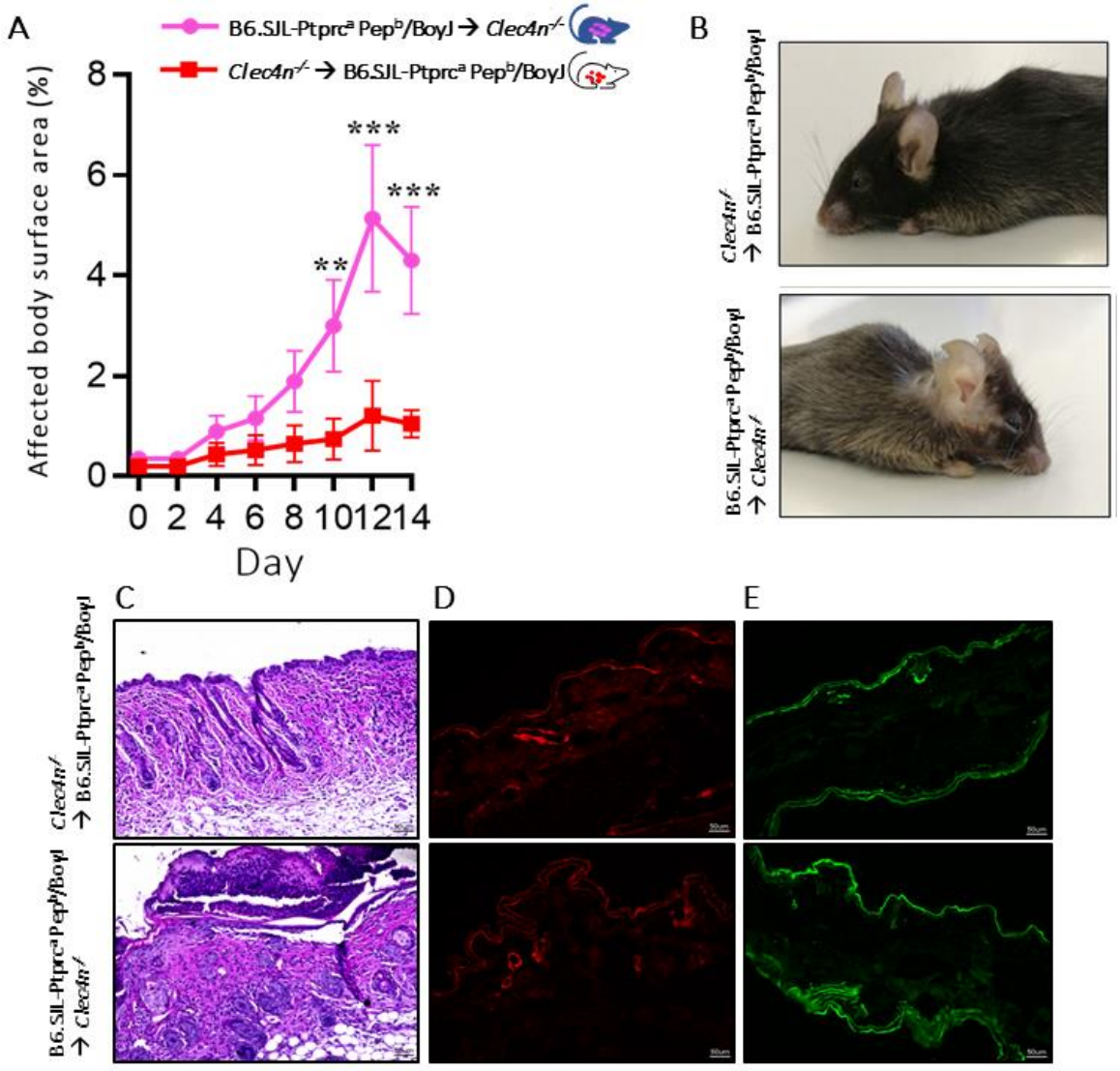

Figure 16 Radiosensitive hematopoietic cells are responsible for EBA disease.

After generating the bone marrow chimera mice, the EBA model was induced as previously described. (A) Clinical score of affected body surface area of B6.SJL-Ptprc^a Pep^b/BoyJ → *Clec4n*$^{-/-}$ and

Clec4n$^{-/-}$ → B6.SJL-Ptprc^{a} Pep^{b}/BoyJ mice through 14 days of scoring time. (B) Exemplary clinical pictures showing a clear difference in the phenotype of the two groups reflecting our observation in the clinical score. (C) Histopathological analysis demonstrating typical detachment of dermal-epidermal junction during EBA in the B6.SJL-Ptprc^{a} Pep^{b}/BoyJ → *Clec4n*$^{-/-}$ mice while, in the *Clec4n*$^{-/-}$ → B6.SJL-Ptprc^{a} Pep^{b}/BoyJ mice did not show tissue damage. Immunohistochemistry analysis reveals the presence of rabbit anti-mCol7c IgG (D) and C3 deposition (E) in both groups of chimera mice, highlighting the presence of inflammation despite the black and white phenotype shown in the clinical score. (All data are presented as mean ± SEM; * $p \leq 0.05$; Scale bar, 50µm).

3.1.2.1 Bone-marrow cells are the drivers of disease progression in the EBA mouse model

To understand the contribution of which type of cells is responsible for EBA disease, the reconstitution of hematopoietic versus non hematopoietic cells, in both B6.SJL-Ptprc^{a}Pep^{b}/BoyJ and *Clec4n*$^{-/-}$ that have been irradiated, as previously described in the bone marrow chimera experiment, was evaluated. Hematopoietic cells are predominantly radiosensitive cells, while non-hematopoietic cells are usually radioresistant. After 14 days of EBA induction, mice were euthanized, and BM cells were collected for FACS analysis. Staining procedure can be found in paragraph 2.2.5.1. Results observed in figure 17, demonstrated a clear BM cells reconstitution from donors to recipients B6.SJL-Ptprc^{a}Pep^{b}/BoyJ → *Clec4n*$^{-/-}$ (CD45.1) and *Clec4n*$^{-/-}$ → B6.SJL-Ptprc^{a}Pep^{b}/BoyJ (CD45.2). Each population was gated for Ly6G PerCP-Cy5.5 and a high percentage of neutrophils was observed in group *Clec4n*$^{-/-}$ → B6.SJL-Ptprc^{a}Pep^{b}/BoyJ (52,48%) compared to B6.SJL-Ptprc^{a}Pep^{b}/BoyJ → *Clec4n*$^{-/-}$group (25.06%). The data demonstrated a near complete replacement of the original bone marrow with the bone marrow of the donor mice. This composition of the bone marrow, taken together with the clinical manifestation of disease showed in Figure 16, highlights the importance of Dectin-2 on radiosensitive bone marrow cells for the progression of the disease making it an essential component that is likely important during early stages of inflammation after the autoantibodies have bound their antigen at the DEJ.

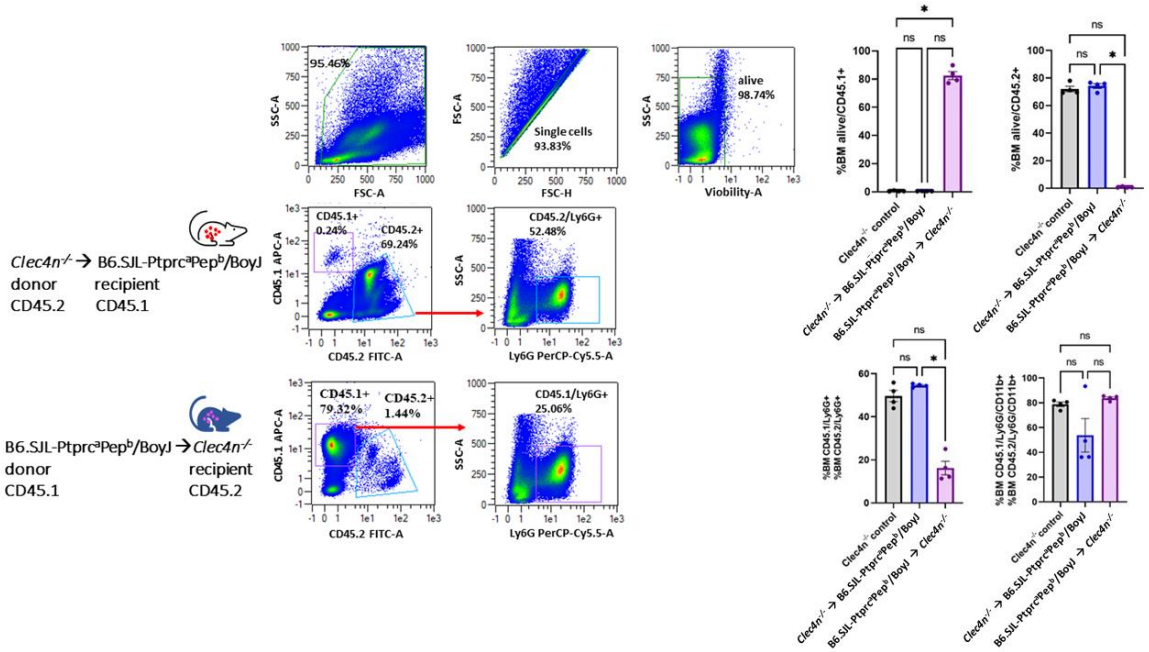

Figure 17 Bone-marrow cells are the drivers of disease progression in the EBA mouse model.

Representative illustration of FACS analysis of BM chimera experiment. BM cells were collected on day 14 of EBA mouse model and analyzed in B6.SJL-Ptprc^{a} Pep^{b}/BoyJ → *Clec4n*$^{-/-}$ compared to the *Clec4n*$^{-/-}$ → B6.SJL-Ptprc^{a} Pep^{b}/BoyJ mice. Cells were labeled with CD45-1 APC (1:200). CD45.2 FITC (1:75), Ly6G PerCP-Cy5.5 (1:50) and CD11b APC-Vio 770 (1:50). The results showed a net cut of the CD45.1 (B6.SJL-Ptprc^{a} Pep^{b}/BoyJ → *Clec4n*$^{-/-}$) and CD45.2 (*Clec4n*$^{-/-}$ → B6.SJL-Ptprc^{a} Pep^{b}/BoyJ) population. Neutrophils, stained with Ly6G marker, are more abundant in *Clec4n*$^{-/-}$ → B6.SJL-Ptprc^{a} Pep^{b}/BoyJ mice compared to the B6.SJL-Ptprc^{a} Pep^{b}/BoyJ → *Clec4n*$^{-/-}$ mice. Data were analyzed with two-way ANOVA and presented a mean ± SEM (n=4); *P < 0.05; **P < 0.01; ***P < 0.001.

3.2 Studying the biological effects of Dectin2 on neutrophils functions

3.2.1 Neutrophils acquire Dectin-2 expression upon exposure to GM-CSF

GM-CSF stimulates the proliferation and differentiation of granulocytes not only in bone-marrow but, also in circulating mature neutrophils. To investigate the importance of Dectin-2 expression on neutrophils surface during inflammation, we wanted to investigate, after 40 hours stimuli, whether C57BL/6J WT bone-marrow-derived neutrophils have a different behaviour compared to the *Clec4n*$^{-/-}$ neutrophils. The procedure of Ab intracellular staining was followed with the same protocol

already described in methods. Briefly, bone-marrow derived neutrophils were isolated from C57BL/6J WT and *Clec4n*$^{-/-}$ mice. Cells were counted and 500x10^6/mL were plated in a 6 well plate with and without GM-CSF, respectively. Samples were incubated for 40 hours and, subsequently, prepared to be labelled with Viobility-dye (1:100), Dectin-2-APC (1:10) or Dectin-2 Isotype (1:10) as control. 10^4 cells were acquired on the MACSQuant Analyzer 10 cytometer and analyzed with MACSQuantifyTM software. The results demonstrated a significant shift and upregulation of Dectin-2+ cells of 39.4% out of the entire C57BL/6J WT neutrophils population that was absent in the *Clec4n*$^{-/-}$ cells (Figure 18). To prove results were consistent, the isotype was used as a control. These results suggested that during EBA inflammation, after a long exposure time, 40 hours priming, neutrophils express the C-type lectin receptor to drive the response. There was no expression of Dectin-2 observed in neutrophils unstimulated (figure not showed).

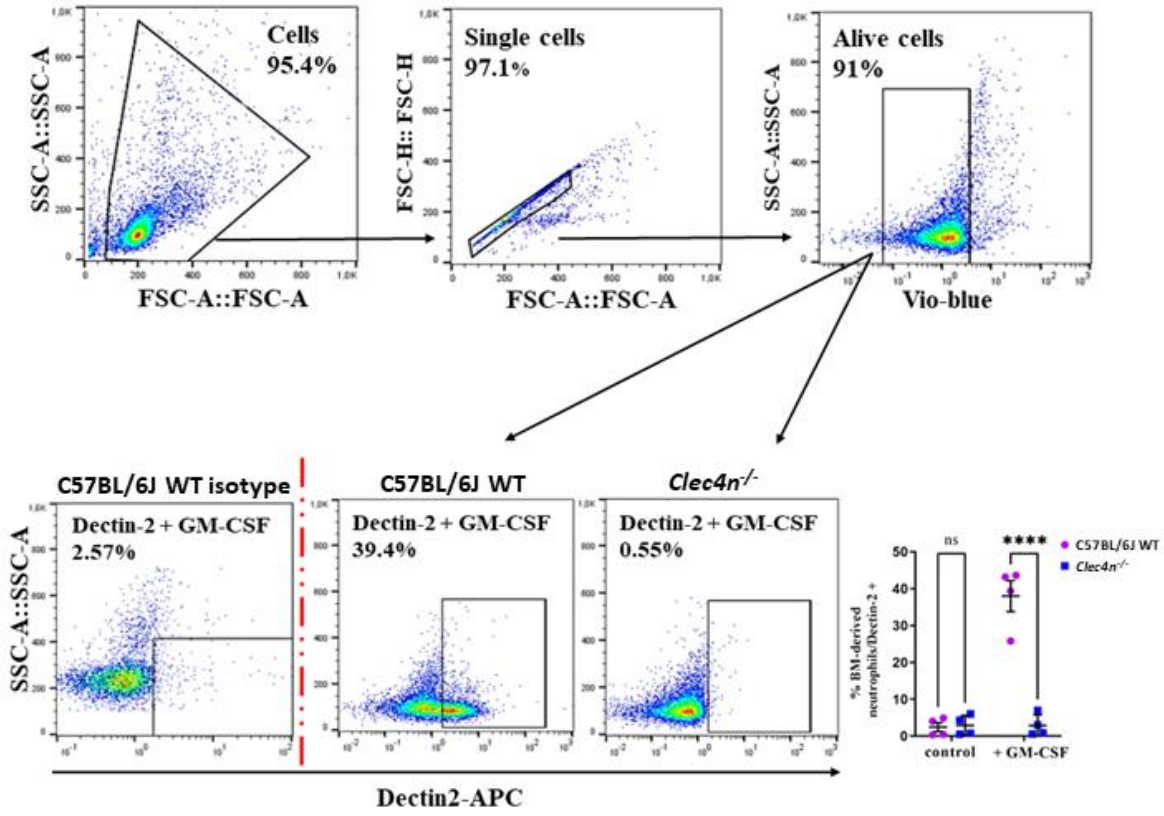

Figure 18 C57BL/6J WT BM-derived neutrophils express Dectin-2 upon 40 h GM-CSF stimulation.

BM-derived neutrophils were isolated from healthy naïve C57BL/6J WT and *Clec4n*$^{-/-}$ mice and stimulated for 40 hours with GM-CSF *in vitro*. Cells were stained for cell viability, then fixed,

permeabilized and labelled with the respective antibodies. Representative experiment of BM-derived neutrophils Dectin-2 expression upon 40 hours GM-CSF stimulation C57BL/6J WT and *Clec4n*$^{-/-}$ cells were gated from alive cells to C57BL/6J WT Isotype (2,57%), C57BL/6J WT (39,4%) and *Clec4n*$^{-/-}$ (0,55%). The graph shows the percentage of the Dectin-2+ expressing cells and its significant increase in the C57BL/6J WT neutrophils upon GM-CSF stimulation. Data were analyzed with two-way ANOVA and presented as mean ± SEM (n=4); *P < 0.05; **P < 0.01; ***P < 0.001.

3.2.2 Neutrophils migration towards the chemoattractant C5a is Dectin-2-independent

As mentioned before, neutrophils priming is a potent concept to accelerate the recruitment of cells to the site of inflammation and to elicit, in a more efficient way, effector functions of neutrophils. Circulating neutrophils live in a basal state with a limited capacity to respond to an insult but once they are exposed to pro-inflammatory factors like cytokines, chemokines and bacterial or viral products they undergo structural changes that initiate transmigration behaviour and prepare the cells to effectively engage against the pathogen. To understand if the absence of Dectin-2 on neutrophils had a relevant impact on their migration towards a stimulus, neutrophils were freshly isolated from the bone marrow following the method described above. The anaphylatoxin complement component 5a (C5a) is a potent chemoattractant with a key function in the pathogenesis of EBA and thus induces strong migration of the granulocytes toward the chemoattractant. Thus, we wanted to investigate whether Dectin-2 played a role in the C5a-mediated mobilization of the PMNs. Briefly, 24- well plate BM-derived neutrophils were loaded in the upper compartment into a Transwell insert with a mesh bottom of 3 µm pore size, without and with 10 nM C5a, which communicates with the bottom part where only control (3% BSA), chemokinesis (10 nM C5a) were loaded. The plate was incubated for 2 hours at 37 °C. Subsequently, only the neutrophils migrated through the transwell mesh to the bottom part were measured and analyzed in MACSQuant devise. While chemotaxis was induced in both C57BL/6J WT and *Clec4n*$^{-/-}$ cells, obtained results demonstrated that there was no significant difference between the two groups when cells were stimulated with 10 nM C5a (Figure 19). There are other publications where different molar concentrations were used and the experiment was performed

also with 5 nM and 1 nM C5a (data are not showed). No difference was found. Both groups, C57BL/6J WT and *Clec4n*$^{-/-}$ cells, responded the same way. As are large inter-assay variation was observed, the fold change of the chemotaxis for each assay was calculated, Figure 19 B, to better visualize and describe the ratio of induce migration and allow better interpretation of potential differences, yet no significant difference in the Transwell-migration towards C5a could be found between C57BL/6J WT and *Clec4n*$^{-/-}$ neutrophils.

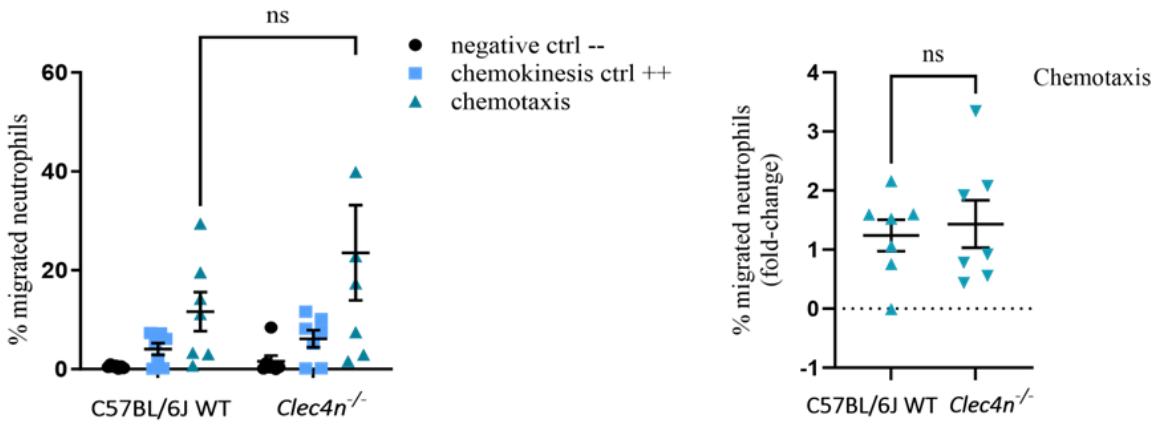

Figure 19 C57BL/6J WT and *Clec4n*$^{-/-}$ BM-derived neutrophils migration towards C5a. (A) BM-derived neutrophils migration expressed in percentage towards 10 nM C5a in C57BL/6J WT and *Clec4n*$^{-/-}$ mice. (B) Migration of BM-derived neutrophils towards C5a analyzed as fold-change. Results are expressed as ± SEM of n=7. 2-way ANOVA, multiple comparison and Wilcoxon test were used respectively, *P < 0.05; **P < 0.01; ***P < 0.001.

3.2.3 Dectin-2 is important for the release of LTB_4 by neutrophils to drive inflammation

Migration of neutrophils to an inflamed tissue is mediated by the release of primary chemoattractants that promote their mobilization and, subsequently their secretion of secondary chemoattractants, i.e., LTB_4 to which they are exposed, due to the formation of a gradient that promotes the recruitment of the granulocytes and other cells. The process is important to favour the robustness to the primary chemoattractants signal supported also by the presence of the immune complex (IC) to induce inflammation. In this study, *in vitro* experiments were performed by mimicking the response of neutrophils upon IC stimulation to study whether Dectin-

2 is essential to promote the release of LTB_4 by PMNs. Briefly, freshly isolated neutrophils (10^6 /mL) from the BM were incubated in a plate pre-coated with IC for 1 h at 37 °C. Subsequently, cells were centrifuge at 400 x g for 5 minutes and the supernatant was collected. Following the LTB_4 ELISA protocol, samples were measured in the Tecan plate reader device. The graphs in Figure 20 showed the release of the chemoattractant LTB_4 by C57BL/6J WT and *Clec4n*$^{-/-}$ neutrophils in response to IC. In this case, C57BL/6J WT littermates were used as a control and were not separated from the Janvier C57BL/6J WT because of the same tendency. The results are presented as fold-change because of the high levels of variation. Despite this, the tendency within the individual experiments demonstrated that *Clec4n*$^{-/-}$ cells release less LTB_4 compared to the C57BL/6J WT. To highlight the tendency, the variable change was measured between the two groups. The log transformed data was used to be subsequently transformed to be normally distributed. The calculation was made to assess that the difference in the means of the log transformed data corresponds to their ratio in the original scale. Data obtain suggested that the expression of Dectin-2 on neutrophils membrane is important for the release of LTB_4. Although data did not show a complete abrogation of the release of the leukotriene by *Clec4n*$^{-/-}$ cells, the results suggest there to be a disruption through a Dectin-2 dependent mechanism diminishing the release of LTB_4.

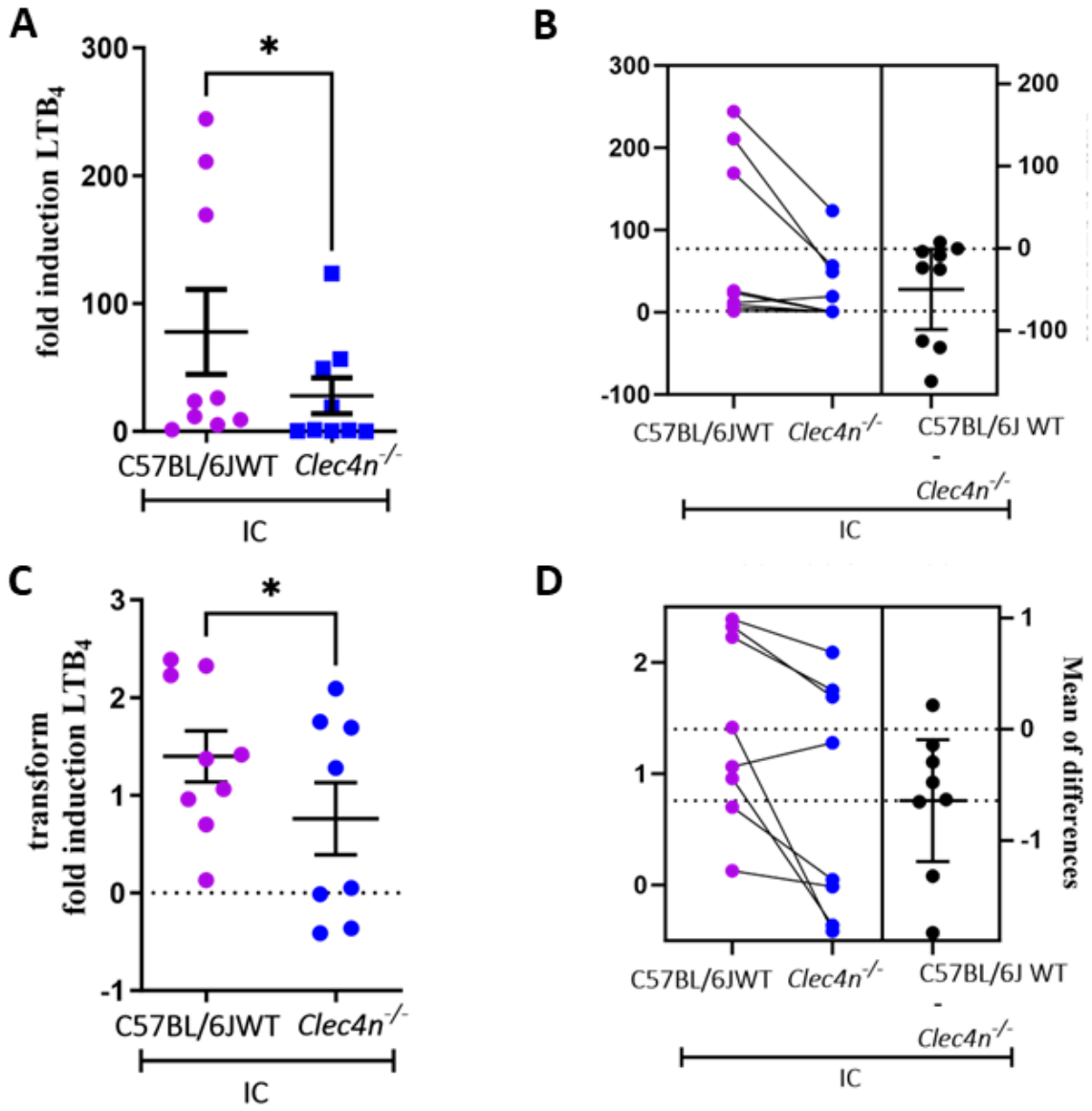

Figure 20 Dectin-2 is important for LTB_4 release by bone-marrow derived neutrophils upon IC stimulation.

BM-neutrophils of healthy naïve C57BL/6J WT and *Clec4n*$^{-/-}$ mice were isolated and stimulated with immune complexes (IC) to measure the release of Leukotriene B4 (LTB_4). Measurement of the fold-change in C57BL/6J WT and *Clec4n*$^{-/-}$ BM-derived neutrophils response upon IC stimulation. (A) Fold-change (B) Estimation plot of the fold-change. (C) Transform of the fold-change and (D) estimation plot of the transform data. Data were normalized and were presented as mean ± SEM; n=9 mice per group; t-test for the fold-change data and paired t-test for the transform log2, respectively; *P < 0.05; **P < 0.01; ***P < 0.001.

3.2.4 Neutrophils ROS release is Dectin-2 independent

Among the cytotoxic products released by neutrophils during their effector phase, another hallmark of inflammation is the release of ROS. To investigate whether Dectin-2 expression may be indispensable in neutrophils to drive the inflammation, in EBA, the release of the reactive oxygen species was measured in C57BL/6J WT and *Clec4n*$^{-/-}$ bone-marrow derived neutrophils. The *in vitro* experiment was performed following the stablished protocol in our laboratory. Briefly, 10^6/mL cells isolated from the bone-marrow were plated in a pre-coated IC plate and the extent of ROS production was quantified using luminol-enhanced chemiluminescence. The measurement was monitored for 2 hours. Based on the obtained results, both C57BL/6J WT and *Clec4n*$^{-/-}$ bone-marrow neutrophils response to IC stimulation did not show a significant difference in the release of ROS. The response in both IC stimulated groups was increased compared to the unstimulated controls but not between the two groups (Figure 21).

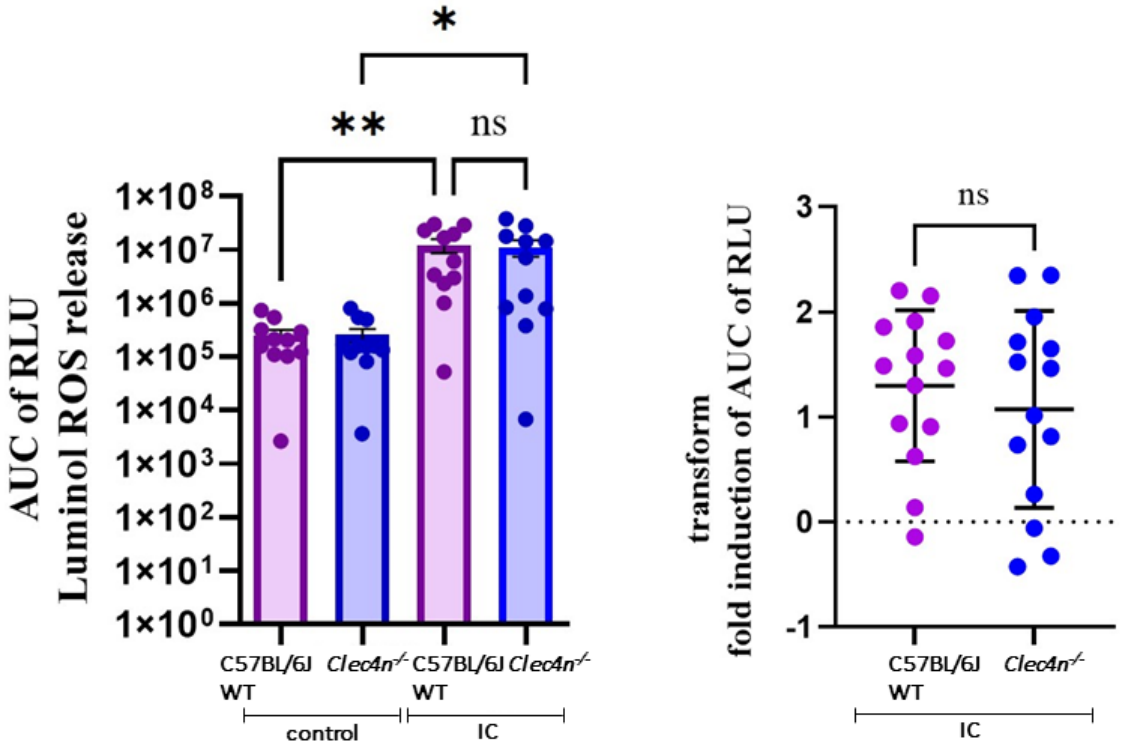

Figure 21 *In vitro*: ROS release is Dectin-2 independent in both C57BL/6J WT and *Clec4n*$^{-/-}$ neutrophils.

C57BL/6J WT and *Clec4n*$^{-/-}$ BM-derived neutrophils were loaded into an IC coated plate, and ROS production was measured as emitted light in relative light units (RLU) in duplicate for 2h at 37˚C. Data is presented as mean ± SEM (n=11); One-way ANOVA test.

3.3 Cooperation of Dectin2 and FcγRIV on neutrophils

3.3.1 Neutrophils specific FcγRIV-KO mice are completely protected from induction of antibody-transfer EBA

Epidermolysis bullosa acquisita is a severe autoimmune skin disease. It is characterized by autoantibodies against type VII collagen. The recruitment of neutrophils is essential for the development of blistering autoimmune dermatoses (pemphigoid), which cause damage to the skin in the tissue through the release of superoxides and proteases. This exposed role of neutrophils in the development of pemphigoid diseases implies that receptors on neutrophils, through which they are recruited into the skin and activated, play a significant role in the pathogenesis of pemphigoid diseases. In recent years, using the passive EBA mouse model as a prototypical example of pemphigoid disease, the research groups at the department of dermatology in Lübeck have identified the receptor FcγRIV as an essential receptor for pemphigoid. However, the cells on which this receptor play their central role in the pathogenesis of pemphigoid diseases have not yet been identified. FcγRIV is expressed on a range of cell types and is also highly expressed on neutrophils, so it is possible that the action of this receptor on neutrophils could be essential for the pathogenesis of pemphigoid diseases. The exact knowledge of the site of action of this receptor in pemphigoid diseases would contribute significantly to the understanding of the pathogenesis of these diseases and enable the development of selective therapies. The experiment set up was the same as described above. Briefly, to induce passive EBA, MRP8-Cre- ires/GFP mice and four neutrophils specific FcγRIV-KO (MRP8^{Cre} x FcγRIV$^{flx/flx}$) mice were injected with 50 µg of affinity purified rabbit anti-mCol7c IgG into the neck, right foreleg, and back on day 0, 2 and 4. Mice were monitored and scored for 14 days. On the termination day, samples were harvested and collected for further analysis. The neutrophil

specific FcγRIV conditional KO mice were specifically knocked out only on neutrophils, due to the expression of the Cre recombinase on under the control of the MRP8 promoter region. While the MRP8-Cre- ires/GFP developed severe signs of erythema and crusts on the ears and alopecia around the eyes, starting from day 4 of the experiment, FcγRIV-KO mice remained completely resistant to the disease and did not show EBA lesions on their skin on day 4 of the experiment. Figure 22 A showed the clinical score of experimental EBA in MRP8-Cre- ires/GFP and FcγRIV-KO mice. Since the beginning of the clinical observation/scoring, Throughout the entire clinical evaluation period there was a significant raise of the clinical manifestation in the MRP8-Cre- ires/GFP mice while, in contrary, the FcγRIV-KO mice demonstrated a complete protection with no presence of lesions in the skin. MRP8-Cre- ires/GFP mice exhibited EBA-lesions spread to their entire parts of the body; figure 22 B represented the development of crusts and erosions on the head and neck regions, right foreleg, and trunk. Histopathological analysis of the lesional skin, showed separation of derma-epidermal junction and mononuclear cellular infiltration. Despite lack of dermal-epidermal separation in FcγRIV-KO mice both groups of mice showed the immunofluorescence staining of C3 and linear deposition of IgG, figure 22 D and E, respectively. In the study, only a small group of mice were compared due to the limited stock of material. Nevertheless, the promising results obtained can be confirmed in the future by analysing a larger sample size.

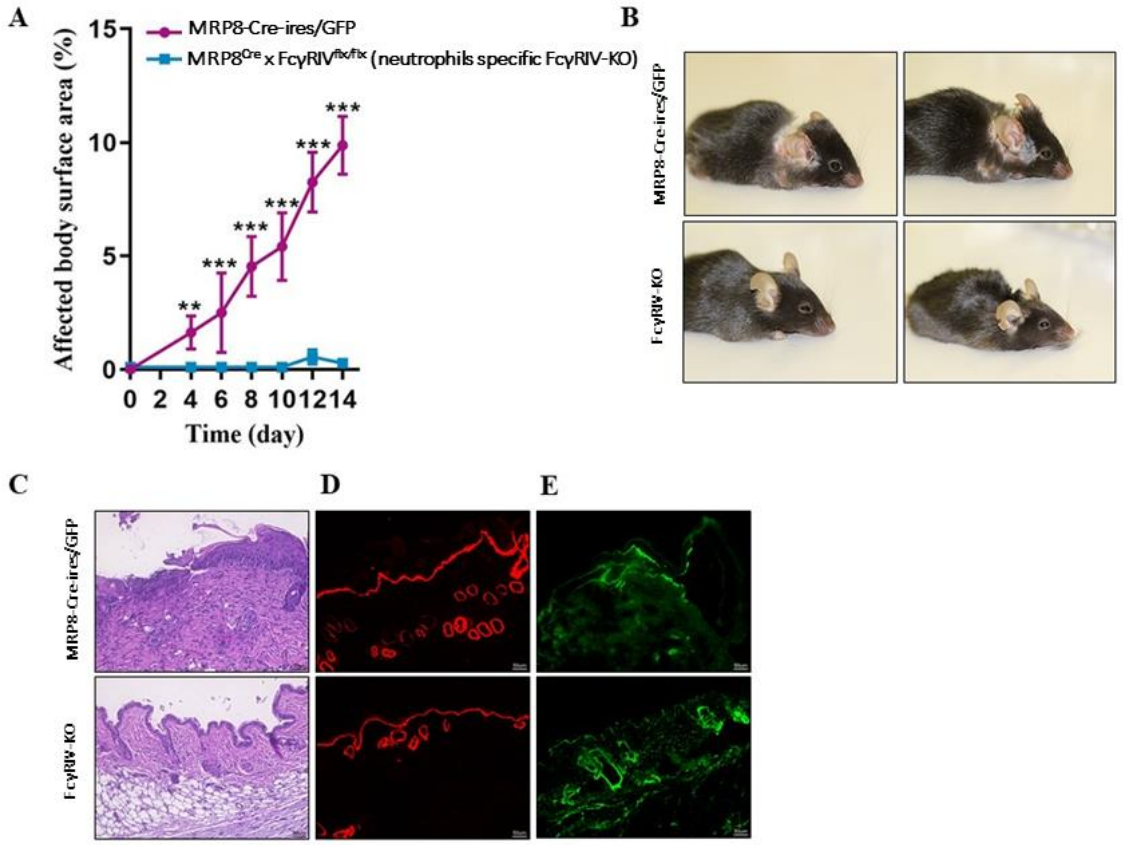

Figure 22 The expression of the FcγRIV on neutrophils is important for their recruitment in the EBA pathogenesis.

The passive EBA mouse model was induced in MRP8-Cre-ires/GFP and FcγRIV-KO mice by injection of anti-mCol7c antibodies as describe before. (A) Clinical score of experimental EBA in MRP8-Cre-ires/GFP (●) vs. FcγRIV-KO (■). Mice with FcγRIV deficiency on neutrophils showed a complete protection from the disease induction compared to MRP8-Cre-ires/GFP animals (n=1); (B) Representative clinical pictures of MRP8-Cre-ires/GFP and FcγRIV-KO mice on day 14 of the experiment; erosion and alopecia are manifested only in the MRP8-Cre-ires/GFP mice; (C) Histological sections of lesional skin highlight the separation of the derma-epidermal junction in the MRP8-Cre-ires/GFP mice and an abundant cellular infiltrate. In contrast, there is no evidence of skin inflammation in the FcγRIV-KO animals; Immunohistochemistry analysis reveal the presence of rabbit anti-mCol7c IgG (D) and C3 deposition (E) in both MRP8-Cre-ires/GFP and FcγRIV-KO mice, highlighting the presence of inflammation despite the black and white phenotype shown in the clinical score. (All data are presented as mean ± SEM; Two-Way ANOVA; *P < 0.05; **P < 0.01; ***P < 0.001; Scale bar, 50µm).

3.3.1.1 Neutrophils require the cooperation between FcγIV receptor and Dectin-2 to elicit their function in EBA

To investigate whether neutrophils and the expression of the FcγRIV receptor, on their surface, are the main source to drive skin inflammation, peripheral blood, bone-marrow and lesional skin (ears) from MRP8-Cre-ires/GFP and FcγRIV-KO mice were collected on day 14 of EBA. The procedure of Ab staining was followed with the same protocol already described in methods. Samples were analyzed from single cells and gated for Ly6G-Percp-Vio700, Ly6C-FITC, FcγRIV-PE and Dectin2-APC. To identified cells other than neutrophils, the Ly6C marker was used as it is expressed on DC, subset of monocytes, macrophages, and lymphocytes. When blood was analyzed, two populations were observed: in MRP8-Cre-ires/GFP mice, most cells were represented by neutrophils (33.3%) and a minority of other cells (7%) compared to the FcγRIV-KO mice where only 11.63% were positive stained for neutrophils and 7.68% positive stained for other cells, figure 23 A and B. These results suggested that neutrophils require the cooperation of FcγIV receptor and Dectin-2 to elicit their function in EBA; indeed, a high percentage of Ly6G expression was observed in MRP8-Cre-ires/GFP compared to FcγRIV-KO. Thus, the constant percentage of other cells found like immature neutrophils or monocytes/macrophages, both in MRP8-Cre-ires/GFP and FcγRIV-KO mice, demonstrated that neutrophils could be predominant for the disease. This can be confirmed by going to the next observation where neutrophils were 87.16% positive for FcγIV receptor compared to the FcγRIV-KO mice (9.68%) as expected. In both groups, the intermediate cells were positive for FcγIV receptor (MRP8-Cre-ires/GFP 38.27% and FcγRIV-KO 25.11%) highlighting the fact that even though other cells were recruited in the blood during inflammation, only neutrophils and their FcγIV receptor highly expressed. Moreover, when neutrophils positive for FcγIV receptor were analyzed to investigate whether its absence may compromise the expression of Dectin-2, surprisingly the C-type lectin receptor was higher expressed in MRP8-Cre-ires/GFP but not in the FcγRIV-KO mice. In line with this, I could hypothesize that when the inflammation occurs both, expression Dectin-2 and FcγIV receptor

cooperation was required for the egression of the granulocytes from the bone marrow into the blood.

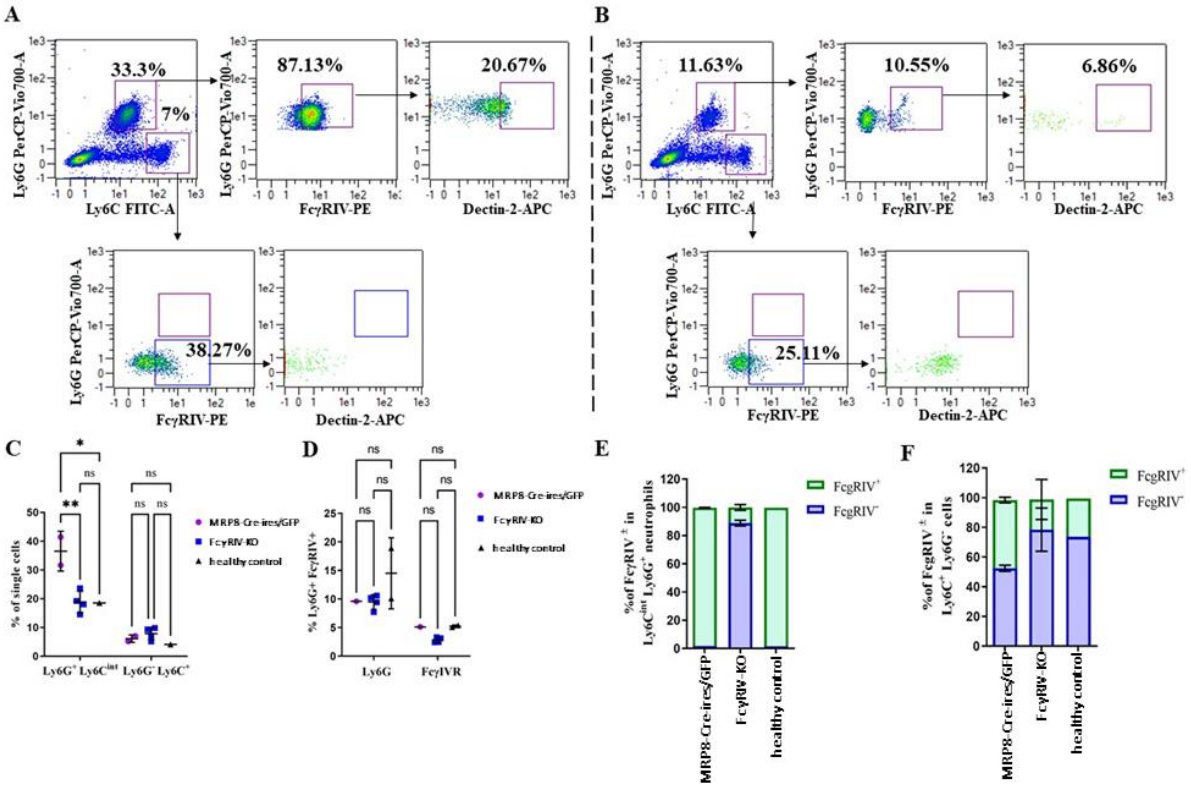

Figure 23 Representative illustration of the expression of FcγIV receptor on neutrophils in mice blood after EBA induction.

After induction of EBA by antibody transfer, blood samples were collected at the end of the experiment on day 14 for further flow cytometry analysis. Expression of FcγRIV on neutrophils (87.13%) and on other cells (38.27%) and expression of Dectin-2 on Ly6G+ FcγRIV+ in both MRP8-Cre-ires/GFP (A) and FcγIV-KO mice (B). Graph illustration of FACS gating strategy (C-F). All data are presented as mean ± SEM; * $p \leq 0.05$. Two-way ANOVA test, multiple comparison.

In the bone marrow, figure 24 A and B, both groups showed a percentage of ~ 31% represented by neutrophils from which 95.05% expressed the FcγIV receptor compared to the 19.15% that may be considered an unspecific binding. In this case, no expression of Dectin-2 was detectable. These results suggested that there was the same ratio in the production of neutrophils in the bone marrow that was

decreased when the granulocytes migrated into the blood. This can be explained by the fact that during the transmigration, the expression of FcγRIV on neutrophils is important for their mobilization to the blood flow. The FcγRIV-KO mice may not have the ability to capture the signal that is released by other cells in the blood with a consequent decrease in the recognition of a stimuli and so their bound with the selectins.

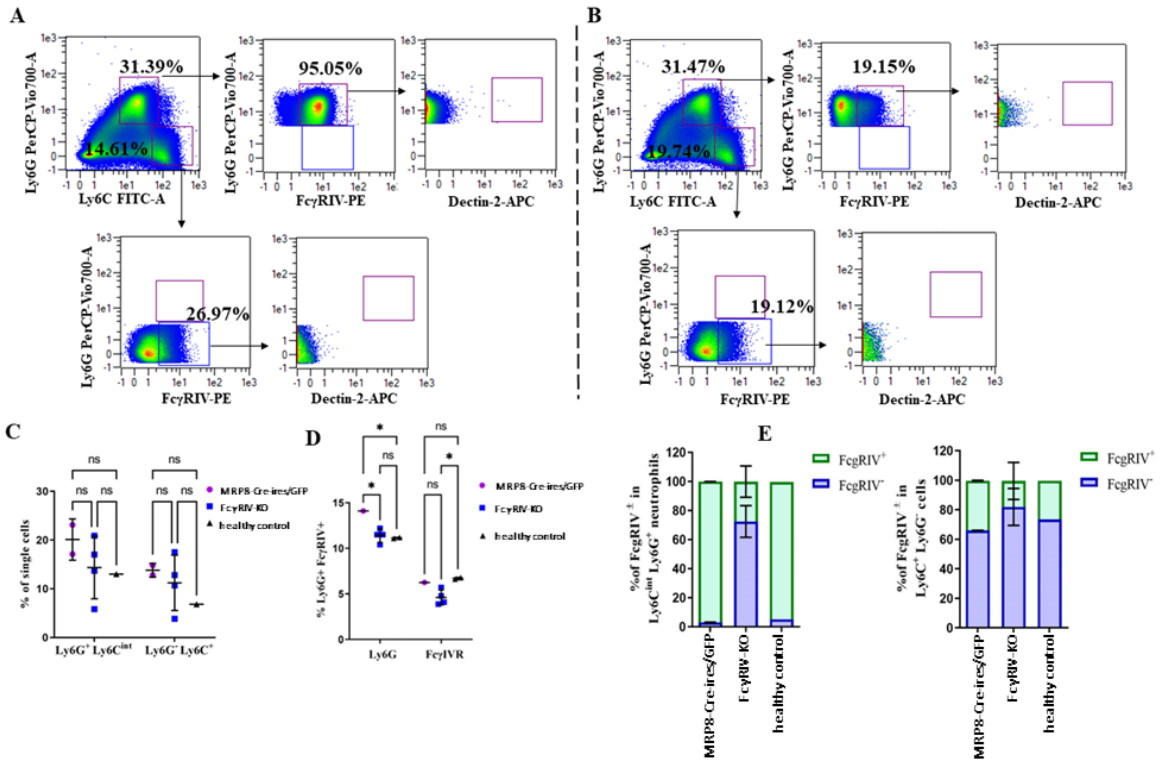

Figure 24 Representative illustration of the expression of FcγIV receptor on neutrophils in the bone marrow of mice after EBA induction.

After induction of EBA by antibody transfer, bone marrow samples were collected at the end of the experiment on day 14 for further flow cytometry analysis. Expression of FcγRIV on neutrophils (95.05%) and on other cells (19.15%) and expression of Dectin-2 on Ly6G+ FcγRIV+ in both MRP8-Cre-ires/GFP (A) and FcγIV KO mice (B). Graph illustration of FACS gating strategy (C-F). All data are presented as mean ± SEM; * $p \leq 0.05$. Two-way ANOVA test, multiple comparison

Interesting, in the lesional skin (ears), Figure 25, three different populations were observed: neutrophils, an intermediate state of possible neutrophils, and other cells

(DC or monocytes/macrophages). A significant difference in cells positive for Ly6G was observed in MRP8-Cre-ires/GFP (36.23%) and in FcγRIV-KO mice (2.14%). Each population was analyzed to investigate the importance of FcγIVR presence on neutrophils and as expected, no expression of the receptor was observed on FcγRIV-KO mice. The possible reason may be that on day 14 of the EBA experiment, neutrophils had already elicited their function by signalling through FcγRIV to release anti-inflammatory factors and are no longer in the skin; in the other hand, other cell types came further to assist in the wound healing and so by expressing the molecule to help in the release of cytokines and chemokines.

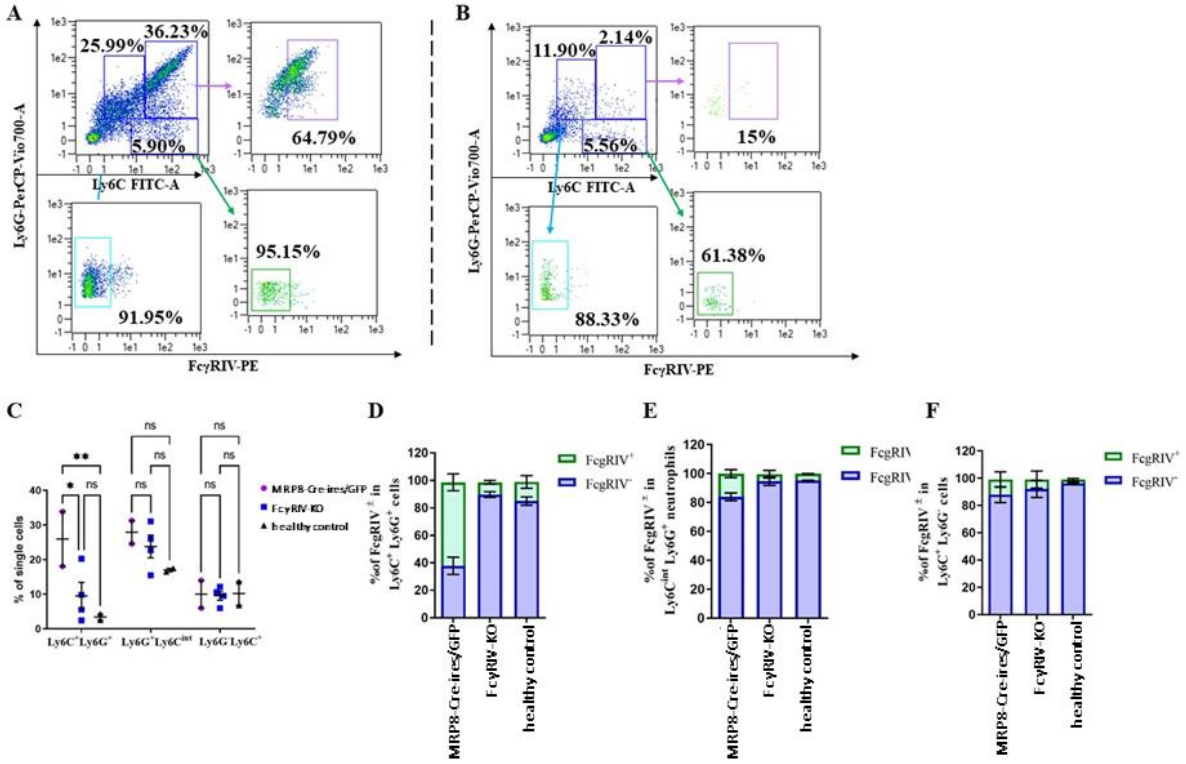

Figure 25 Representative illustration of the expression of FcγIV receptor on neutrophils in the lesional skin (ears) of MRP8-Cre-ires/GFP and FcγRIV-KO mice after EBA induction.

After induction of EBA by antibody transfer, skin samples were collected at the end of the experiment on day 14 for further flow cytometry analysis. Expression of FcγRIV on neutrophils (64.79%), intermediate cells (DC or monocytes/macrophages) (25.99%) and on other cells (5.90%) in MRP8-Cre-ires/GFP (A) and on neutrophils (2.14%), intermediate cells (DC or monocytes/macrophages)

(11.90%) on other cells (5.56%) in FcγRIV-KO mice (B). Graph illustration of FACS gating strategy (C-F). All data are presented as mean ± SEM; * $p \leq 0.05$. Two-way ANOVA test, multiple comparison

3.3.2 Dectin-2 collaborates with FcγRIV to induce the release of ROS but not of LTB_4 from neutrophils

Based on the previous results that highlighted the importance of FcγRIV for neutrophils activation, I wanted to investigate whether, *in vitro*, the inhibitory anti-FcγRIV antibody (9E4 kindly donated by Falk Nimmerjahn group) nullified the release of both LTB_4 and ROS from neutrophils in response to rabbit IgG-ICs. Briefly, neutrophils were isolated from the C57BL/6J WT bone marrow as previously described in methods. Briefly, 10^6/mL cells were stimulated with IC and treated, in two separate pre-coated plates, with anti-FcγRIV (1:100) and Purified Armenian Hamster IgG (1:100) as isotype control. Cells were measured to assess ROS release and LTB_4 concentration. Figure 26 represented a significant decrease in ROS release when neutrophils are stimulated with IC and treated with anti- FcγRIV; in contrast, there was no difference in LTB_4 concentration. These findings confirmed my previous hypothesis about the importance of FcγRIV expression on neutrophils to drive an inflammation which, in this case, additionally favored ROS release.

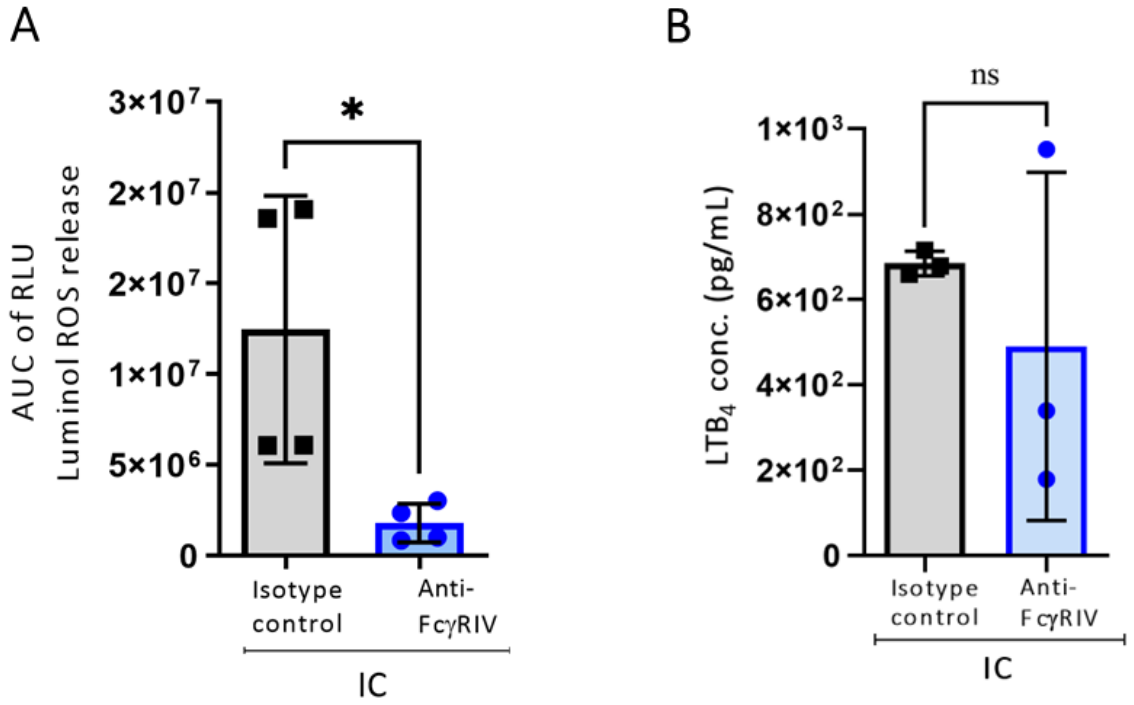

Figure 26 Dectin-2 interacts with FcγRIV to drive inflammation.

Graphic representation of ROS measurement in (A) BM-derived C57BL/6J WT neutrophils treated with anti-FcγRIV (1:100) and Purified Armenian Hamster IgG (1:100) as isotype control upon IC stimulation (n=4). (B) Graphic representation of LTB4 measurement of BM-derived C57BL/6J WT neutrophils treated with anti-FcγRIV (1:100) upon IC stimulation (n=3). Isotype was used as control in both experiments. Data were analyzed with two-way ANOVA and presented as ± SEM (n=3); *P < 0.05; **P < 0.01; ***P < 0.001.

3.3.3 Dectin-2 enhances FcγRIV-triggered immune responses of neutrophils *in vitro*

To follow the hypothesis from our previous results where neutrophils, stimulated with GM-CSF for 40 hours, showed Dectin-2 internalization in the C57BL/6J WT BM-derived neutrophils after being primed we wanted to investigate whether FcγRIV is internalized too. The extracellular staining on PMNs for the Vioblue (1:100), and the Abs Ly6G-APC-Vio (1:10) and FcγRIV-PE (1:10) was followed with the protocol described in the section “methods”. Briefly, BM-derived neutrophils, C57BL/6J WT

and *Clec4n*$^{-/-}$, were freshly isolated and 10^6 cells/mL were incubated with the IC coated high binding plate for 1 hour. After, incubation, neutrophils were collected, centrifuged, and resuspended in MACS buffer. The results displayed clearly lower surface density of the surface marker, FcγRIV, in C57BL/6J WT neutrophils stimulated with IC (86.98%). Compared to the unstimulated C57BL/6J WT and *Clec4n*$^{-/-}$ and with the stimulated *Clec4n*$^{-/-}$, whereas the expression remained constant with a percentage of 91.55%, 90.05% and 92.82%, respectively, Fig.27 A. The shedding state observed only in C57BL/6J WT upon IC stimulation gave us the conclusion that Dectin-2 likely collaborates with FcγRIV for down-stream signal that leads to the release of ROS and LTB_4 to, subsequently, erosions on the skin. Also, from our previous results, we showed the expression of Dectin-2 only after 40 hours upon GM-CSF stimulation is visible only intracellularly, while after only 1 hour of IC stimulation, FcγRIV is expressed in large amount on the surface of neutrophils and only a small portion internalized. The interplay between Dectin-2 and FcγRIV may be a timing game. It can be that due to the long time required for Dectin-2 to be activated is directly proportional to FcγRIV internalization. Likely, this hypothesis drives us to strongly think there is a dimerization between the two proteins to be in contact and to signal downstream. There is no significant change between unstimulated C57BL/6J WT and *Clec4n*$^{-/-}$ upon stimulation showing once again the importance of Dectin-2 in tissue-driving inflammation.

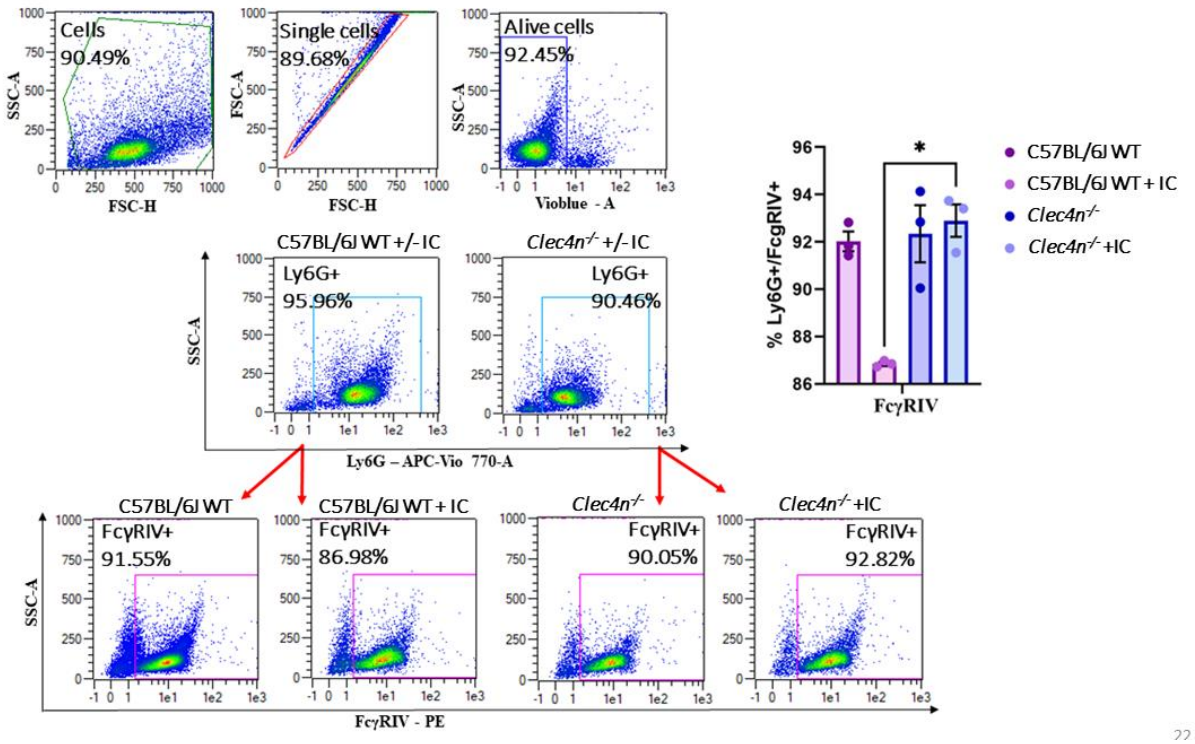

Figure 27 FcγRIV is internalized after immune-complex stimulation

In vitro FACS analysis of C57BL/6J WT and *Clec4n*$^{-/-}$ BM-derived neutrophils. (A) Cells (10^6 cells/mL) were incubated with IC for 1h and subsequently labeled with Vio-blue (1:100), Ly6G-APC-Vio 770 (1:10) and FcγRIV-PE (1:10) markers. From alive cells (92.45%), neutrophils (Ly6G+) resulted in the same percentage in both C57BL/6J WT (95.6%) and *Clec4n*$^{-/-}$ (90.46%); Subsequently, the expression of FcγRIV on neutrophils was measured in C57BL/6J WT and *Clec4n*$^{-/-}$ unstimulated and IC stimulated. The results showed a significant decrease of the expression of FcγRIV in the WT with IC stimulation (86.98%) compared to the C57BL/6J WT and *Clec4n*$^{-/-}$ unstimulated (91.55% and 90.05%, respectively) and *Clec4n*$^{-/-}$ IC stimulated (92.82%). (B) Graphic illustration of BM-derived neutrophils. Data were analyzed with two-way ANOVA and presented as ±SEM (n=3); *P < 0.05; **P < 0.01; ***P < 0.001

DISCUSSION

4.1 Requirement of Dectin-2 for the progression of EBA

Recruitment of immune cells into peripheral tissue is a hallmark of tissue inflammation. In autoimmune diseases, loss of self-tolerance and expansion of self-reactive immune cells lead to tissue damage. Neutrophils that are the first cells migrating to the site of inflammation constitutively express several cell-surface receptors (Hadebe et al., 2018) that stimulate the phagocytosis and intracellular killing of microbes bound to them, although some also signal through other pathways to trigger responses such as cytokine production. These phagocytic receptors include several members of the C-type lectin-like family like for example Dectin-2 specifically studied in this project. Previous studies showed that Dectin-2 is essential for the competent host defense against *C. albicans* infection whereas *Clec4n*$^{-/-}$ mice were more susceptible to infection (Ifrim et al., 2016). Based on these results, I sought to elucidate the role of Dectin-2 in the pathogenesis of EBA using the antibody-transfer EBA mouse model (Sitaru et al., 2005). The EBA antibody-transfer model is a rapid and well-reproducible mouse model that provides a unique tool to study the effector phase of Ab-induced skin inflammation *in vivo*. Yet, this model does not allow us to identify the contribution of LTs to mechanisms leading to the loss of tolerance in EBA.

To address the first aim of the study, the antibody-transfer EBA mouse model was induced in the C57BL/6J WT and *Clec4n*$^{-/-}$ mice. These mice lack the presence of the gene *Clec4n* that encodes for the protein Dectin-2 which function is, most likely to recognize the sugar presents on the IgG. Starting from day 4, C57BL/6J WT mice developed severe signs of erythema and crusts on the ears and alopecia over the body, whereas *Clec4n*$^{-/-}$ remained completely resistant to the disease and did not show EBA lesions on their skin. My results were the opposite to the ones from *C. albicans* experiment mentioned previously. At first, I thought that no inflammation occurred *Clec4n*$^{-/-}$ mice, therefore we were curious to scrutinize what really happened at the histopathological level. By harvesting from both C57BL/6J WT and *Clec4n*$^{-/-}$ mice lesional skin and stained with H&E, we observed extraordinary results

where, indeed, a derma-epidermal separation was visible in C57BL/6J WT but not in the *Clec4n*$^{-/-}$ mice. Moreover, C57BL/6J WT lesional skin presented infiltration by white blood cells/PBMCs where nothing was observed in the equivalent skin regions of *Clec4n*$^{-/-}$ mice. Thus, I wanted to investigate the deposition of IgG and C3 in both groups, expecting no sign of inflammation was present at the histopathological level of *Clec4n*$^{-/-}$ mouse skin. Surprisingly, both C57BL/6J WT and *Clec4n*$^{-/-}$ skin sections showed a deposition of IgG and C3. To summarize, at first observation, It has been seen a complete protection from EBA in *Clec4n*$^{-/-}$ mice compared to the C57BL/6J WT with indeed a severe disease on day 8; thus, at the histopathological level, C57BL/6J WT showed a detachment of dermis and epidermis at the dermal-epidermal junction, but nothing was observed in the knock-out lesional sections; the split formation that I observed is the hallmark in the EBA phenotype which is not observed though in the *Clec4n*$^{-/-}$. Based on these results, I thought even though the inflammation took place also in *Clec4n*$^{-/-}$ mice, somehow the recruitment of cells as a response to the inflammation is stopped; therefore, the typical external reaction that is observed in WT mice and so the erosions, blisters, and scars, was not observed in the *Clec4n*$^{-/-}$ mice. I hypothesized that might be a lack of signal transfer from immune complex binding to downstream signaling pathways at the mRNA level of genes important to produce cytokines and chemokines essential for the initiation and propagation of the inflammation and the recruitment of neutrophils to the damaged tissue.

To address this hypothesis, I profiled the main genes involved in EBA pathogenesis; on day 14, mice were harvested and lesional skin (or equivalent skin regions if no lesions were observed) was collected for RNA screening. By analyzing the mRNA levels of *Clec4n*, *Il-17*, *Il -23*, *Cxcl2*, *Il -1β*, *Tnf-α* and *Csf2*, we observed a significant decrease of the pro-inflammatory factor IL-1β and the chemokine CXCL2 in *Clec4n*$^{-/-}$ mice compared to the C57BL/6J WT where we observed *Cxcl2* and *Il-1β* mRNA were significantly more abundant in lesional skin of C57BL/6J WT mice than at corresponding skin sites of *Clec4n*$^{-/-}$ mice. CXCL2 has been already described to be released by neutrophils and by the endothelial cells to facilitate addition cells to the injured tissue (Reutershan et al., 2006). CXCL2 expression has the main function of managing the migration of leukocytes (homing) in the respective anatomical locations in inflammatory and homeostatic processes. Therefore, the absence of

Dectin-2 leads to a disruption in the downstream signaling and, consequently, neutrophils do not produce CXCL2 able to act as a chemoattractant. This may explain why mice deficient for Dectin-2 do not show any visible skin inflammation as neutrophil cannot migrate but, presence of neutrophils in the skin, as my results showed, can lead us to think, in contrast, that Dectin-2 is not CXCL2-dependent. However, tissue analysis is always made on day 14 and not in the initial hours/day of the *in vivo* EBA mouse model; presence of neutrophils at this stage can be given by an amplification effect by resident cells, recruiting more white blood cells. There might be either severely reduced cell recruitment or an abrogate immune cell retention in *Clec4n*$^{-/-}$ mice. Also, IL-1β is involved in the release of pro-inflammatory factors that subsequently favor the recruitment of more immune cells, like neutrophils and to increase the inflammatory chemokines like CXCL2. Production of ROS to maximize neutrophils function in destroying the pathogen is promoted by the recognition of receptors expressed on their surface membrane. The interaction receptor-pathogen initiates the transmission of a signal that spreads downstream to activate all the processes indispensable for the release of the pro- and inflammatory factors (Takeuchi and Akira, 2010). This is due to an efficient expression of IL-1ß to promote the release of ROS and It was observed how the expression of the cytokine is decreased and so, consequently neutrophils ROS response upon IC stimulation is quite weak.

The expression of Dectin-2 has been mainly found in hematopoietic cells such as neutrophils, eosinophils, dendritic cells, and monocytes/macrophages and up-regulated on induction of inflammation. However, its expression was found in non-hematopoietic cells such as Langerhan cells in the skin and in the Kupfer cells in the lung. To distinguish whether Dectin-2 expression on neutrophils or on tissue-resident macrophages and dendritic cells is essential for the induction of skin inflammation, we generated bone marrow chimera between B6.SJL-Ptprc^{a} Pep^{b}/BoyJ and *Clec4n*$^{-/-}$ mice according to an irradiation protocol designed to preserve the recipient's tissue-resident myeloid cells while replacing blood leukocytes by donor cells, as previously described (Sadik et al., 2012). For the generation of chimera, Pepboy mice were used as to allow distinguishing donor and recipient cells by their expression of CD45.1 and CD45.2. The expected origin of myeloid cells in the bone marrow, peripheral blood and in the skin was confirmed by

FACS analysis and immunofluorescence staining for CD45.1 and CD45.2, and cell type-specific cell surface markers. Comparing phenotypes EBA *Clec4n*$^{-/-}$ mice, reconstituted with B6.SJL-Ptprc^{a} Pep^{b}/BoyJ BM (B6.SJL-Ptprc^{a} Pep^{b}/BoyJ → *Clec4n*$^{-/-}$) and B6.SJL-Ptprc^{a} Pep^{b}/BoyJ mice reconstituted with *Clec4n*$^{-/-}$ BM (*Clec4n*$^{-/-}$ → B6.SJL-Ptprc^{a} Pep^{b}/BoyJ), we found that B6.SJL-Ptprc^{a} Pep^{b}/BoyJ → *Clec4n*$^{-/-}$ developed severe skin inflammation while, Clec4n-/- → B6.SJL-Ptprc^{a} Pep^{b}/BoyJ, in contrast, were protected from disease. These results further supported the idea that radiosensitive-hematopoietic cells are the cellular source of Dectin-2 expression in this model. This is not in line with a mouse model of atherosclerosis in which deletion of hematopoietic Dectin-2 did not alter the percentage of mild (42%) and severe (58%) atherosclerosis compared to the C57BL/6J WT mice (Thieme et al., 2019). They found no effect on the cytokines secretion while I observed a decrease in the pro-inflammatory factor IL-1β and the chemokines CXCL2. When the BM-derived cells from both the lines were analyzed, a clear distinction between CD45.1 and CD45.2 was observed, and additionally, confirmed my hypothesis of a fully reconstitution of the hematopoietic cells in the BM. In contrary, when cells in the blood and skin were analyzed, I did not find any traces of Dectin-2. It potentially demonstrates that BM-derived cells are responsible for the progression of the disease. I would like to highlight the high variability of Dectin-2 function in different diseases that makes also complicated to define only one way to function. A possible explanation may be the fact of the targeted ligand and its structure composition in EBA that might be different in the other inflammatory diseases. Thus, cells were analyzed on day 14 of the disease which let us think the expression of Dectin-2 on resident cells in the skin and blood already lost the ability to express it at high levels. On the other hand, the constant production of hematopoietic cells in the BM during inflammation is highly under a continuous stimulus by GM-CSF, LTB_4 to make the cells effective by being primed.

4.2 Biological effects of Dectin2 on neutrophils functions

With my results indicating the requirement of Dectin-2 for the progression of EBA, I wanted to address the significance of the C-type lectin receptor for neutrophils activity *in vitro*. As previously report (Yao et al., 2015), stimulation of neutrophils with

10 ng/ml GM-CSF increased the expression of Dectin-2 on the cell surface. To address the question whether the importance of primed neutrophils is required to elicit their function during inflammation, the Reactive Oxygen Species (ROS) activity and Leukotriene B4 (LTB_4) expression were measured in C57BL/6J WT and *Clec4n*$^{-/-}$ BM-derived cells after priming the cells for approximately 2 days with GM-CSF. ROS are chemically reactive molecules containing oxygen that could be very harmful when found as peroxides, superoxide, hydroxyl radical and more that can damage our cells. There are two sources of ROX generation: 1) exogenous pathway caused by radiation, pollution, drugs and 2) endogenous pathway due to the presence of inflammation in our body. In EBA, the activation of granulocytes by ICs at the dermal-epidermal junction is considered the primary trigger for granulocytes to unleash of reactive oxygen species (ROS) and proteases, which subsequently degrade the dermal-epidermal adhesion complex resulting in the formation of subepidermal clefts (Chiriac et al., 2007; Kasperkiewicz et al., 2012; Liu et al., 2000; Liu et al., 1998; Shimanovich et al., 2004). The stimulation of neutrophils by ICs at the DEJ may also induce the release of leukotriene B4 (Chou et al., 2010), which initiates and amplifies the recruitment of neutrophils to the DEJ and is consequently a prerequisite for the eruption of inflammatory skin lesions (Sezin et al., 2017; Sezin et al., 2019). Based on my current understanding of the mechanisms mediating the effector phase of EBA, dermal-epidermal separation occurs following binding of anti-Col7 Abs to type VII collagen and recruitment of neutrophils into the skin. I wanted to investigate the importance of ROS release by PMNs to induce blisters formation. Therefore, BM-derived neutrophils from both C57BL/6J WT and *Clec4n*$^{-/-}$ mice were isolated and stimulated with IC for 1 hour. Following measurement of ROS activity and LTB_4 release, the *in vitro* results presented in this work demonstrated there was a difference between unstimulated and stimulated neutrophils. However, no difference in ROS activity between IC stimulated C57BL/6J WT and *Clec4n*$^{-/-}$ neutrophils was observed. The previously shown decrease of the pro-inflammatory factor IL-1ß at the mRNA level of *Clec4n*$^{-/-}$ mice in the passive EBA mouse model which turned is most likely responsible for the induction of ROS. This latter is generated in stimulated neutrophils mainly by NADPH oxidase and myeloperoxidase-hydrogen peroxide-chloride systems. Accordingly, it was shown that NADPH oxidase system

is required to induce tissue damage in EBA (Chiriac et al., 2007). At the cellular level, NADPH oxidase can be activated by a large collection of chemicals, physical, environmental, and biological factors including LTB_4 (Jiang et al., 2011; Perkins et al., 1995). Thus, in addition to its chemotactic effects on neutrophils, LTB_4 was previously shown to stimulate neutrophil degranulation. When the leukotriene B4 expression was analyzed by IC stimulated PMNs there was a slight decrease of LTB_4 in *Clec4n*$^{-/-}$ BM-derived neutrophils compared to the C57BL/6J WT. I do not know whether there might be a possible link between ROS and LTB_4 release in neutrophils, but Kiung-Jin Chou and collaborators suggested that 5-LOX derived ROS are involved in many pathological and inflammatory response. However, the specific signaling pathways involved in the generation of ROS requires further studies. Based on my results it might be that ROS are released in a Dectin2-indipendent manner while its presence, on neutrophils, is important for LTB_4 release.

4.3 Neutrophils require the cooperation between FcγIV receptor and Dectin-2 to elicit their function in EBA

The dilemma about the C-type lectins is the fact that there are so many that can interact with many different pathogens. Therefore, when you knock-out one of them it is very difficult to see a biological consequence when one receptor is missing there are other receptors that can also do the same job. C-type lectin receptors can act as “strict PRR” for example upon ligation directly signal to activate the innate and adaptive immune response; they can modulate the immune responses by helping to find the right immunity to detected pathogen and can directing cargo for antigen processing/presentation. I already mentioned above the different groups of C-type lectin receptors. Dectin-1 is the most studied protein (Sancho et. Al, 2012) and it is expressed on myeloid cells like macrophages, neutrophils, dendritic cells; it recognizes β-1 glucans present in the cell wall of fungi and some bacteria independently from Ca^{2+} and lacks the motif EPN/QPN for binding mannose and galactose. It has instead an ITAM-like (hemITAM) motif that directly triggers the signaling pathway by recruiting Syk. Studies on Dectin-1 demonstrated that Dectin1

KO mice were more susceptible to *C. albicans*. Surprisingly, another study conducted by Marakalala and collaborators demonstrated that other strains of *C. albicans* can vary their cell wall and so other PRR can recognize it and not anymore by Dectin-1 (Marakalala et, al, 2013). One of the Dectin-2 recognition pathogen is *C. albicans* as well and here we can see there is an overlapping of the recognition pathway with Dectin-1. It recognized α-mannans present in the fungal cell wall but the only difference with Dectin-1 is the process by which it signals. When *Clec4n*$^{-/-}$ mice were infected with *C. albican* and analyzed, they were more susceptible to *C. albicans* (Ifrim, et al., 2016) like Dectin-1 result. The difference between the two proteins is that Dectin-2 requires an adaptor molecule (Kerscher et al., 2013) and only through this attachment it can be expressed on the surface, and it is required for downstream signaling. It was demonstrated that our passive EBA mouse model showed protection of the *Clec4n*$^{-/-}$ mice from the disease. In this case, Dectin-2 was knocked out in all the cells. Therefore, it was not known which specific cell was responsible for driving inflammation. To answer this question, an *in vivo* passive EBA mouse model was performed comparing MRP8-Cre-ires/GFP and neutrophils specific FcgRIV-KO (MRP8^{Cre} x FcγRIV$^{flx/flx}$) mice. The standard protocol was followed by injecting COLVII on day 0, 4 and 6 and we scored the mice from day 6 until day 14. Surprisingly our results showed a complete protection of the disease in the FcγRIV KO mice. When lesional skin was analyzed, deposition of C3 and IgG was observed in both MRP8-Cre-ires/GFP and FcγRIV^{-}KO at the histological level. Also, a split of the dermal-epidermal junction in MRP8-Cre-ires/GFP compared to the FcγRIV^{-}KO was observed. To make further robust my conclusion, I analyzed BM, blood, and skin cells. In the MRP8-Cre-ires/GFP BM, it was observed a notable number of FcγRIV expressed on neutrophils and intermediate cells while, how it was expected no expression of FcγRIV on neutrophils and intermediate cells in the FcγRIV^{-}KO. No Dectin-2 expression was detected. In the blood, we observed a low expression level of neutrophils and FcγRIV on their surface in MRP8-Cre-ires/GFP where in FcγRIV^{-}KO also low expression of neutrophils and no FcγRIV as expected. Instead, we did see the expression Dectin-2 on neutrophils in MRP8-Cre-ires/GFP and not in FcγRIV KO. In the skin of MRP8-Cre-ires/GFP mice, high expression of neutrophils was observed compared to the FcγRIV^{-}KO where almost no expression of PMNs was observed. One of the explanations is that in the BM, neutrophils are still unprimed, therefore they still do not acquire a mature stage where we can see

Dectin-2 expression to elicit its function whereas FcγRIV is already formed. When neutrophils start to migrate to the blood, they are attracted by chemoattractants and so they are primed and become mature, so they express Dectin-2 and FcγRIV. Once the granulocytes arrived from the blood to the inflamed skin as effector cells, they release ROS to boost their role as phagocytes and release ROS. Although it is known in the skin there are resident macrophages and other type of cells and neutrophils, it can be that EBA pathogenesis is not in its peak anymore on day 14. This could explain why we did not see any expression of Dectin-2. In support to our hypothesis, a study conducted by Kasperkiewicz et al., suggests that neutrophils activation following exposure to pathogenic rabbit anti-mCol7c IgG requires FcγRIV binding to the Fc portion of Col7c IgG. Thus, the disease was restored in γ-chain deficient mice locally reconstituted with WT neutrophils, but not with γ-chain deficient neutrophils (Kasperkiewicz et al., 2012). We can conclude that neutrophils are the main cause of EBA manifestation thus, the expression of Dectin-2 on their surface is important to drive inflammation.

4.4 Dectin-2 collaborates with FcγRIV to release ROS but not LTB_4 from neutrophils

EBA is characterized by the presence of immunoglobulin (Ig) G auto-antibody molecules suggesting that several factors influence the ability to induce inflammation and skin pathology. IgGs recognize antigens through their two Fab domains and are in turn recognized through their Fc portion by specific Fcγ receptor on the cell surface of neutrophils. The IgGs affinity to a specific Fcγ receptor depends on their subclasses and their glycosylation pattern. In mice, it has been shown IgG1 has high-affinity for the inhibitory FcγRIIb while IgG2a has a high-affinity

for activating FcγRIV. To elucidate the role of Dectin-2 and its collaboration with FcγRIV specifically, to trigger inflammation we wanted to confirm the importance of FcγRIV in EBA. I performed an *in vitro* experiment by stimulating C57BL/6J WT BM-derived neutrophils with IC and, subsequently treated with anti-FcγRIV (kindly donated by Falk Nimmerjahn laboratory) and FcγRIV Abs isotype as a control. My results showed, clearly, a significant decrease in ROS production by C57BL/6J WT neutrophils treated with anti-FcγRIV Ab compared to the Isotype. In contrast, I did not see any difference in LTB_4 expression with or without anti-FcγRIV Ab and the isotype upon IC stimulation.

4.5 Dectin-2 is expressed only when neutrophils are primed

During quiescent phase, neutrophils do not express many receptors on their surface until it is required to elicit their function when an inflammation occurs. The chemokine GM-CSF is known to be a potent prime factor for neutrophil activation during EBA pathogenesis. Not only, the pro-inflammatory factor leads neutrophils to become mature also, it is capable recruiting neutrophils from the bone marrow into the blood. I previously showed Dectin-2 was not detected in the skin and in the bone marrow but instead in the blood. The reason might depend on the timeline of EBA. I saw that WT neutrophils expressing FcγRIV was 95.05% in the bone-marrow and 87.13% blood respectively while in the skin the percentage of neutrophils dropped down to 64.79%. Dectin-2 was only detectable in the blood with a low percentage of 20.67%. In *Clec4n*$^{-/-}$ mice not even a significant percentage of the expression of FcγRIV on neutrophils was comparable to the WT analysis. Although the presence of neutrophils into inflamed tissues has always been confirmed by many studies it might be that mice inflamed tissue harvested on day 14 is already in a reminiscence stage. This can explain why Dectin-2 is not detectable. Because it was demonstrated that Dectin-2 collaborates with FcγRIV to recognize the autoantibodies, in EBA, thus GM-CSF promotes the expression of both receptors it can be that at day 14 of EBA the inflammation process was about to end. Therefore

a cell migration assays *in vitro* with unprimed neutrophils was performed to understand whether they were able to migrate toward a potent chemoattractant, the anaphylatoxin C5a. Results showed there was no difference of migration in both cell lines and migration itself was not at a high level. I hypothesized that neutrophils needed to be primed and their functions are limited for a period maybe shorter than 14 days of EBA inflammation.

4.6 Dectin-2 is expressed intracellularly upon recognition of autoantibodies

To confirm my hypothesis, I sorted C57BL/6J WT and *Clec4n*$^{-/-}$ cell lines by treating them for 40 hours and analyzed Dectin-2 expression on neutrophils at the intracellular level. It was already seen that the expression of Dectin-2 was detectable after 72 hours treatment with GM-CSF. In line with this, it was observed an extraordinary shift in the C57BL/6J WT BM-derived neutrophils population where *Clec4n*$^{-/-}$ cells did not show. I then built a new hypothesis stating that upon “priming” process, during inflammation, the granulocytes express Dectin-2. In our specific case, only after 40 hours with GM-CSF treatment. This linked us back to the timeline point where it can be that on day 4 of the EBA pathology there is a maximum expression of the receptors on neutrophils membrane surface that is reduced or not even detected on day 14. Furthermore, with these results we can say once Dectin-2 recognizes the sugar chain of the IgGs is turning intracellularly together with FcγRIV.

4.7 FcγRIV is expressed intracellularly when interacting with Dectin-2

Following the thesis that Dectin-2 goes intracellularly upon recognition of autoantibodies I wanted to investigate whether FcγRIV follows the same process. I performed *in vitro* staining of the receptor after stimulation of C57BL/6J WT and *Clec4n*$^{-/-}$ neutrophils with and without IC. My results confirmed my theory: C57BL/6J WT BM-derived neutrophils treated with IC showed a significant decreased of FcγRIV expression compared to the unstimulated one and no difference was showed in both unstimulated and IC treated *Clec4n*$^{-/-}$ BM-derived neutrophils. FcγRIV, which

are both multimeric receptors non-covalently associated with a transmembrane adaptor protein, the Fc-receptor γ-chain (FcRγ), which carries an ITAM motif in its intracellular tail. Since this non-covalent association is required for the stabilization of the receptor complex, the FcRγ-associated receptors are not expressed on the cell surface in the absence of FcRγ.

CONCLUSION

Based on my findings, the C-type lectin receptor Dectin-2 seems to play an important role as regulator of neutrophil response to EBA skin inflammation. Results from *in vivo* passive EBA mouse model demonstrated that *Clec4n*$^{-/-}$ mice were protected from the disease compared to the C57BL/6J WT mice. Thus, lesional skin sections presented separation of derma-epidermal junction and mononuclear cellular infiltration in the C57BL/6J WT mice group while, lack of dermal-epidermal separation was observed in *Clec4n*$^{-/-}$ mice group.

The pro-inflammatory factor IL-1ß and the chemokine CXCL2 expression were significantly reduced in the skin *Clec4n*$^{-/-}$ mice, therefore I hypothesized Dectin-2 expressed on neutrophils was crucial for the formation of the CXCL2 structure to allow, subsequently, neutrophils transmigration. In contrast to the low expression of *Il-1ß*, *in vitro* experiments showed no significant difference in the release of ROS in both groups, C57BL/6J WT and *Clec4n*$^{-/-}$ BM-derived neutrophils treated with IC. On the other hand, I did see a slight decrease in LTB_4 release in *Clec4n*$^{-/-}$ BM-derived neutrophils compared to the C57BL/6J WT.

To gain insights into the mechanism of Dectin-2 in the experimental EBA, it was important to define the cellular source and target cells of Dectin-2 knowing that hematopoietic cells are radiosensitive while non-hematopoietic cells are radioresistant. Therefore, chimera experiment was performed by irradiating both B6.SJL-Ptprc^{a}Pep^{b}/BoyJ and *Clec4n*$^{-/-}$ mice that, subsequently, were reconstituted with donors B6.SJL-Ptprc^{a}Pep^{b}/BoyJ BM cells into the recipients *Clec4n*$^{-/-}$ mice (B6.SJL-Ptprc^{a}Pep^{b}/BoyJ → *Clec4n*$^{-/-}$) and donors *Clec4n*$^{-/-}$ BM cells into recipients B6.SJL-Ptprc^{a}Pep^{b}/BoyJ mice (*Clec4n*$^{-/-}$ → B6.SJL-Ptprc^{a}Pep^{b}/BoyJ). Results showed a full replacement of BM cells from the donors into the recipients; therefore,

I hypothesized BM cells were the source of EBA initiation. This is an interesting finding for a potential treatment for patients suffering from skin disease such as EBA. The severe erosion of the skin is not only a constant struggle in the daily life of patients but indeed poses a serious risk to their survival. As many diseases, EBA cannot be cured by drugs; in parallel to my main project, I was able to test the antibiotic dapsone in EBA murine model: dapsone was able to mitigate inflammation when I treated C57BL/6J WT and *Clec4n*$^{-/-}$ BM-derived mouse neutrophils by reducing their recruitment and so, subsequently, ROS release and LTB_4 in response to immune complex (Murthy et al., 2021). However, the mode of action of dapsone is unknown and cannot cure EBA. Instead, BM transplant consists of taking away the malfunctioning deficient BM cells to resupply the body with healthy new blood (from healthy patients) to recreate the immune system of that individual. As mentioned above, results from my chimera experiment showed BM cells were fully replenished in both groups of mice and, also when recipients B6.SJL-Ptprc^{a}Pep^{b}/BoyJ mice were replenished with donors *Clec4n*$^{-/-}$ mice, surprisingly no manifestation or slight presence of blisters on body surface was observed. This highlights the fact we may use cells as medication, instead of drugs, to cure the autoimmune blistering disease. I would like to mention the work done by Dr. Yamanaka who altered skin cells and made them into the cells called induced pluripotent stem cells from mouse to embryonic and adult fibroblast cultures by defined (Takahashi and Yamanaka, 2006). However, we cannot take skin cells from EBA patients and make them pluripotent embryonic stem cells because they all have genetic error. Therefore, my suggestion would be to further investigate the DNA of EBA mice skin cells and use the “gene editing technologies” to try to replace the genetic error with good DNA. Once DNA is corrected, the idea is to produce a large amount of these new cells for BM transplant. This can help to possibly find a cure.

Furthermore, It was interesting to investigate whether neutrophils acquired Dectin-2 expression upon exposure to GM-CSF as this potent chemoattractant is able to prime neutrophils that, subsequently, are able to elicit their maximal function during inflammation; therefore, I performed an *in vitro* experiment where both C57BL/6J WT and *Clec4n*$^{-/-}$ BM-derived neutrophils were incubated with GM-CSF for 40h; subsequently, cells were analyzed by flow cytometry and results demonstrated a

clear shift of the C57BL/6J WT population positive for Dectin-2 compared to the *Clec4n*$^{-/-}$ population. In addition, to confirm the hypothesis of the importance of primed neutrophils, in EBA inflammation, a migration assay was performed with unstimulated neutrophils migrating towards one of the most potent chemoattractants, C5a. No difference was observed between C57BL/6J WT and *Clec4n*$^{-/-}$ in terms of migration and so this result additionally supported the importance of neutrophils to be primed.

AAbs have different affinities for Fcγ receptors, and the *in vitro* results presented in this work demonstrated that there is a cooperation between the FcγIV receptor and Dectin-2. I wanted to investigate whether neutrophils are the major source of Dectin-2 and that this latter cooperated with FcγIV receptor. I performed an *in vivo* passive EBA mouse model by comparing MRP8-Cre-ires/GFP and neutrophils specific FcγRIV-KO (MRP8^{Cre} x FcγRIV$^{flx/flx}$). mice. My results indicated FcγRIV-KO mice were protected from induction of antibody-transfer EBA. From these findings, it would be interesting to further investigate, with the fluorescence resonance energy transfer (FRET), whether there is a co-aggregation directly between FcγRIV and Dectin-2 on the surface membrane in a quiescent phase of the cells and upon IC stimulation; by co-expressing Dectin-2 and FcγRIV in human embryonic kidney (HEK293) cells, widely used in research due to their easy way to grow in suspension and easy to be transfected.

Once Dectin-2 recognizes the AAbs bound to the DEJ/autoantigen COL7c and colocalized with FcγIV receptor, one of the studies to be considered is to analyze the cascade signal where kinase cascades are implicated. This can be evaluated by monitoring neutrophils at different time points with and without IC treatment and to analyze through the western-blot technique the phosphorylation of the kinases involved in the signaling pathway.

Another future investigation would be measuring the expression of integrins, under different conditions, to evaluate whether they may affect the expression of Dectin-2 not only on neutrophils but also on macrophages and mature monocytes.

LITERATURE

Anaya, J.M., Shoenfeld, Y., Yehuda S., Rojas-Villarraga, A., Roger, A. L. (2013). Autoimmunity: from Bench to Bedside. El Rosario University Press (digital).

Amulic B, Cazalet C, Hayes GL, Metzler KD, Zychlinsky A (2012) Neutrophil function: from mechanisms to disease. Annu.Rev.Immunol. 30, 459-489.

Adrover, J. M., Nicolás-Ávila, J. A., and Hidalgo, A. (2016). Aging: a temporal dimension for neutrophils. Trends Immunol. 37, 334–345.

Arancibia, S.A., et al., Toll-like receptors are key participants in innate immune responses. Biol. Res. 2007; 40:97–112.

Barcellos-de-Souza, P., Canetti, C., Barja-Fidalgo, C. and Arruda, M.A. (2012). Leukotriene B (4) inhibits neutrophil apoptosis via NADPH oxidase activity: redox control of NF-κB pathway and mitochondrial stability. Biochim. Biophys. Acta 1823, 1990–1997.

Barrett, N.A., Rahman, O. M., Fernandez, J. M., Parsons, M. W., Xing, W., Austen, K. F., & Kanaoka, Y. (2011). Dectin-2 mediates Th2 immunity through the generation of cysteinyl leukotrienes. Journal of Experimental Medicine, 208(3), 593–604.

Bernard, P., Prost, C., Aucouturier, P., et al., The subclass distribution of IgG autoantibodies in cicatricial pemphigoid and epidermolysis bullosa acquisita J Invest Dermatol, 97 (1991), pp. 259-263.

Beutler BA. TLRs and innate immunity. Blood. 2009; 113:1399–1407.

Bieber, K., Sun, S., Ishii, N., Kasperkiewicz, M., Schmidt, E., Hirose, M., Westermann, J., Yu, X., Zillikens, D., & Ludwig, R. J. (2010). Animal models for autoimmune bullous dermatoses. Experimental Dermatology, 19(1), 2–11.

Borregaard N (2010) Neutrophils, from marrow to microbes. Immunity. 33, 657-670.

Borregaard N, Kjeldsen L, Sengelov H, Diamond MS, Springer TA, Anderson HC, Kishimoto TK, Bainton DF. Changes in subcellular localization and surface

expression of L-selectin, alkaline phosphatase, and Mac-1 in human neutrophils during stimulation with inflammatory mediators. J. Leukoc. Biol. 1994; 56:80–87. Briggaman, R. A., & Wheeler, C. E. (1975). The epidermal dermal junction. Journal of Investigative Dermatology, 65(1), 71–84.

Brogden, N.K., Mehalick, L., Fischer, C.L., Wertz, P.W., and Brogden, K.A. (2012). The emerging role of peptides and lipids as antimicrobial epidermal barriers and modulators of local inflammation. Skin Pharmacol. Physiol. 25, 167-181.

Bruhns, P., Iannascoli, B., England, P., Mancardi, D.A., Fernandez, N., Jorieux, S., et al., Specificity and affinity of human Fc{gamma} receptors and their polymorphic variants for human IgG subclasses. Blood. (2009) 113:3716–25.

Bruhns, P. and Jonsson, F. Mouse and human FcR effector functions. Immunological Reviews 2015 Vol. 268: 25–51

Chen, M., Marinkovich, M. P., Veis, A., Cai, X., Rao, C. N., O'Toole, E. A., & Woodley, D. T. (1997). Interactions of the amino-terminal noncollagenous (NC1) domain of type VII collagen with extracellular matrix components. Journal of Biological Chemistry, 272(23), 14516–14522.

Chiffoleau, E. (2018). C-type lectin-like receptors as emerging orchestrators of sterile inflammation represent potential therapeutic targets. Frontiers in Immunology, 9(FEB), 1–9.

Chiriac, M.T., Roesler, J., Sindrilaru, A., Scharffetter-Kochanek, K., Zillikens, D., and Sitaru, C. (2007). NADPH oxidase is required for neutrophil-dependent autoantibody-induced tissue damage. J. Pathol. 212, 56–65.

Chomczynski P, Mackey K. (1995) Short technical report. Modification of the TRIZOL reagent procedure for isolation of RNA from Polysaccharide-and proteoglycan-rich sources. Biotechniques 19(6): 942-5.

Damoiseaux, J. (2013). Bullous Skin Diseases: Classical Types of Autoimmune Diseases. Scientifica, 2013, 1–5.

Decout, A., Silva-Gomes, S., Drocourt, D., Blattes, E., Rivière, M., Prandi, J., Larrouy-Maumus, G., Caminade, A.M., Hamasur, B., Källenius, G., Kaur, D., Dobos, K.M., Lucas, M., Sutcliffe, I.C., Besra, G.S., Appelmelk, B.J., Gilleron, M., Jackson,

M., Vercellone, A., Tiraby, G., & Nigou. J. Deciphering the molecular basis of mycobacteria and lipoglycan recognition by the C-type lectin Dectin-2 (2018)

Drickamer, K., & Taylor, M. E. (2015). Recent insights into structures and functions of C-type lectins in the immune system. Current Opinion in Structural Biology, 34, 26–34.

Edwards, G., Diercks, G. F. H., Seelen, M. A. J., Horvath, B., Van Doorn, M. B. A., & Damman, J. (2019). Complement activation in autoimmune bullous dermatoses: A comprehensive review. Frontiers in Immunology, 10(JUN), 1–8.

El-Benna J, Dang PM, Gougerot-Pocidalo MA. Priming of the neutrophil NADPH oxidase activation: role of p47phox phosphorylation and NOX2 mobilization to the plasma membrane. Semin. Immunopathol. 2008; 30:279–289.

Elias, P.M. (2015). Stratum corneum acidification: how and why? Exp. Dermatol. 24, 179-180.

Gaffen, S. L., Jain, R., Garg, A. V., and Cua, D. J. (2014). The IL-23-IL-17 immuneaxis: from mechanisms to therapeutic testing. Nat. Rev. Immunol. 14, 585–600.

Garrod, D. and Chidgey, M. (2008). Desmosome structure, composition and function. Nat. Rev. vol 1778, 572-587.

Fischer, W. W., Hemp, J., Valentine J. S. (2016). How did life survive Earth's great oxygenation? Curr. Opin. Chem. Biol. 31, 166–178.

Gammon, W.R., Merritt, C.C., Lewis, D.M., Sams, W.M., Carlo, J.R., and Wheeler, C.E. (1982). An in vitro model of immune complex-mediated basement membrane zone separation caused by pemphigoid antibodies, leukocytes, and complement. J. Invest. Dermatol. 78, 285–290.

Goletz, S., Zillikens, D., & Schmidt, E. (2017). Structural proteins of the dermal-epidermal junction targeted by autoantibodies in pemphigoid diseases. Experimental Dermatology, 26(12), 1154–1162.

Gordy, C., Pua, H., Sempowski, G. D., and He, Y. W. (2011). Regulation of steady-state neutrophil homeostasis by macrophages. Blood 117, 618–629.

Görgens, A., Radtke, S., Möllmann, M., Cross, M., Dürig, J., Horn, P. A., et al., 198692(2013). Revision of the human hematopoietic tree: granulocyte subtypes derive from distinct hematopoietic lineages. Cell Rep. 3, 1539–1552.

Graham, L. M., & Brown, G. D. (2009). The Dectin-2 family of C-type lectins in immunity and homeostasis. Cytokine, 48(1–2), 148–155.

Hadebe, S., Brombacher, F., & Brown, G. D. (2018). C-type lectin receptors in asthma. Frontiers in Immunology, 9(APR), 1–11.

Häger,M., Cowland, J. B., and Borregaard,N. (2010).Neutrophil granules in health and disease. J. Intern. Med. 268, 25–34.

Haider M, Dambuza IM, Asamaphan P, Stappers M, Reid D, Yamasaki S, et al., (2019) The pattern recognition receptors Dectin-2, mincle, and FcRγ impact the dynamics of phagocytosis of Candida, Saccharomyces, Malassezia, and Mucor species. PLoS ONE 14(8): e0220867.

Harris ES, McIntyre TM, Prescott SM, et al., The leukocyte integrins. J Biol Chem 2000, 275:23409–23412.

Higham, A., Cadden, P., Southworth, T., Rossall, M., Kolsum, U., Lea, S., Knowles, R. and Dave Singh. Leukotriene B4 levels in sputum from asthma patients. ERJ Open Res.

Jiao, J., Dragomir, A. C., Kocabayoglu, P., Rahman, A. H., Chow, A., Hashimoto, D., et al., (2014). Central role of conventional dendritic cells in regulation of bone marrow release and survival of neutrophils. J. Immunol. 192, 3374–3382.

Joo, K.M., Hwang, J.H., Bae, S., Nahm, D.H., Park, H.S., Ye, Y.M., and Lim, K.M. (2015). Relationship of ceramide-, and free fatty acid-cholesterol ratios in the stratum corneum with skin barrier function of normal, atopic dermatitis lesional andnon-lesional skins. J. Dermatol. Sci. 77, 71-74.

Kasperkiewicz, M., Nimmerjahn, F., Wende, S., Hirose, M., Iwata, H., Jonkman, M.F., Samavedam, U., Gupta, Y., Möller, S., Rentz, E., et al., (2012a). Genetic identification and functional validation of FcγRIV as key molecule in autoantibody-induced tissue injury. J. Pathol. 228, 8–19.

Kerrigan, A. M., & Brown, G. D. (2011). Syk-coupled C-type lectins in immunity. Trends in Immunology, 32(4), 151–156.

Kerscher, B., Willment, J. A., & Brown, G. D. (2013). The Dectin-2 family of C-type lectin-like receptors: An update. International Immunology, 25(5), 271–277.

Kim, H. K., De La Luz Sierra, M., Williams, C. K., Gulino, A. V., and Tosato, G. (2006). G-CSF down-regulation of CXCR4 expression identified as a mechanism for mobilization of myeloid cells. Blood 108, 812–820.

Koga, H., Prost-Squarcioni, C., Iwata, H., Jonkman, M. F., Ludwig, R. J., & Bieber, K. (2019). Epidermolysis bullosa acquisita: The 2019 update. Frontiers in Medicine, 6(JAN).

Janeway C.A. Jr., Medzhitov R. Innate immune recognition. Annu Rev Immunol. 2002;20:197–216.

Lehman, J.S., Camilleri, M. J., & Gibson, L. E. (2009). Epidermolysis bullosa acquisita: Concise review and practical considerations. International Journal of Dermatology, 48(3), 227–236.

Ludwig,R.J., Recke, A., Bieber, K., Müller, S., de Castro Marques, A., Banczyk, David., Hirose, M., Kasperkiewicz, M., Ishii, N., Schmidt, E., Westermann, J., Zillikens, D. and Ibrahim, S.M. (2011). Generation of Antibodies of Distinct Subclasses and Specificity Is Linked to H2s in an Active Mouse Model of Epidermolysis Bullosa Acquisita. Journal of Investigative Dermatology, Volume 131, Issue 1, January 2011, Pages 167-176.

Ludwig, R. J. (2013). Clinical Presentation, Pathogenesis, Diagnosis, and Treatment of Epidermolysis Bullosa Acquisita. ISRN Dermatology, 2013, 1–25.

Malhotra, V., & Erlmann, P. (2011). Protein export at the ER: Loading big collagens into COPII carriers. EMBO Journal, 30(17), 3475–3480.

McGonagle, D. and McDermott (2006). A Proposed Classification of the Immunological Diseases. PloS Med. 3(8): e297

Mehren, C. R., & Gniadecki, R. (2011). Epidermolysis bullosa acquisita: Current diagnosis and therapy. Dermatology Reports, 3(3), 2–5.

Mihai, S., & Sitaru, C. (2007). Immunopathology and molecular diagnosis of autoimmune bullous diseases. Journal of Cellular and Molecular Medicine, 11(3), 462–481.

Mihai, S., Chiriac, M. T., Takahashi, K., Thurman, J. M., Holers, V. M., Zillikens, D., Botto, M., & Sitaru, C. (2007). The Alternative Pathway of Complement Activation Is Critical for Blister Induction in Experimental Epidermolysis Bullosa Acquisita. The Journal of Immunology, 178(10), 6514–6521.

Miura, T., Kawakami, T., Kanno, E., Tanno, H., Tada, H., Sato, N., Masaki, A., Yokoyama, R., Kawamura, K., Kitai, K., Takagi, N., Yamaguchi, K., Yamaguchi, N., Kyo, Y., Ishii, K., Imai, Y., Saijo, S., Iwakura, Y., Tachi. M. 2019. Dectin-2-Mediated Signaling Leads to Delayed Skin Wound Healing through Enhanced Neutrophilic Inflammatory Response and Neutrophil Extracellular Trap Formation. J. invest. Dermatol.

Moudgil K.D., Choubey D. Cytokines in autoimmunity: Role in induction, regulation and treatment. J. Interferon Cytokine Res. 2011; 31:695–703.

Murthy, S., Schilf, P., Patzelt, S., Thieme, M., Becker, M., Kröger, L., Bremer, T., Derenda-Hell, A., Knebel, L., Fagiani, F., Ibrahim, S.M., Schmidt, E., Zillikens, D. and Sadik C.D. Dapsone Suppresses Disease in Preclinical Murine Models of Pemphigoid Diseases. J Invest Dermatol. 2021 Nov., 141(11):2587-2595.

Nandakumar, K.S., and Holmdahl, R. (2006). Antibody-induced arthritis: disease mechanisms and genes involved at the effector phase of arthritis. Arthritis Res. Ther. 8, 223.

Nguyen, A. V., & Soulika, A. M. (2019). The dynamics of the skin's immune system. International Journal of Molecular Sciences, 20(8), 1–53.

Nimmerjahn, F., Bruhns, P., Horiuchi, K., Ravetch, J. FcγRIV: A Novel FcR with Distinct IgG Subclass Specificity. 2005. Immunity

Noris, M., & Remuzzi, G. (2013). Overview of complement activation and regulation. Seminars in Nephrology, 33(6), 479–492.

Oostingh, G.J., Sitaru, C., Zillikens, D., et al., Subclass distribution of type VII collagen-specific autoantibodies in patients with inflammatory bowel disease J Dermatol Sci, 37 (2005), pp. 182-184.

Ono M, Bolland S, Tempst P, Ravetch JV. Role of the inositol phosphatase SHIP in negative regulation of the immune system by the receptor Fc(gamma)RIIB. Nature. (1996) 383:263–6.

Oyoshi, M.K., He, R., Li, Y., Mondal, S., Yoon, J., Afshar, R., Chen, M., Lee, D.M., Luo, H.R., Luster, A.D., et al., (2012a). Leukotriene B4-driven neutrophil recruitment to the skin is essential for allergic skin inflammation. Immunity 37, 747–758.

Peters-Golden, M., Canetti, C., Mancuso, P., Coffey, M.J. Leukotrienes: underappreciated mediators of innate immune responses. J Immunol 2005; 174:589–594

Petit, I., Szyper-Kravitz, M.,Nagler, A., Lahav,M., Peled, A.,Habler, L., et al., (2002).

Rankin SM. The bone marrow: a site of neutrophil clearance. J. Leukoc. Biol. (2010); 88:241–251.

Rose, N.R and Bona, C. (1993). Defining criteria for autoimmune diseases (Witebsky's postulates revisited). Immunol Today, 14(9):426-30.

Sadik, C.D., and Luster, A.D. (2012). Lipid-cytokine-chemokine cascades orchestrate leukocyte recruitment in inflammation. J. Leukoc. Biol. 91, 207–215.

Reutershan J, et al., Critical role of endothelial CXCR2 in LPS-induced neutrophil migration into the lung. J. Clin. Invest. 2006; 116:695–702.

Saijo, S., Ikeda, S., Yamabe, K., Kakuta, S., Ishigame, H., Akitsu, A., Fujikado, N., Kusaka, T., Kubo, S., Chung, S. hyun, Komatsu, R., Miura, N., Adachi, Y., Ohno, N., Shibuya, K., Yamamoto, N., Kawakami, K., Yamasaki, S., Saito, T., … Iwakura, Y. (2010). Dectin-2 recognition of α-mannans and induction of Th17 cell differentiation is essential for host defense against candida albicans. Immunity, 32(5), 681–691.

Sakai, L. Y., Keene, D. R., Morris, N. P., & Burgeson, R. E. (1986). Type VII collagen is a major structural component of anchoring fibrils. Journal of Cell Biology, 103(4), 1577–1586

Santi, C. G., Gripp, A. C., Roselino, A. M., Mello, D. S., Gordilho, J. O., de Marsillac, P. F., & Porro, A. M. (2019). Consensus on the treatment of autoimmune bullous dermatoses: Bullous pemphigoid, mucous membrane pemphigoid and epidermolysis bullosa acquisita – Brazilian society of dermatology. Anais Brasileiros de Dermatologia, 94(2), 33–47.

Samavedam U. K., K. Kalies, J. Scheller, H. Sadeghi, Y. Gupta, M. F. Jonkman, E. Schmidt, J. Westermann, D. Zillikens, S. Rose-John, R. J. Ludwig. 2013. Recombinant IL-6 treatment protects mice from organ specific autoimmune disease by IL-6 classical signalling-dependent IL-1ra induction. J. Autoimmun. 40: 74–85.

Scapini P, Cassatella MA. Social networking of human neutrophils within the immune system. Blood. 2014; 124:710-719. DOI: 10.1182/ blood-2014-03-453217

Sitaru, C., S. Mihai, C. Otto, M. T. Chiriac, I. Haußer, B. Dotterweich, H. Saito, C. Rose, A. Ishiko, and D. Zillikens. 2005. Induction of dermal-epidermal separation in mice by passive transfer of antibodies to type VII collagen. J. Clin. Invest. 115: 870 – 878.

Sitaru, C. (2007). Experimental models of epidermolysis bullosa acquisita. Exp. Dermatol. 16, 520–531.

Stark,M. A., Huo, Y., Burcin, T. L.,Morris,M. A., Olson, T. S., and Ley, K. (2005). Phagocytosis of apoptotic neutrophils regulates granulopoiesis via IL-23 and IL-17. Immunity 22, 285–294.

Stefanidakis M, et al., Intracellular and cell surface localization of a complex between alphaMbeta2 integrin and promatrix metalloproteinase-9 progelatinase in neutrophils. J. Immunol. (2004); 172:7060–7068.

Tager, A.M., Dufour, J.H., Goodarzi, K., Bercury, S.D., von Andrian, U.H., and Luster, A.D. (2000). BLTR mediates leukotriene B(4)-induced chemotaxis and adhesion and plays a dominant role in eosinophil accumulation in a murine model of peritonitis. J. Exp. Med. 192, 439–446.

Takahashi, K. and Yamanaka, S. (2006). Induction of pluripotent stem cells from mouse embryonic and adult fibroblast cultures by defined factors. Cell; 126(4):663-76.

Takeuchi O. and Akira S. Pattern recognition receptors and inflammation. Cell 140: 805–820, 2010.

Thannickal VJ. and Fanburg BL. Reactive oxygen species in cell signaling. Am J Physiol Lung Cell Mol Physiol 279: L1005–L1028, 2000.

Tanya Sezin , Matthias Krajewski2 , Adam Wutkowski2 , Sadegh Mousavi1 , Lenche Chakievska3 , Katja Bieber3 , Ralf J. Ludwig3 , Markus Dahlke4 , Dirk Rades4 , Franziska S. Schulze3 , Enno Schmidt3 , Kathrin Kalies5 , Yask Gupta3 , Paul Schilf3 , Saleh M. Ibrahim3 , Peter Ko¨nig5 , Dominik Schwudke2 , Detlef Zillikens1 and Christian D. Sadik (2017). The Leukotriene B4 and its Receptor BLT1 Act as Critical Drivers of Neutrophil Recruitment in Murine Bullous Pemphigoid-Like Epidermolysis Bullosa Acquisita. Journal of Investigative Dermatology 137, 1104-1113

Van den Berg, L. M., Gringhuis, S. I., & Geijtenbeek, T. B. H. (2012). An evolutionary perspective on C-type lectins in infection and immunity. Annals of the New York Academy of Sciences, 1253(1), 149–158.

Villas, B. H. (1998). Flow cytometry: an overview. Cell Vision: The Journal of Analytical Morphology, 5(1), 56–61.

Von Vietinghoff, S., and Ley, K. (2008). Homeostatic regulation of blood neutrophil counts. J. Immunol. 181, 5183–5188. doi: 10.4049/jimmunol.181.8.5183.

Von Vietinghoff, S., and Ley, K. (2009). IL-17A controls IL-17F production and maintains blood neutrophil counts in mice. J. Immunol. 183, 865–873.

Walko, G., Castañón, M. J., & Wiche, G. (2015). Molecular architecture and function of the hemidesmosome. Cell and Tissue Research, 360(3), 529–544. https://doi.org/10.1007/s00441-015-2216-6

Wegener, H., Paulsen, H., & Seeger, K. (2014). The cysteine-rich region of type VII collagen is a cystine knot with a new topology. Journal of Biological Chemistry, 289(8), 4861–4869. https://doi.org/10.1074/jbc.M113.531327

G-CSF induces stem cell mobilization by decreasing bone marrow SDF-1 and up-regulating CXCR4. Nat. Immunol. 3, 687–694. doi: 10.1038/ni813

Woodley D T, Ram R, Doostan A et al., Induction of epidermolysis bullosa acquisita in mice by passive transfer of autoantibodies from patients. J Invest Dermatol 2006: 126: 1323–1330.

Yancey, K. B. 2005. The pathophysiology of autoimmune blistering diseases. J. Clin. Invest. 115: 825– 828.

Yokomizo, T. (2014). Two distinct leukotriene B4 receptors, BLT1 and BLT2. J. Biochem. (Tokyo).

Yonekawa, A., Saijo, S., Hoshino,Y., Miyake, Y., Ishikawa, E., Suzukawa, M., a Inoue, H., Tanaka, M., Yoneyama, M., Oh-hora, M., Akashi, K., and Sho Yamasaki (2014). Dectin-2 Is a Direct Receptor for Mannose-Capped Lipoarabinomannan of Mycobacteria. J.immuni.

Walcheck B, Kahn J, Fisher JM, Wang BB, Fisk RS, Payan DG, Feehan C, Betageri R, Darlak K, Spatola AF, Kishimoto TK. Neutrophil rolling altered by inhibition of L-selectin shedding in vitro. Nature. 1996; 380:720–723.

Zhu, L.L., Zhao, X.Q., Jiang, C., You, Y., Chen, X.P., Jiang, Y.Y., Jia, X.M. and Xin Lin. C-Type Lectin Receptors Dectin-3 and Dectin-2 Form a Heterodimeric Pattern-Recognition Receptor for Host Defense against Fungal Infection. (2013). J.immuni.

PUBLICATIONS

S. Murthy, P. Schilf, S. Patzelt, M. Thieme , M. Becker, L. Kröger , T. Bremer, A. Derenda-Hell, L. Knebel, F. Fagiani, S.M. Ibrahim , E. Schmidt, D. Zillikens, C.D. Sadik. Dapsone Suppresses Disease in Preclinical Murine Models of Pemphigoid Diseases. J Invest Dermatol. 2021 Nov., 141(11):2587-2595

D.A. East, F. Fagiani, J. Crosby, N.D. Georgakopoulos, H. Bertrand, M. Schaap, A. Fowkes, G. Wells, M. Campanella. PMI: a ΔΨm independent pharmacological regulator of mitophagy. Chem Biol. 2014 Nov 20; 21(11):1585-96